JECN

Journal of Epilepsy and Clinical Neurophysiology

ISSN 1676-2649

Volume 26 | Number 1 | Year 2020

ABSTRACTS PRESENTED AT THE 7TH BRAINN CONGRESS BRAZILIAN INSTITUTE OF NEUROSCIENCE AND NEUROTECHNOLOGY (BRAINN-UNICAMP)

JANUARY 25th - 27th 2021 - CAMPINAS, SP, BRAZIL

J Epilepsy Clin Neurophysiol 2020; 26(1): 1-39

www.jecn.org

JECN Journal of Epilepsy and Clinical Neurophysiology

Órgão Oficial da Liga Brasileira de Epilepsia

Indexada no LILACS – Literatura Latino-americana e do Caribe em Ciências da Saúde LILACS 25 years

CORPO EDITORIAL

EXPEDIENTE

Editor Consultivo – Arthur Tadeu de Assis
Editora Executiva – Ana Carolina de Assis
Editora Administrativa – Atha Comunicação Editora
Contato – revistajecn@outlook.com

Ficha Catalográfica

Journal of Epilepsy and Clinical Neurophysiology (Revista de Epilepsia e Neurofisiologia Clínica) / Liga Brasileira de Epilepsia. – Vol. 26, n.1, jul 2020.

v.1, 1995 – JLBE: Jornal da Liga Brasileira de Epilepsia
v. 2 a 7 (n. 2, jun. 2001) Brazilian Journal of Epilepsy and Clinical Neurophysiology (Jornal Brasileiro de Epilepsia e Neurofisiologia Clínica)
Publicação trimestral.
ISSN 1676-2649

CDD: 616.8
CDU: 616.853(05)
616.8-092(05)
616.8-073(05)

Índice para Catálogo Sistemático:

Epilepsia – Periódicos – 616.853(05);
Neurofisiologia – Periódicos – 616.8-092(5);
Eletroencefalografia – Periódicos – 616.8-073(05);
Eletroneuromiologia – Periódicos – 616.8.073(05);
Neurologia – Fisiologia – Periódicos – 616.8-092(05).

Coordenação editorial, criação, diagramação, tradução e produção gráfica Atha Comunicação e Editora - E-mail: 1atha@uol.com.br

JECN Journal of Epilepsy and Clinical Neurophysiology

Contents/Sumário/Contenido

ABSTRACTS PRESENTED AT THE 7TH BRAINN CONGRESS BRAZILIAN INSTITUTE OF NEUROSCIENCE AND NEUROTECHNOLOGY (BRAINN-UNICAMP)

JANUARY 25TH - 27TH 2021 - CAMPINAS, SP, BRAZIL

JECN Journal of Epilepsy and Clinical Neurophysiology

JECN Journal of Epilepsy and Clinical Neurophysiology

JECN Journal of Epilepsy and Clinical Neurophysiology

JECN Journal of Epilepsy and Clinical Neurophysiology

ABSTRACTS PRESENTED AT THE 7TH BRAINN CONGRESS BRAZILIAN INSTITUTE OF NEUROSCIENCE AND NEUROTECHNOLOGY (BRAINN-UNICAMP)

JANUARY 25TH - 27TH 2021 - CAMPINAS, SP, BRAZIL

A 5-FIVER LONGITUDINAL CLINICAL AND NEUROIMAGING STUDY IN SCA3/MJD

T.J.R. Rezende[1], C.C. Piccinin[1], P. Moyses, J.L.R. Paiva[1], A.R.M. Martinez, F. Cendes[1], M.C. França Jr[1]

[1]Department of Neurology, School of Medical Sciences, Unicamp, Brazil.

Introduction: Machado Joseph disease (MJD) is the most common autosomal dominant ataxia worldwide. However, the natural history of MJD is still unknown since there is a lack of longitudinal studies, mainly with long-term follow-up. Hence, we performed a 5-year longitudinal multimodal neuroimaging study in MJD patients to understand the disease's natural history and to uncover biomarkers for clinical trials. **Methods:** We enrolled 23 MJD patients and 22 healthy controls. All subjects underwent 3T MRI and clinical evaluations (by SARA scale) in two time-points with mean interval of 5.0 years for patients and 4.6 years for controls. To assess basal ganglia and infra tentorial white matter, we employed MRICloud. Cerebellar gray and white matters were assessed using Ceres-Suit and SpineSeg for cervical spinal cord. In all group analyses, we used the rate of degeneration ANOVA was performed to assess group differences using age and sex as covariates. Effect sizes (ES) were calculated for each statistically significant result including SARA. **Results:** We found progressive and widespread cerebellar atrophy with the highest effect size (ES:2.0) (Figure 1). The cerebral deep

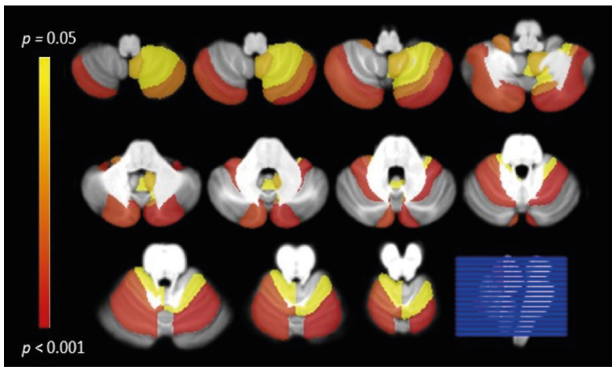

Figure 1. Cerebellar grey matter regions that presented significant progressive damage after 5 years of follow-up in patients with MJD. Color-coded bar represents p-values.

GM showed significant changes and with smallest ESs in left putamen, left thalamus and right medulla. Diffusion parameters revealed progressive radial diffusivity abnormalities in the corticospinal tracts, left superior and right inferior cerebellar peduncles (ES:1.29). We did not find progressive spinal cord damage. In contrast to imaging results, clinical scale showed ES of 0.82 what represent a mean difference in SARA scale comparing the two time points of 3.48 points. **Discussion/Conclusions:** Longitudinal changes in MJD affects mostly cerebellum, infratentorial white matter and basal ganglia, which provided large effect sizes when compared to clinical scale. This is a key point since SCA3/MJD is a rare disease, and the use of a marker with larger sensitivity to change implies in a smaller sample size needed for phase II clinical trials, for instance.

A PILOT STUDY EVALUATING BRAIN FUNCTIONAL CHANGES ASSOCIATED TO THE BEHCREATIVE ENVIRONMENT

E. Partesotti[1], J. A. Feitosa[2,3], J. Manzolli[1], G. Castellano[2,3]

[1]Interdisciplinary Nucleus for Sound Studies, NICS, UNICAMP; [2] Neurophysics Group, IFGW, UNICAMP; [3]BRAINN.

Introduction: This paper describes a pilot study on the development of a Digital Musical Instrument (DMI) for therapeutic purposes. We developed an interactive technology – *BehCreative* – and run the pilot experiment to investigate functional brain changes using resting state functional magnetic resonance imaging (rs-fMRI) data. We believe that daily use of such technology will improve functional connectivity and plasticity of the subject's brain. We adopted theoretical concepts such as Creative Empowerment, Motion Fluidity and Virtual Affordance. **Materials and Methods:** We run the pilot with two participants at NICS Lab in an octophone environment for five sessions (each with maximum duration of five minutes) and we collected MRI data at the Clinics Hospital of UNICAMP in two instances, pre-first and post last session. We attributed audio-visual feedbacks to the left and right arm's subject position. The visual was projected respectively in front of and to the two sides of the subject. We collected the *jerk* – a type of body acceleration – to calculate the Motion Fluidity (MF) and give the audio feedback. MF sets the degree of dissonance or consonance that the subjects hear while performing. Furthermore, we collected *a priori* six specific arm's movements of the two subjects which we named Virtual Affordance (VA) and we assigned to specific sounds. The rs-fMRI data were analyzed in the same way described in [1]. The degree of the obtained graphs was computed for the two moments data were acquired, as well as degree changes between these moments. **Results:** Subject 1 (S1) commenced exploration with a slow jerk, remaining mainly in the dissonant phase, thus generating only black and white feedback in the first few sessions. Subject 2 (S2), instead, presented a more sustained jerk, maintaining more consonant phases and displaying colored feedback while also hearing VA. S2 stressed the feeling of control experienced – and thus Creative Empowerment – in the fifth session. The curve of Motion Development evidences that S1 began to use a constant jerk gradually. Instead, S2 gradually begun to use silence. Regarding brain analyses, S1 showed degree increase in the visual cortex (VC), and in the prefrontal cortex (PC) in the motor system. The second subject showed the largest degree increase in the anterior PC. **Discussion/Conclusion**: Degree increases found for S1 in VC possibly underlie alertness and higher attention, and in the motor cortex they could be related to movement improvement. For S2, degree changes in the anterior PC, could be related to an increase in the calibration of MF and self-awareness during the daily practice. Indeed, the anterior PC is responsible for strategic processes in memory recall and cognitive control of behavior, which facilitate the attainment of the chosen goal; in turn this is particularly important when referring to the rewarding system. Eventually, a creative and compositional curve is observable in the use of VA together with the performance of the jerk in S2 while for S1, results show that is not completely aware of VA but instead presents a more regular MF compared to the jerk of the 1 session. These findings can be correlated to the concept of Creative Empowerment [2] linked to the reward circuit. Nevertheless, from these initial results we cannot strongly assert that there is an activation of the rewarding circuit and adaptation related to the training of this DMI.

We have designed and run a pilot study with a technology that could be used as a creative instrument, and its usage depends on the adaptation of the subjects and the reward circuit experienced during the performance. A future experiment will follow with 21 subjects and a more stable environment.

References: [1] Feitosa JA et al., doi: 10.1109/NER.2019.8717143. [2] Partesotti E et al., doi:10.1080 /08098131.2018.1490919

A PIPELINE FOR COPY NUMBER VARIATION DETECTION USING SNP-ARRAY DATA

B. Henning[1,3], T. K. de Araujo[1,3], I. Lopes-Cendes[1,3], B. S. Carvalho[2,3]

[1] Department of Medical Genetics and Genomic Medicine, School of Medical Sciences; [2]Department of Statistics, Institute of Mathematics, Statistics and Scientific Computing; University of Campinas (UNICAMP); [3]Brazilian Institute of Neuroscience and Neurotechnology (BRAINN), Campinas, SP, Brazil.

Introduction: Genetic factors are believed to play a role in approximately 80% of patients with epilepsy [1,2]. Particularly, copy number variation (CNV) has contributed to elucidating the etiology in several cases [1]. CNVs are deletions or duplications of stretches of DNA that can be the cause of diseases or only normal genomic variation [3]. SNP-array is the platform of choice for CNV detection in the clinical setting [4]. Several algorithms to detect CNVs using SNP-array data are available, each one with its advantages and limitations. A common drawback is that highly sensitive algorithms also display a high number of false positive detection. Our main goal is to develop a pipeline for CNV detection using SNP-array data with lower false positive rate and yet higher sensitivity. Here we present preliminary results of a pipeline that combines three distinct statistical approaches for CNV detection, the parent-specific circular binary segmentation (PSCBS) [5], the penalized least square method from copynumber R package [6], and the Bayesian approach with expectation-maximization from the genome alteration detection analysis (GADA) [7]. **Materials and Methods:** We identified the CNVs from 741 subjects, 408 patients with mesial temporal lobe epilepsy (MTLEHS) or genetic generalized epilepsy (GGE) and 333 control subjects, using the Genome-Wide Human SNP Array 6.0 (Affymetrix). Our pipeline for CNV detection is based on four steps: 1) array normalization performed with the rawcopy algorithm [8]; 2) CNV segmentation performed by the three algorithms independently. 3) Algorithms intersection performed by finding the regions found as altered by the three algorithms; 4) CNV calling by defining the altered regions as duplications or deletions. We merged the CNVs identified among control subjects to define the set of CNVs found in healthy subjects, which we consider the effect may be less relevant as contributor to the etiology of epilepsy. Thus, we removed the set of CNVs on healthy subjects from the patients to obtain the case-exclusive CNVs. We filtered the case-exclusive CNVs by estimating the pathogenic impact of the CNVs to obtain the set of selected CNVs to be validated by quantitative polymerase chain reaction (qPCR) [9]. **Results and discussion:** The set of CNVs selected to be validated by qPCR included 13 CNVs and we validated all of them, a 100% of CNV validation rate. In comparison, a similar study followed the same steps of running an algorithm for CNV detection, filtering the predicted CNVs by pathogenicity, and validating the selected CNVs with qPCR [10]. They used the PennCNV algorithm, which is one of the most commonly used algorithms for CNV detection and they were able to validate 6 CNVs out of 49 selected for validation, which is equivalent to a 12% of validation rate. **Conclusion**: The pipeline developed by the combination of the PSCBS, GADA and copynumber algorithms is promising as a sensitive method for CNV detection with a low rate of false positives. Currently we are improving the CNV detection from the chromosomes X, and Y. As a future work, we aim to use the optimized version of this method as a tool for generating the ground truth data to test and validate methods for CNV detection using next-generation sequencing data.

References: [1] Myers CT and Mefford HC, doi: 10.1186/s13073-015-0214-7; [2] Hildebrand MS et al., doi:10.1136/ jmedgenet-2012-101448; [3] Olson H et al., doi:10.1002/ana.24178; [4] Zhang X et al., doi:10.1186/1471-2105-15-50; [5] Olshen et al., doi: 10.1093/bioinformatics/btr329; [6] Nilsen et al., doi: 10.1186/1471-2164-13-591; [7] Pique-Regi et al., doi: 10.1186/1471-2105-11-380; [8] Mayrhofer et al., doi: 10.1038/srep36158; [9] Kearney et al., doi: 10.1097/GIM.0b013e3182217a3a; [10] Mafra et al.,10.1007/s10815-016-0822-1

A PYTHON TOOL FOR THE AUTOMATIC TILLING OF MICROSCOPY IMAGES

J.B.C. Silva [1], P. M. Bartmeyer [2], L. Rittner [3], F.J. Von Zuben[1]

[1] LBiC, FEEC, UNICAMP , [2] Labore, FEEC, UNICAMP, [3] MICLab, FEEC, UNICAMP.

Introduction: Light microscopy and electron microscopy are used to image nerves in the brain and spinal cord. These techniques provide high magnification images by taking pictures of small pieces each time. In this way, the final image will be a composition of the individual images. The higher the magnification, the larger the number of individual images, and the higher the tilling process time. There are automatic tools for image tilling, such as ImageJ and PhotoShop. Photoshop can merge a large number of images, but since it has no scientific purpose, it creates distortion, resizing, and background filling. On the other hand, ImageJ[1] avoids these problems, but it can generate low-quality matches between the individual images(Fig. 1a). Therefore, some research groups choose to do this task manually which can take many hours. This work proposes an automatic image tilling process, reducing the runtime compared to manual processes and improving the tilling quality without adding any artifact to the composed image. **Materials and Methods:** The proposed tilling method uses the template matching technique [3] with template-based approach and with a cross correlation as similarity metric. It compares small regions of the image to be merged (templates) with the area of the current composed image. The program decides for the highest similarity region if the similarity metric satisfies a minimum threshold value. If the similarity value does not reach the threshold value, it composes a list to be analyzed later. The process ends when all images are added in the current composed image. The performance of the proposed tilling program is measured by visually comparing the matches between the final obtained composed image and the stitched image using ImageJ. **Results:** Experiments used 44 individual images, and the method merged 35 images correctly, and 9 images were excluded from the composition. Even though some images were blurred (Fig.1b - below), the limits of individual images are indistinguishable in a visual inspection (Fig.1c - highlighted in Fig.1d). The experiments were held in a AMD® Phenom(tm) ii x4 965

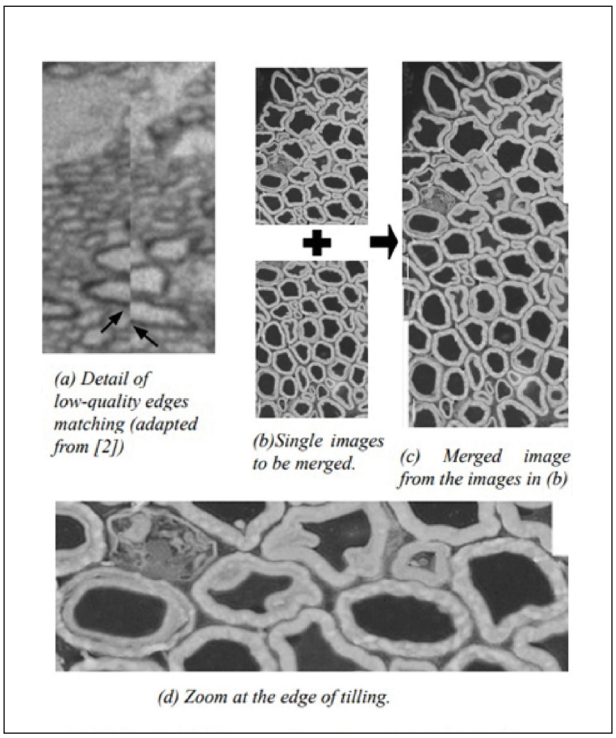

Figure 1. Sample of tilling image process and the detail of the adges matching.

processor × 4 with 16Gb of memory. **Discussion:** A visual inspection of the composed image shows perfect border matches. The method is also able to merge most of the images creating a high quality partial image. The images do not need to be sequential thus avoiding the necessity of a previous sorting of the images and reducing human intervention during the process. The run time is a great benefit of this method since the manual method takes an average of 3 hours and the proposed method takes 65,3 minutes in the same machine. **Conclusion:** The proposed technique does not require human intervention in the tilling process and improves the final image quality. It also contributes to other future analysis, such as cells border calculation, since the method

preserves the cells structures. A comparison with quantitative quality metrics of the proposed approach for light microscopy images is the next focus of the research. Finally, there is room for improvement on code efficiency, and therefore, on run time reduction.

References: [1] S. Preibisch et al., doi:10.1093/bioinformatics/btp184; [2] Available in https://osf.io/s8mfp/; [3] P. Swaroop et al., doi:10.5120/ijca2016912165

A WEARABLE DEVICE FOR VIRTUAL ENVIRONMENT CONTROL IN NEUROREHABILITATION THERAPY

M. M. Jurioli[1], B. C. S. M. Guedes [2,3], S. E. Ferreira-Melo[2,3], A. F. Brandao[3,4], C. F. M. Toledo[1]

[1]Instite of Mathematics and Computer Science, ICMC, USP; [2]School of Medical Sciences, FCM, UNICAMP, [3]Brazilian Institute of Neuroscience and Neurotechnology, BRAINN, UNICAMP; [4]Physics Institute Gleb Wataghim, IFGW, UNICAMP.

Introduction: Stroke is one of the leading causes of disability worldwide [1], in more than 80% of the cases, the patient presents some motor impairments [2]. Post-stroke's treatments using Virtual Reality (VR) with conventional physiotherapy can optimise the recovery process [3]. This study presents a preliminary result of a wearable device development to control a 3D environment, designed for use as a complementary therapy tool for rehabilitation. **Materials and Methods:** The equipment consists of a tracking device that can simulate the movement of the patient in the VR environment (emulated in a smartphone). The movement itself can be amplified in the simulated environment, in other words, a small range of motion (real life) can be translated in a bigger one (VR) if it's necessary for the rehabilitation treatment, and vice versa. The device developed hopes to simplify communication and usability. It presents an IMU (I) to track motion; a Bluetooth (III) to communicate with the smartphone, and a microcontroller (II) to process the inputs from the IMU. A jigsaw puzzle developed to validate the device (Figure 1(B)). There are several settings in the puzzle to help the therapist customise the difficulty for each patient, such as the sensibility (how the patient's movement control the VR environment). You can select the image from a menu, and the hitbox shows the precision for the patient to put the picture in the correct place. **Results:** A preliminary evaluation, with 13 healthy subjects, run to get the device's viability to control the VR software. The device, placed in the voluntary's forearm (Figure 1(A)), allows them to control

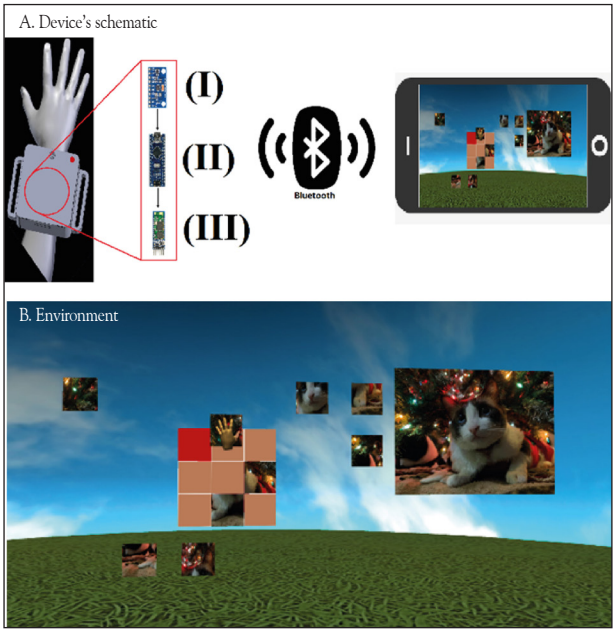

Figure 1. Hardware's and software's prototypes.

and complete a 3x3 jigsaw puzzle in the VR environment. In this test, 85% of the subjects affirmed that the device could control all functions in a 3D environment. **Discussion:** The test with healthy subjects concluded that the device presents a good way to control the virtual environment. This 3D environment's software needs to be evaluated by kinesiology experts to improve it for rehabilitation needs. The second phase of tests is to evaluate the system with post-stroke patients. This test includes the evaluation of the patient's recovery improvement and the therapist's evaluation of the software. **Conclusion:** The device can provide a helpful and easy way to control rehabilitation procedures involving virtual reality environments. It's a tracking device that provides the opportunity to develop all kinds of VR rehabilitation environments, for upper and lower limbs.

References: [1] https://www.who.int/healthinfo/global_burden_disease/en/; [2] Turolla A et all., doi: 10.1186/1743-0003-10-85; [3] McEwen et al., doi: 10.1161/STROKEAHA.114005362.

ACOUSTIC AND THERMAL FIELD SIMULATION FOR THE FOCUSED ULTRASOUND NEUROMODULATION TECHNIQUE

P. C. Andrade[1], E. T. Costa[2]

[1,2] Biomedical Engineering Dept, FEEC, UNICAMP.

Introduction: This study aims to simulate acoustic fields and volume rates of heat deposition generated by a focused ultrasound source used for neuromodulation technique. Ultrasound neuromodulation has been studied to modulate the Central and Peripheral Nervous Systems to treat different pathologies like Parkinson disease, Alzheimer, depression, essential tremor, obsessive compulsive disorder, chronic pain, anxiety disorders amongst others, acting on the neural stimulated region [1]. The success of the ultrasound neuromodulation technique depends on the accuracy of the ultrasonic focal point. However, transcranial focused ultrasound stimulation (tFUS) presents difficulties due to the huge ultrasound skull attenuation [2]. Thus, in order to prevent any damage to patients, we decided to begin with simulations of thermal field, generated by the absorption of mechanical waves across the various transcranial layers. We also simulated the ultrasonic waves (US) to verify the depth and spatial resolution of focused ultrasound field. It is expected that those difficulties of tFUS be overcome and that our results help to expand the knowledge of this technique. **Materials and Methods:** A 2D computational model was developed to evaluate thermal and acoustic pressure maps generated by tFUS through the human skull. A human MRI skull DICOM file from Calgary-Campinas Public Brain MR dataset was used to construct a computational ultrasound phantom. The brain characteristics, such as medium density, sound speed and attenuation coefficient, were set to be equal to water parameters at 37ºC. Other characteristics as density, thermal conductivity and specific heat values used for a cranial bone were set as showed in [3] and the acoustic parameters for the cranial bone were set as showed in [4]. The model used is a computer simulation of ultrasound propagation from an external transducer to a target in the deep brain, passing through superficial soft tissue and propagating through bone and brain tissue. We set transducers parameters as: 0.25 and 0.5 MHz center frequencies, 110 mm outer diameter, 44 mm inner diameter and 110 mm radius of curvature [5]. The stimulation pulse length was set as 10 ms, which is sufficient for US to achieve steady state. The simulations were performed using the open source k-Wave toolbox for MATLAB® [6]. **Results:** From the simulated 2D acoustic mapping for 250 and 500 kHz frequencies, it was possible to notice the acoustic wave attenuation provoked by the human skull. Higher frequencies provide much higher spatial resolution than lower frequencies. However, higher frequencies increase heat deposition. **Discussion/Conclusion**: In conclusion, we have shown that the selected parameters were sufficient to reach deep targets in human brain. Higher frequencies, such as 500 kHz, allow for higher spatial resolution, which is interesting for techniques such as brain mapping. On the other hand, higher frequencies are more absorbed by the skull and converted into heat, becoming a risk to the patient as compared to lower frequencies. Future studies intend to create a 3D mapping and perform longer time stimulation protocols in order to investigate the heat deposition rate.

References: [1] Fini, M *et al.*, doi: 10.1080/09540261.2017.1302924. [2] Robertson J. L. B et al., doi: 10.1121/1.4976339. [3] Legon, W *et al.*, doi: 10.1002/hbm.23981. [4] Nahirnyak, V et al., doi: 10.1016/j.ultrasmedbio.2007.02.005. [5] Pouliopoulos, A. N. *et al.* doi: 10.1016/j.ultrasmedbio.2019.09.010. [6] Treeby, B. E. *et al.*, doi: 10.1117/1.3360308.

AMYGDALA AND HIPPOCAMPAL T2 SIGNAL CHANGES IN TEMPORAL LOBE EPILEPSY ASSOCIATED WITH MAJOR DEPRESSIVE DISORDER

M. E. R. Barbosa[1,2], L. R. Pimentel-Silva[1], M. H. Nogueira[1], T. J. R Rezende[1], C. L. Yasuda[1], F. Cendes[1]

[1]University of Campinas, Campinas, SP [2]Pontifícia Universidade Católica de Campinas, Campinas, SP.

Introduction: Temporal lobe epilepsy (TLE) is the most common form of epilepsy in adults. This disease is frequently associated with psychiatric comor-

bidities and a higher risk of developing major depressive disorder (MDD) when compared to general population [1]. Studies suggest a bidirectional relationship between epilepsy and mood disorders, indicating possible pathogenic pathways shared by these diseases [2]. However, the mechanisms involved are not fully understood. As the amygdala and the hippocampus play an important role in psychiatric disorders and T2 signal changes might translate gliotic dysfunction in this region, we hypothesize that the measure of T2 signal in TLE and MDD may be useful to better understand possible mechanisms that lead to the coexistence of these diseases [3]. **Materials and Methods:** We included 60 individuals, namely: TLE-only (n=11), TLE-MDD (n=13), MDD-only (n=19) and controls (n=17). We obtained 3mm thick T2 coronal multi-echo images using a 3T MRI scanner (Philips Achieva). We processed relaxometry using Aftervoxel (http://www.bergo.eng.br/academic/aftervoxel/). Briefly, we manually quantified a hyperintense signal area in two slices for each amygdala and three slices for each hippocampus (head, body and tail) bilaterally, carefully avoiding regions of CSF and articfacts [4]. MDD was diagnosed based on the structured clinical interview for DSM-V. Ipsi- and contralateral T2 signal were evaluated using MANOVA and Tukey or Games-Howell post hoc tests. We set $p<0.05$ as significant. Statistical analyses were performed using SPSS v.24 (IBM, Armonk). **Results:** We found a significant difference between groups in the ipsilateral amygdala [$F(3,56)=16,70$, $p<0.001$] but not in the contralateral amygdala [$F(3,56)=2,44$, $p=0.73$]. For the hippocampus, the difference between groups was significant both in the ipsilateral [$F(3,56)=17,48$, $p<0,001$] and contralateral [$F(3,56)=8,48$, $p<0,001$] side. Post-hoc comparisons showed increased ipsilateral T2 signal in TLE-MDD ($p<0,001$) and TLE-only ($p=0,003$) compared to controls and in TLE-only compared to MDD ($p=0,019$) in the amygdala. We also found an ipsilateral increase in TLE-MDD compared to TLE-only ($p=0.031$) in the amygdala. However, it did not remain significant after multiple comparisons corrections. For the hippocampus, the T2 signal was increased in TLE-MDD ($p=0,002$) and TLE-only ($p=0,005$) compared to controls, and in TLE-only ($p=0,010$) and TLE-MDD ($p=0,004$) compared to MDD. **Discussion/Conclusion**: In conclusion, our data suggest that the comorbid association of TLE and MDD might influence T2 signal changes, restricted to the epileptogenic focus in the amygdala and being more diffuse for the hippocampal region. **Acknowledgements:** FAPESP #2019/08390-9.

References: [1] Harden, C. et al, doi:10.2165/00023210-200216050-00002; [2] Kanner AM. Dialogues Clin Neurosci 10(1): 39-45, 2008; [3] Briellmann RS et al, doi:10.1136/JNNP.2006.104521; [4] Kubota YK et al, doi:10.1016/j.yebeh.2015.04.001

AN IN-DEPTH LOOK AT CANDIDATE LOCI FOR MESIAL TEMPORAL LOBE EPILEPSY

P. H. M. Magalhães[1], E. M. Bruxel[1], M. C. P. Athie[1], Marina K.M. Alvim[2], R. Secolin[1], Clarissa L. Yasuda[2], F. Cendes[2], I. Lopes-Cendes[1]

1.Department of Medical Genetics and Genomic Medicine, 2. Department of Neurology; School of Medical Sciences, University of Campinas (UNICAMP), and the Brazilian Institute of Neuroscience and Neurotechnology (BRAINN), Campinas, SP, Brazil.

Introduction: Mesial temporal lobe epilepsy (MTLE) is the most common form of focal epilepsy in the adult population, and most patients are refractory to treatment with antiepileptic drugs. MTLE is a genetically complex disease for which the identification of predisposing genes is, for the most part, still elusive. Recent genomic association studies discovered a few genomic regions that could harbor genetic variants that predispose to MTLE. Among these, there is the locus on the chromosome (ch) 2q24.3. Multiple association studies detected signs indicating association at this locus [1,2,3]. Interestingly, the *SCN1A* gene is in this same location, and mutations in *SCN1A* have been extensively associated with monogenic forms of epilepsy, especially in the developmental encephalopathies. In addition, this same chromosomal location harbors interesting candidates, such as those that encode other ion channel subunits, which could also be involved in the predisposition to MTLE. Moreover, two other loci were previously linked to MTLE in a recent genome-wide association study: 3q25.31 and 6q22.31 [3]. It has been recognized that the genetic architecture of the population can influence genetic variants for complex disorders. Thus, patients from different populations may have different combinations of predisposing variants. Therefore, this project aims to look deeper into these candidate loci in patients with MTLE using association analysis combined with the re-sequencing of the candidate region(s) identified in our cohort of patients. **Materials and Methods:** Genome-Wide Human SNP Array 6.0 (Thermo Fisher, Waltham, Massachusetts, United States) was used to obtain SNP-array data from our cohort to better define the candidate regions for subsequent target re-sequencing. For this study, we analyzed only the SNPs located within the three candidate regions previously determined and located on chs 2q24.3, 3q25.31 and 6q22.31. The p values obtained in the association analysis were adjusted for multiple comparisons. After that, MiSeq target Next-Generation Sequencing (Illumina, San Diego, California, United States) will be used for sequencing the candidate regions identified in the target association study. Data will be aligned using the Burrows-Wheeler Aligner algorithm. Variants will be detected by the Genome Analysis Toolkit and identified using the Variant Effect Predictor software. **Results:** The local association test performed in 472 patients and 415 controls identify a significant association at the locus on ch 2q24.3 ($p=0,03301$). However, results on the two other candidate loci were less clear with suggestive signals but not reaching statistical significance. **Conclusion:** We were able to find a significant genetic association on ch 2q24.3 in our cohort of patients with MTLE. In addition, we achieved a fine genetic mapping of the candidate region, which can be now sequenced to identify putative causative variants predisposing to MTLE; thus, contributing to the ongoing worldwide collaborative studies to unravel the genetics of the complex epilepsies. **Supported by:** CAPES; FAPESP.

References: [1] Anney RJL et al., doi: 10.1016/S1474-4422(14)70171-1; [2] Kasperavičiute, D et al., doi: 10.1093/brain/awt233 [3] International League Against Epilepsy Consortium on Complex Epilepsies, DOI: 10.1038/s41467-018-07524-z

ANALYSIS OF CANDIDATE SNPS IN PATIENTS WITH GENETIC GENERALIZED EPILEPSY

F. S. Kaibara[1], I. L. Cendes[2], R. Secolin[3]

[1] Genetics Dept., FCM, UNICAMP, [2]Genetics Dept., FCM, UNICAMP, [3]Genetics Dept., FCM, UNICAMP.

Introduction: Genetic Generalized epilepsy (GGE) is the most common type of generalized epilepsy, whose main characteristic is the occurrence of recurrent seizures with no specific region of origin in the brain. In addition, the seizure spreads rapidly along both brain hemispheres [1]. Evidence of genetic factors has been extensively reported in patients with GGE. In this context, GWASs have identified 52 genetic variants that predispose to GGE, which are generally located in genes encoding ionic channels and synaptic vesicles. However, these reported studies were based mostly on European and Chinese populations, and the GWAS results could not be transferable to admixed American populations. Therefore, the present study aims to assess the existence of an association between the 52 candidate SNPs and the disease phenotype in Brazilian patients with GGE. **Materials and Methods:** We used data from SNP-array genotypes of 427 individuals, including 87 patients with GGE and 340 controls. Among the 52 candidate variants identified for GGE in the literature, we found 17 in the SNP-array dataset. In order to assess the statistical power to detect genetic association between the SNPs and GGE, we estimated the statistical power and effect size by the G*POWER v.3.1.9.2 software, according to the following parameters: logistic regression; two-tail; probability of alpha error $p=0.003$ (adjusted for 17 multiple tests); statistical power=0.8; sample total size=427; other parameters default. The results of the statistical power show that the sample has 80% of chance of detecting a genetic association with effect size, estimated by odds ratio, lower than 0.64 (protection against the disease) or higher than 1.56 (increased susceptibility to the disease). **Results:**. All 17 candidate SNPs presented allelic frequencies higher than 0.01 in Brazilian control individuals. However, four SNPs were not in Hardy-Weinberg equilibrium, therefore not suitable for further analysis, since they might present spurious results because of biased genotypic distribution due to evolutional processes rather than the association itself. According to the logistic regression analysis, one SNP showed evidence of association with GGE (rs9788, nominal $p=0.03663$ (OR=1.44; IC95%=1.02 - 2.08). However, the result did not hold after Bonferroni's correction for multiple tests (corrected $p=0.6226$). Interestingly, the SNP rs1046276 also showed evidence of association, even after the correction for multiple tests (nominal $p=0.00039$; corrected $p=0.00536$; OR=0.42; IC95%=0.36 - 0.75). However, this last SNP is not in Hardy-Weinberg equilibrium, and it is not possible to determine if the difference in the genotypic distribution is due to a real association or just a result of the evolutionary processes and population demography. **Discussion/**

Conclusion: The assessment of the 17 candidate SNPs available in the SNP-array did not show evidence for association in Brazilian patients with GGE. Since these SNPs were previously related to GGE in other populations, we suggest that the genetic structure of the Brazilian patients with GGE could be different in comparison with European and Chinese patients. Our results strengthen the hypothesis of non-transferability of GWAS results from one population to another. However, even though we presented enough statistical power to detect association using the Brazilian cohort, a larger sample size would be desirable to better access SNPs rs9788 and rs1046276. It was also important to point it out that there are other 35 candidate SNPs which were not available in the SNP-array dataset. Therefore, the next step of this project will be the imputation of these 35 SNPs from the SNP-array dataset, which is a computational and statistical process that identifies SNPs stemming from a different source of genome data, according to parameters as linkage disequilibrium.

References: [1] Berg AT, Berkovic SF, Brodie MJ, Buchhalter J, Cross JH, Van Emde Boas W, et al. Revised terminology and concepts for organization of seizures and epilepsies: Report of the ILAE Commission on Classification and Terminology, 2005-2009. Epilepsia. 2010;51(4):676-85.

ANALYSIS OF CONTACT SITES AND MORPHOLOGY OF MITOCHONDRIA AND ER IN A CELLULAR MODEL OF PARKINSON'S DISEASE

I. Geacomini[1], R. Raeisossadati[1], M. F. R. Ferrari[1]

[1] Neurodegeneration Cell Biology Laboratory, IB, University of São Paulo.

Introduction and Hypothesis: Parkinson's disease (PD) is the second most prevalent neurodegenerative disorder [1, 2]. Besides the degeneration of the dopaminergic neurons in the substantia nigra [2], the presence of Lewy bodies, and microgliosis is the hallmark of the disease [3]. Emerging data have been shown that the α-synuclein has an influence on neuronal mitochondrial dynamics[4], and direct interaction with the mitochondrial outer membrane, which interfere the mitochondrial fusion and fission [5]. Overexpression of the α-synuclein can also impair the endoplasmic reticulum function via ER stress[6]. Recently, it has been shown that α-synuclein can interact directly with mitochondria-associated endoplasmic reticulum membranes (MAMs) [7]. In this study we aim to evaluate how different α-synuclein mutations (A30p, A53T, WT) can alter the MAMs in the dopaminergic differentiated cells from SH-SY5Y cell line. **Objective:** We aim to evaluate the morphology of mitochondria and endoplasmic reticulum in the presence of different *SNCA* mutations, also investigate the mitochondria - ER contact site differences. **Materials and Methods:** The SH-SY5Y cell will be transduced and differentiated into dopaminergic neurons. The morphology of the mitochondria and ER will be evaluated with the mito-tracker and ER-tracker. The differentiated cells will be co-transfected with Mito-dsRed and Sce61-GFP plasmids, and Split-GFP (figure1) to investigate how different *SNCA* mutations can influence on the contact site. **Relevance:** Different cell lines, and human postmortem brain samples, were utilized to investigate the role of MAMs in the different cellular processes [7-9]. Further studies are necessary to understand how *SNCA* mutations can alter the MAMs in human dopaminergic neurons.

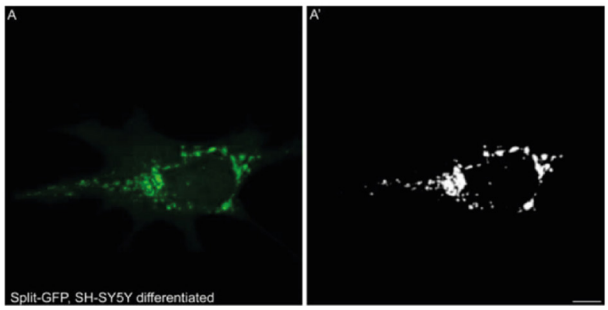

Figure 1. Visualization of ER-mitochondria contact site with Split-GFP. (A, A') The green signal demonstrates the contact site in the SH-SY5Y-derived neurons. Scale 15 μm.

References: [1] Dorsey ER et al., doi: 10.1212 / 01.wnl.0000247740.47667.03, **[2]** Wirdefeldt K et al., doi: 10.1007 / s10654-011-9581-6, **[3]** Dexter DT et al., doi: 10.1016 / j.freeradbiomed.2013.01.018, **[4]** Pozo Devoto VM et al., doi: 10.1242/dmm.026294, **[5]** Nakamura K et al., doi: 10.1074 / jbc.M110.213538, **[6]** Colla E, doi: 10.3389/fnins.2019.00560, **[7]** Guardia-Laguarta C et al., doi: 10.1523/JNEUROSCI.2507-13.2014, **[8]** Guardia-Laguarta C et al., doi: 10.1002/mds.26239 e **[9]** Calì T et al., doi: 10.1016 / j.bbadis.2013.01.004

ANALYSIS OF TISSUE EXPRESSION OF GLIAL MARKERS IN WHITE MATTER OF THE TEMPORAL ANTERIOR POLE AND PARAHIPPOCAMPAL GYRUS OF PATIENTS WITH HIPPOCAMPAL SCLEROSIS

Vítor Henri Baldim[1], Bruna Cunha Zaidan[1], Marina Koutsodontis Machado Alvim[2], Enrico Ghizoni[2], Helder Tedeschi[2], Fernando Cendes[2], Fabio Rogerio[1]

[1] Pathology, FCM, UNICAMP, [2] Neurology, FCM, UNICAMP.

Introduction and Hypothesis: Epilepsy is the most common neurological disease. Epileptic seizures consist of sudden transient episodes of abnormal electrical activity in groups of neurons of a given region that may spread throughout the cortex [1]. In neuroimaging studies, it is possible to observe white matter changes in patients with temporal lobe epilepsy (TLE) associated with hippocampal sclerosis (HS). Previous studies, emphasizing comparisons between patients with refractory TLE, report tissue alterations as demyelination (reversible myelination decrease) in this topography [2]. The present study aims to verify a possible difference regarding the tissue expression of glial markers in the white matter of the anterior pole of the temporal lobe and the parahypocampal gyrus of pacientes with HS compared with specimens from individuals submitted to necropsy without history of neurological disease. **Objective:** To study histopathological alterations of the white matter of brain specimens from patients who undergone surgery to treat TLE associated with HS. Particularly, it will be described microscopic findings detected by means of special staining and/or immunohistochemistry related to oligodendrocyte, atrocytic and microglial populations. **Materials and Methods:** Analysis of histological sections of specimens from individuals subjected to surgery due to refractory TLE and HS (n = 15) and specimens from individuals submitted to necropsy without history of neurological disease (controls; n = 10) will be made by means of immunohistochemical staining for CNPase, GFAP and Iba-1 for oligodendrocyte, astrocyte and microglial populations, respectively. Additionally, myelin integrity will also be assessed by using Luxol Fast Blue special staining. Photodocumentation of microscopic fields (40x) from the superficial (within 500 μm from the gray/white matter boundary (GWMB)) and the deep white matter (500 μm from the gray/white matter boundary (GWMB)) will be followed by digital analysis with the ImageJ® software (treshold methodology). **Relevance:** The present study focus on comparing histological findings from epilepsy patients and individuals without previous history of any neurological disease. Such study design is original and may provide future histological and/or neuroimaging investigations with data to better differentiate pathological features associated with epilepsy.

References: [1] Steinhauser, C. et al; Neuroscience, 323: 157–169, 2016. [2] Eijsden, P.V. et al. Epilepsia, 52(4): 841–845, 2011.

ASSESSMENT OF BLOOD–BRAIN BARRIER PERMEABILITY AND MICROVASCULAR CHANGES TO DIFFERENTIATE PSEUDO AND TRUE PROGRESSION IN PATIENTS WITH GLIOBLASTOMA

W.S. Loos[1,2], L.B. Andersen[1,2], R.J. Sevick[1,2], R.M. Lebel[1-3], and R. Frayne[1,2]

[1]Departments of Radiology and Clinical Neuroscience, Hotchkiss Brain Institute, University of Calgary. [2]Seaman Family MR Research Centre, Foothills Medical Centre, and [3]General Electric Healthcare, Calgary, AB, Canada.

Introduction and Hypothesis: One outcome of the glioblastoma (GBM) therapy is pseudoprogression (PP), a condition that mimics tumor progression (TP) on magnetic resonance (MR) images immediately after treatment [1]. PP results from short-lasting (a few months) brain changes caused by surgery, chemotherapy and/or radiation therapy. The accurate separation of PP and TP is important because patients with TP can require a change in their treatment. Histologically, changes to blood–brain barrier (BBB) permeability and microvascular proliferation are associated with TP. PP tends to only have changes in permeability. Dynamic contrast-enhanced MR (DCE-MR) imaging is a method for interrogating the microcirculation and BBB status [2]. We have implemented a technique to acquire DCE-MR images with high temporal and spatial resolution, allowing us to estimate high-resolution, quantitative permeability and microvascular proliferation maps [3]. We hypothesized that permeability and microvascular proliferation maps can differentiate TP from PP. **Objective:** The objective of this study is to evaluate if high resolution quantitative permeability and microvascular proliferation maps can help differentiating TP from PP. **Materials and Methods:** Forty-three (43) patients with histopathologically confirmed glioblastoma were included in this study and received at least 2 MR exams about every 2 months. A total of 165 scans were acquired on a 3-T

scanner (Discovery MR750; General Electric). DCE-MR images acquired a time series of T1-weighted images before, during and after the arrival of an injected contrast agent in the brain. A sparsely sampled acquisition technique was used [3] and images were reconstructed with high temporal (~5s) and spatial resolution (<2 mm^3). The relationship between the observed image contrast and the underlying brain physiology was described by pharmacokinetic models. Modelling requires the vascular input function (VIF) and the relaxation time of the brain tissue (T1 map). The VIF was measured in the transverse sinus and the T1 map was computed using the variable flip angle method. The Patlak pharmacokinetic model [4] was used to describe the leakage rate of the contrast to the extravascular extracellular space (K^{trans}) and the blood plasma volume tissue (v_p). Figure 1 shows example K^{trans} and v_p maps in a patient 4 months after tumour resection. Due to the BBB disruption leakage of the constrast into the extravascular extracellular space (increased K^{trans}) and neoangiogenesis (increased v_p) is observed. After we complete reconstructing the datasets and generating K^{trans} and v_p maps, our next step will consist of determining if there is a statistical significant difference between K^{trans} and v_p in patients with TP and PP. **Relevance:** Early differentiation of TP and PP can provide better treatment management in patients with glioblastoma [1]. Conventional MR imaging does not allow differentiation of TP and PP. The analysis of the BBB integrity and microvascular changes may be useful in making this distinction.

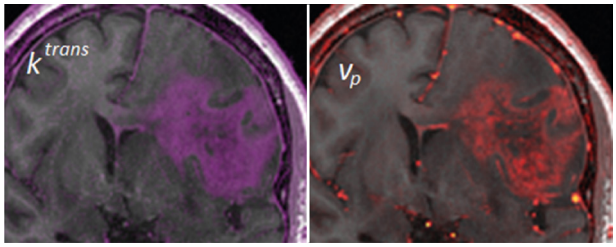

Figure 1. Ktrans and vp maps on T1-weighted image, showing vessel leakage (left) and microvascular changes (right) expected from tumor growth. Patient was imaged 4 months post-surgery.

References: [1] Radbruch A, *et al.*, *Neuro-Oncology 2015;* **17**: 151-159 https://doi.org/10.1093/neuonc/nou129. [2] Eilaghi A, *et al.* Biomark Cancer 2016; **8**: 47-59. https://doi.org/10.4137/BIC.S31801. [3] Lebel RM *et al.*, *Magn Reson Med* 2014; **71**: 635-44. https://doi.org/10.1002/mrm.24710. [4] Patlak CS, *et al. J Cereb Blood Flow Metab* 1983; **3**: 1-7. https://doi.org/10.1038/jcbfm.1983.1.

AUTOMATED MRI LABELING USING MACHINE LEARNING

L.Rodrigues[1], A.Lopes[2], B. Campos[3], B.Sgambato[4], D.Silva[5], D.Carmo[1], I.Fantini[1], M.Bento[6], M.Salluzzi[6], R.Souza[6], W.Loos[6], R.Frayne[6], L.Rittner[1]

[1]MicLab - School of Electrical and Computer Engineering (FEEC), Unicamp, Brazil [2]Semantix - Campinas, Brazil [3]Neuroimage Lab, School of Medical Sciences (FCM), Unicamp, Brazil [4]Institute of Physics Gleb Wataghin, Unicamp, Brazil [5]FEEC, Unicamp, Brazil [6]Hotchkiss Brain Institute, University of Calgary.

Introduction: With the increase of medical imaging acquisitions, sites that curate them are receiving a large number of images. The data quality assessment still has many steps performed manually, which is time-consuming and fatiguing. One of these tasks is to check if the image is correctly labeled, where sometimes human mistakes happen. In this work we aim to develop one or more models to perform 6 classification tasks: 1. exam modality (MRI or CT); 2. MRI images (T1, T2, T2*, FLAIR, DWI); 3. CT Angiography images (Non-Contrast - NCCT or contrast -CTA); 4. MRI vendor (GE, Siemens, Philips); 5. CT vendor (GE, Siemens, Philips or Toshiba) and 6. MRI plane (sagittal, coronal, axial). **Materials and Methods:** The dataset is comprised of 717 stroke patients. There are 563 MR exams (22876 images) of 1.5 and 3T and 164 CT exams (23411 images). All data were saved in Nifti format. There are some patients with more than one exam. We have three different vendors for MRI and four for CT. at first, we established a baseline using a support vector machine (SVM) with histogram of gradients (HOG) for all the tasks. Using convolutional neural networks (CNNs) we tried three different approaches: 1. One Shot Multilabel Approach – using one EfficientNet[1] to solve all the tasks at one shot; 2. Divided Multilabel Approach – Resnet50[2], to solve only MRI tasks; 3. Individual trained CNNs – Multiple Resnet50, each one responsible for one single task. **Results/Discussion:** To assess our results, we are using accuracy as metric. Due to dataset unbalancing, we used stratified hold out for data division. Finally, we had 60% of the dataset for training, 20% for validation and 20% for testing. Our results (Tab 1) showed that CNN overcomes traditional SVM in almost every problem. When comparing single shot solutions with individual solutions, it is clear that the later gets better results. **Conclusion**: When dealing with deep learning, the way we input the data can significantly change the final result. For instance, to solve MRI vendor task, it would be better to analyze small patches of the image, including the background, looking for the scanner noise. On the other hand, neither the image background nor small patches helped classifying the MRI plane. Therefore, despite the fact that single shot networks usually bring more information about the data, they seem not to be helpful when tasks are very distinct.

Tabela 1. Accuracy results for baseline and three approaches on the test set.

	Baseline	Individual CNNs	Divided Multilabel	One Shot Multilabel
MRI x CT	0.992	-	-	0.846
CTA x NCCT	0.838	0.824	-	0.877
CT Vendor	0.560	0.911	-	0.740
MRI Vendor	0.405	0.755	0.750	0.740
MRI Sequence	0.564	0.930	0.667	0.830
MRI Plane	0.878	-	0.925	0.902

References: [1] Tan et al., arXiv:1905.11946, [2] He et al, arXiv:1512.03385

AUTOMATIC CORPUS CALLOSUM SEGMENTATION AND PARCELLATION IN DTI: A TOOL FOR VISUALIZATION AND COMPARISON OF RESULTS FROM DIFFERENT METHODS

Thais Caldeira[1], William G Herrera[1], Aline T Lapa[2], Simone Appenzeller[2], Letícia Rittner[1]

[1]Medical Imaging Computing Laboratory, FEEC, UNICAMP – [2]Rheumatology Department, FCM, UNICAMP.

Introduction and Hypothesis: The corpus callosum (CC) is the largest white matter structure in the human brain [1]. Due to its highly organized fibers, analysis with diffusion tensor imaging (DTI) has provided new relevant information about the CC [2]. Most CC studies on DTI are concerned with diffusion measures alongside the structure, which requires its segmentation – determination of its limits – and parcellation – division of the structure in different parts, accordingly with the cortical regions with which they are interconnected. The four most common diffusion measures are: fractional anisotropy (FA), and mean, axial and radial diffusivity (MD, AD, RD). Recent access to larger datasets has required use of fully automated methods for those tasks, which are available for CC studies on DTI, but are often non-generalizable and not robust. In order to allow researchers to perform CC analysis on DTI with confidence, especially when working with large datasets, we implemented the most reputable methods of automated segmentation and parcellation, proposing different quality measurements in a comprehensive graphical user interface that will not only perform the analysis, but allow quality assessment and data exploration. **Materials and Methods:** Three DTI-based segmentation algorithms were implemented: (a) ROQS [3], (b) Watershed [4], and (c) STAPLE [5]. For the parcellation, the implemented algorithms were: (a) Witelson [6], (b) Hofer & Frahm [7], (c) Chao [8]. and (d) Cover [9]. Quality assessment for segmentation is performed in two stages: in the first we detect possible mis-segmentations using the obtained CC shapes and a pretrained support vector machine [10] and by detecting outliers with respect to FA mean. In the second stage the user must evaluate if the detected mis-segmentations are truly errors and can remove them of the analyzed dataset. Furthermore, the developed software allows data exploration for a single individual, a population or comparing populations. **Results:** A first prototype was developed using Python over the Kivy Framework. A dataset containing 176 DTI acquisitions from healthy subjects were used to explore the implemented functionalities. Quality checks were sensitive to segmentation errors and atypical CCs, which were promptly selected and removed. Alongside, visualization techniques allowed data exploration in populational analysis that can, when needed, be thoroughly check in individual analysis (Figure 1). **Discussion/Conclusion:** This work proposes a comprehensive software that allows use of automated methods for segmentation and parcellation of the corpus callosum while mitigating possible errors, especially when analyzing large datasets. It also implements a practical

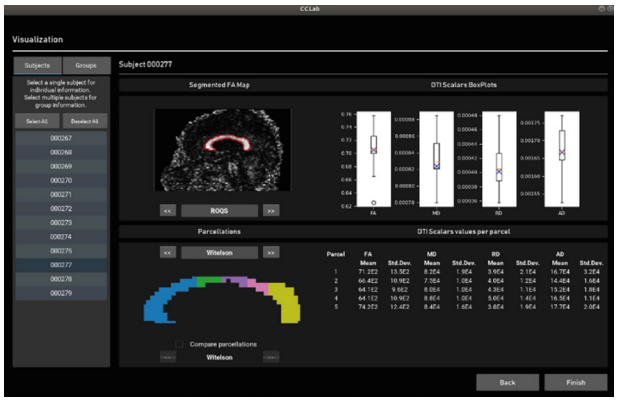

Figure 1. Screen for visualization and data exploration.

form of obtaining and exploring most of information used in DTI studies of the CC, including analysis of possible abnormalities of diffusivity in specific regions or parcels of the structure.

References: [1] Aboitiz F et al., doi:10.1590/S0100-879X2003000400002 [2] Basser P et al., doi:10.1016/j.jmr.2011.09.022 [3] Niogi S et al., oi:10.1016/j.neuroimage.2006.10.040 [4] Rittner L et al. doi:10.1109/sibgrapi.2008.17 [5] Warfield S et al., doi:10.1109/tmi.2004.828354 [6] Witelson S et al., doi:10.1093/brain/112.3.799 [7] Hofer S, doi:10.1016/j.neuroimage.2006.05.044 [8] Chao Y et al., doi:10.1002/hbm.20739 [9] Cover G et al., doi:10.1109/access.2017.2761701 [10] Herrera W et al., doi:10.1007/978-981-13-2517-5_22

BCI BASED ON SSVEP IMPLEMENTED ON RASPBERRY PI

V. M. Barbosa[1], S. N. Carvalho[1,2], H. M. A. Leite[1,2]

[1]Federal University of Ouro Preto (UFOP), Brazil. [2]Brazilian Institute of Neuroscience and Neurotechnology (BRAINN), Brazil.

Introduction: Brain-Computer Interface (BCI) is a system that converts brain signals into application commands [1]. This paper reports the development of an BCI based on Steady State Visual Evoked Potential (SSVEP) on Raspberry Pi using the open-source EEG platform OpenBCI. The solution reported is low cost and easily embeddable in different applications. **Materials and Methods:** In this study we have used the brain signals acquired from one health volunteer. The brain activity was registered at 250 Hz by electroencephalography (EEG) using 8 dry electrodes placed on: O1, Oz, O2, PO3, POz, PO4, Pz e Cz. The volunteer was exposed to four stimuli blinked on a monitor at frequencies: 6, 10, 12 and 15 Hz. The database was composed of 32 trials of 12 s, being 8 replicates of each stimulus. The signal processing was performed in three stages: preprocessing, feature extraction and classification. In the preprocessing, the signal was windowed in 3 s and filtered by Common Average Reference (CAR), in order to eliminate noises and artifacts. The feature extraction was operated by Fast Fourier Transform (FFT) considering the magnitude of spectrum evaluated at visual stimuli frequencies. The classification was operated by a least squares linear discriminant analysis. The accuracy of the offline system was evaluated considering 21.875% of the data and the remained 78.125% was used to train the classifier. For the online system, the classifier was trained with the all 32 trials and evaluated with data collected at run time. **Results:** Table 1 shows the online and offline BCI performance for each frequency. **Discussion/Conclusion**: The implementation of the digital signal processing module of a BCI-SSVEP in Python language, using Raspberry PI and OpenBCI platform was concluded with success. The results show a satisfactory accuracy for offline and online systems. The advantage of using Raspberry PI and OpenBCI is the mobility, low cost and open source platform. As future work, we plan to incorporate more signal processing techniques to increase the hit rates and expand the analysis database. **Acknowledgements:** The authors thank CNPq, Fapesp and UFOP for the financial support.

Table 1. BCI system performance.

	Accuracy (%)				
BCI	6 Hz	10 Hz	12 Hz	15 Hz	MEAN ± STD
Offline	49.99	77.22	50.00	69.44	61.66 ± 14.44
Online	60.00	50.00	60.00	50.00	55.00 ± 5.77

Reference: [1] WOLPAW, Jonathan R. et al. Brain-computer interface technology: a review of the first international meeting. IEEE transactions on rehabilitation engineering, v. 8, n. 2, p. 164-173, 2000.

BIOCHEMICAL ASPECTS AND IDENTIFICATION OF BIOMARKERS TO PREDICTING ANTIDEPRESSANTS RESPONSE

P. T. Carlson[1], L. C. Silva-Costa[1], J. Steiner[2], D. Martins-de-Souza[1]

[1]Laboratory of Neuroproteomics, Biochemistry and Tissue Biology Dept., Institute of Biology, UNICAMP. [2]Department of Psychiatry, University of Magdeburg, Germany.

Introduction and Hypothesis: Major depressive disorder (MDD) is a multifactorial psychiatric disorder which has potentially debilitating consequences and is one of the main causes of suicide worldwide. Up to 30% of the patients respond poorly to antidepressants treatment, and present adverse reactions, exhibiting treatment resistant symptoms as well as difficulties in social and occupational function, decline in physical health and suicidal thoughts [1]. The biochemical changes promoted by antidepressants that may induce an adequate response are not yet well known. Therefore, considering the potential of blood plasma to exhibit drug-induced changes, the analysis of blood plasma from patients with different responses to treatment may help elucidate those biological mechanisms. **Objective:** We aim to propose a panel of proteins that could aid in the prediction of treatment response. Additionally, we will also investigate affected biochemical pathways through blood plasma proteins, enabling us to better elucidate the mechanisms through which antidepressants act. **Materials and Methods:** Blood plasma samples of 10 MDD patients, 5 good responders (GR) and 5 poor responders (PR), were collected from the psychiatric clinic of the University of Magdeburg both prior to starting treatment (T0) and 6 weeks into treatment (T6). The patients were matched for age, gender and smoking habits. The patients considered GR were those whose score on the Hamilton Rating Scale for Depression (HRSD) [2], used to clinically diagnose MDD patients, decreased in over 50%, 6 weeks into treatment. The samples first had their 14 most abundant proteins depleted by immunoaffinity chromatography using a MARS-14 column [3]. After being depleted, the low abundant fraction samples were then digested with trypsin. Finally, the digested samples will be separated by nano liquid chromatography and analyzed by mass spectrometry using a state-of-the-art bottom-up shotgun methodology, run in data independent acquisition mode. Generated data will be processed by Progenesis QI for Proteomics 4.0 and the results analyzed *in silico* through open access algorithms. **Relevance:** MDD is diagnosed by clinical interviews and there are no current methods to predict response to treatment, and those who are poor responders must follow other strategies as a dosage augmentation, change of medication type and even combinations of antidepressants [1]. Taking that into account, finding a potential protein signature that could work as response predictors could help psychiatrists to better adapt the treatment prescribed in order to avoid the patient going through diverse changes in medication in the attempt of getting better. Aside from that, a better knowledge of the biochemical pathways associated to MDD medication can potentially aid in the development of more effective antidepressants.

References: [1] Al-Harbi KS et al., doi: 10.2147/MDER.S33198; [2] Hamilton M., doi:10.1007/978-3-642-70486-4_14; [3] Garcia S., et al., doi: 10.1007/978-3-319-52479-5_15

BSN WEARABLE DEVICE AS GESTURE CONTROL OF E-STREET VIRTUAL REALITY SOFTWARE FOR NEUROREHABILITATION THERAPIES

D. R. C. Dias[1,3], S. T. M. Reis[1], B. C. S. G. Martins[2], L. L. Min[2], A. F. Brandão[3], G. Castellano[3]

[1]Computer Dept, UFSJ, [2]School of Medical Sciences, FCM, UNICAMP, [3]Neurophysics Group, IFGW, UNICAMP.

Introduction: The objective of this project is to facilitate the development of virtual applications aimed at the motor and cognitive rehabilitation. This work proposes to create a Unity game engine asset that manages the main functionalities of a cutting-edge device for body tracking, aiming to contribute to the popularization of a low-cost wearable device. Such a device is named Biomechanics Sensor Node (BSN), composed of a gyroscope, an accelerometer, and a compass, responsible for recording the user's movements. These records are transferred from the BSN to the Unity [1] via Bluetooth Low Energy (BLE), the protocol used in communication. **Materials and Methods:** In the first phase, we carried out a study regarding the BSN tracking device to know all its functionalities and organize the manipulation functions. In the second phase of the work, we developed the communication module, the fusion of the BSN sensors, and packaging the implemented functions. Finally, we used the BSN as an interaction device to the e-Street environment - this application exemplified

the entire process of communication of the smartphone with the BSN using the BLE communication protocol. **Results:** The result of this work was an interaction solution for virtual environments developed using the Unity game engine. For validation purposes, the BSN was used to control the e-Street [2] application - an urban virtual environment for performing space navigation in a 3D city. The scientific bias of the work was to use this combination to help the rehabilitation process of patients with several pathologies, such as, people who suffered a stroke. We used the BSN as an interaction device by tracking the lower limbs (stationary gait) and applying it as an input to the system. To perform the step used by the e-Street application, we captured the information from the Euler angles and the gravity vector. We considered as steps X-values less than or equal to 5 degrees (Euler angles), and Y-values with a variation of 3 units, between -1.5 and 1.5 (gravity vector). **Discussion/Conclusion**: Other studies [3,4] present technological solutions of gesture interaction with higher development cost, also with the purpose of application in rehabilitation therapies. The results obtained demonstrated the effectiveness of communication with the BSN and the potential of the device to be used in the development of various applications aimed at motor and cognitive rehabilitation. The next steps in this research will be patient testing and assessment of the learning curve by the user, therapist impressions (kinesiology specialist), and clinical evaluation of actual functional gain and transfer to everyday tasks.

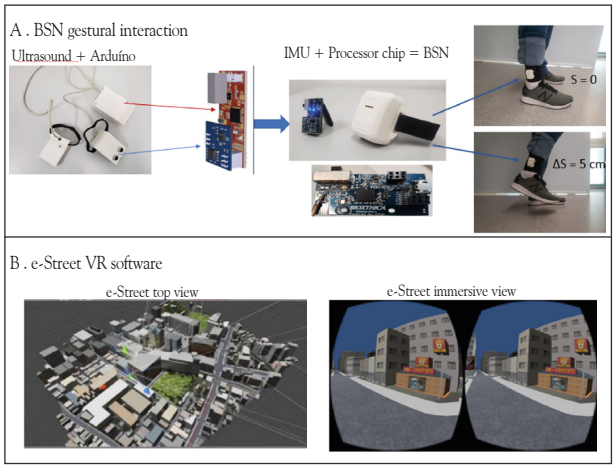

Figure 1. BSN integration with e-Street.

References: [1] Unity https://unity.com/; [2] Brandão A. et al. (2019), BTSym 2017 1(1), 1-8. Springer Cham, DOI https://doi.org/10.1007/978-3-319-93112-8_25; [3] Sveistrup H. (2004), J. Neuroeng. Rehabil. 1(1), 10, 1-8; [4] Fung J. et al (2006), CyberPsychol. Behav. 9(2), 157-162.

CANNABIDIOL(CBD) EFFECTS ON MICE HIPPOCAMPAL GENE EXPRESSION

J. P. D. Machado[1], V. Almeida[2], A. S. Vieira[1]

[1]Laboratory of Electrophysiology, Neurobiology and Behaviour, Dept. Functional and Structural Biology, Institute of Biology, UNICAMP. [2]Laboratory of Neuroproteomics, Dept. Biochemistry and Tissue Biology, Institute of Biology, UNICAMP.

Introduction and Hypothesis: Cannabidiol (CBD) is one of hundreds cannabinoids presents in cannabis plants. CBD interacts indirectly with the endocannabinoid system and also modulates several non-endocannabinoid signaling systems. Thus, this molecule has already been explored as a therapeutic strategy showing neuroprotective, anticonvulsant, and antiepileptic effects under various conditions, both in animal models and in humans. In this study, we will elucidate the gene expression changes produced by CBD treatment in different hippocampus subregions, one of the most studied brain areas, also injured in many diseases. **Objective:** To explore the CBD effect on the transcriptome of different hippocampal subregions, we will sequence and quantify messenger RNAs from the ventral and dorsal hippocampal regions (CA1, CA2, CA3, GD layers) after intraperitoneal administration of CBD for 1 or 7 days and will compare to their controls. After this, we will analyze how much and which genes are differentially expressed and how they may enhance or impair biological process and pathways when compared to control animals. **Materials and Methods:** Adult mice will be separated into three experimental groups: Control (saline) (n=5), one day treatment with CBD (100 mg/kg, 1 dose) and seven days treatment with CBD (100 mg/kg, 1 dose per day for 7 days). Animals will be euthanized 24h after the last administration and their brains processed for laser microdissection using Zeiss PALM LCM. All layers will be bilaterally collected from dorsal and ventral hippocampus of each animal, total RNA will be extracted for each layer and libraries preparation for RNA-Seq in Illumina Hiseq platform. Sequences will be aligned, quantified and compared with the STAR Aligner/DESeq2 pipeline. Gene Ontologies will be analyzed with the Enrichr, STRING, Panther and DAVID bioinformatic free-softwares. **Relevance:** Medical cannabis prescriptions, like CBD extracts and medicines, are becoming more popular as evidences of their effects grows in the scientific community and spread in media platforms. In Brazil, a pro-war on drugs country where CBD is illegal, the number of CBD importation requirements for new patients tripled from 913 to 3.613 in 2015-2018 (Figure 1). Only in 2019, the commercialization of CBD based products for brazilian population became legal. Allied to this, the well-established therapeutics effects remains with unclear details of their gene network activation and therapeutics cellular markers. Thus, these mechanisms may be further elucidated with the RNA-Seq results of this study.

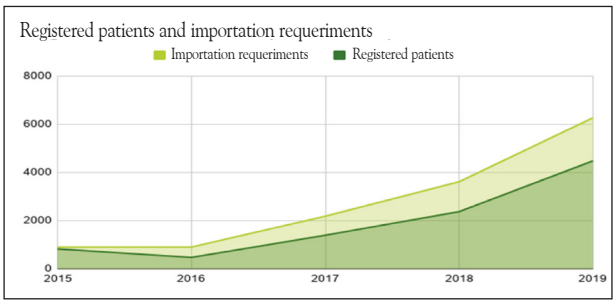

Figure 1. Number of registered patients and importation requirements in Brazil from 2015 to 2018. Data provide from Agência Nacional de Vigilância Sanitária(ANVISA).

CHARACTERIZATION OF THE GENE EXPRESSION PROFILE OF HYPOTHALAMIC PARAVENTRICULAR NUCLEUS CELLS

P. B. Curral[1], A. S. Vieira[1]

[1]Department of Structural and Functional Biology, Institute of Biology, University of Campinas (UNICAMP); and the Brazilian Institute of Neuroscience and Neurotechnology (BRAINN), Campinas, SP, Brazil.

Introduction: The hypothalamic paraventricular nucleus (PVN) plays an important role in the control of sympathetic activity, its cells receive afferences from different regions involved with the processing of visceral sensory information and emotional state of the organism, such as the cingulate and insular cortex. These PVN cells project, among other regions, to the Rostral Ventrolateral Marrow (RVLM) which in turn influences the activity level of preganglionic sympathetic neurons along the spinal cord and brainstem. Thus the PVN consists of a hypothalamic nucleus critical for controlling the sympathetic activity of the organism. However, the molecular profile of this region remain poorly known. Transcriptome analysis allows for extensive mapping of RNA molecules that encode the cellular machinery that makes up cells and tissues, allowing investigation of the set of mechanisms responsible for physiological or pathological conditions. Therefore, the objective of the present study is to use laser capture microdissection and transcriptome analysis using RNAseq to explore the molecular profile of different PVN cell populations. **Materials and Methods:** We used 6 month old male Swiss mice (n=5) (CEMIB-UNICAMP). Animals were deeply anesthesized with isoflurane and brains were collected and immediately frozen. Samples were processed for the production of histological tissue slides and were Laser Capture Microdissection (LCM) using a Zeiss-PALM system. We extracted the Magnocellular (MC) and Parvocellular (PC) regions from the paraventricular nucleus. RNA was extracted using Trizol (Thermo) and cDNA library's were prepared using Truseq (Illumina) library preparation kit according to manufacturer instructions. We ran cDNA libraries on a miSEQ (Illumina) and obtained an average of 1 million paired-end 100 bp reads per sample. **Results:** We found a total of 193 genes differentially expressed when comparing MC to PV cells, (considering an adjusted p-value < 0.1). A number of 152 genes were more expressed in the PC than in MC cells and

42 genes were more expressed in MC than in PC cells. **Discussion/Conclusion**: Our data demonstrates specific molecular components of the MC and PC cell populations. The present data may provide new specific markers for this cells populations and may provide a better understanding of the molecular machinery responsible for each cell population function.

CORTICAL ACTIVITY DURING THE WRITING TASK IN DYSTONIA - A STUDY WITH FUNCTIONAL NEAR INFRARED SPECTROSCOPY (FNIRS)

R. P. Dalle Lucca [1,2], J. B. Balardin[1], D. D. de Faria [1,3,4], A. M. Paulo[1], J. R. Sato[5], C. A. Baltazar[1], V. Borges[3], S. M. C. Azevedo Silva [3,4], H. B. Ferraz[3], P. M. de Carvalho Aguiar [1,3]

[1]Hospital Israelita Albert Einstein, [2]Universidade de São Paulo, [3]Departamento de Neurologia e Neurocirurgia- Universidade Federal de São Paulo, [4]Hospital do Servidor Público Estadual de São Paulo, [5]Centro de Matemática, Computação e Cognição - Universidade Federal do ABC.

Introduction: Dystonia is a movement disorder characterized by involuntary sustained or intermittent muscle contractions causing abnormal postures and/or repetitive twisting movements, typically patterned[1], which can be task specific. Handwriting is a complex highly skilled task and is most common trigger for task specific dystonia. Commonly used neuroimaging techniques such as fMRI and PET impose important physical constraints, limiting previous image studies to assess dystonic patients' brain activity during actual writing. Latter advances in functional near infrared spectroscopy offer a new possibility for investigating cortical areas and the neural correlates of complex motor behaviors non-invasively under naturalistic experimentation. In this context, this study aimed to investigate the cortical activity in focal right upper limb dystonia patients using functional near infrared spectroscopy (fNIRS) during actual writing. **Materials and Methods:** Twenty-one patients with right upper limb idiopathic dystonia (6 with task-specific dystonia) and twenty-one healthy volunteers matched for age and years of education were submitted to a simple right-hand writing task paradigm that consisted of 4 epochs of alternating writing/resting blocks. To test a priori hypotheses that brain activation to simple handwriting in cortical sensorimotor and supplementary motor regions would be less specific in patients than in controls, we defined right and left primary motor (M1) and somatosensory (S1) and supplementary motor area (SMA) ROIs. Differences between groups on changes in both deoxy and oxy-Hemoglobin (HbO_2) and for each ROI were then compared using Mann Whitney tests. **Results:** Channels exhibiting increased HbO_2 for the writing task compared to the resting condition in the patient and control groups are described in Fig. A. In controls, a lateralization predominantly to the left side was observed in most of the central channels covering the primary motor and somatosensory cortices. A more bilateral pattern of activation was observed in patients. In the ROI-based group analysis, between-group differences were observed in two of the five ROIs: left M1 ($p = 0.022$) and S1 ($p = 0.022$) exhibited increased HbO_2 in patients in relation to controls (Fig. B). **Discussion/Conclusion**: Overactivity findings on M1 and S1 are in agreement with previous studies of the writing task in non-ecological conditions, including imagined writing task[2,3,4], reinforcing the role of these areas in dystonia and the sensorimotor processing impairment hypothesis. As symptoms in dystonia are very specific to the task, we believe the pattern of brain activation is as much as specific, therefore the importance of an experimental set that mimics real life conditions. To our knowledge, this is the first study to measure cortical activity during actual writing in ecological conditions (subjects sited in anatomical position, in less noisy environment, using traditional paper and pen) in focal upper limb dystonia patients, outlining the potential of fNIRS for the study of the movement disorders in unconstrained environments.

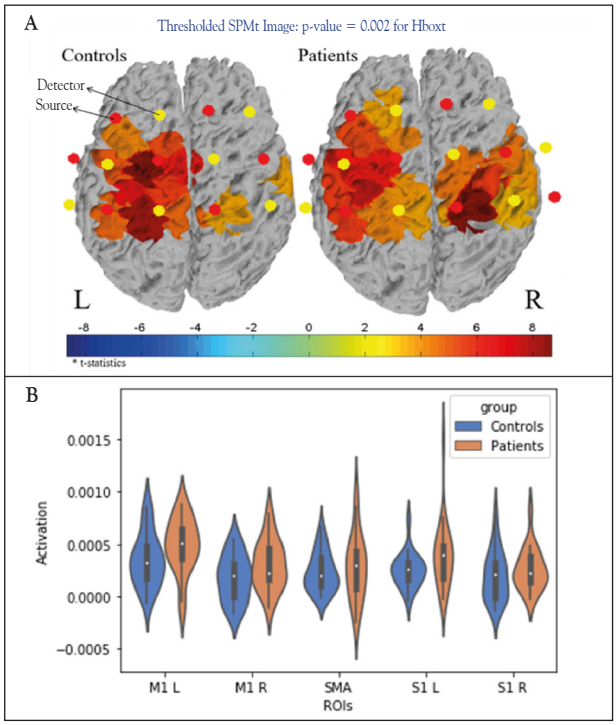

Figure 1. Figure A. Activation maps from the channel-wise analysis showing the mean activation of each group: controls (left) and patients (right). The map for patients confirms the trend for bilateral activation. Small red and yellow circles represent sources and detectors, respectively. Results for each channel were Bonferroni corrected for multiple comparisons (p-value <0.002). Figure B. Violin plots comparing the activation between controls (C), in blue, and patients (P), in red, in ROI's M1 Left (M1 L), M1 Right (M1 R), SMA, Somatosensory Left (S1 L) and Somatosensory Right (S1 R), where activation is given by the difference between writing and resting beta coefficients (e.g. coefficients of activation) (Activation [dimensionless] = writing – resting). Box plots inside the violins are conventional box plots, where the white dot represents the median and outlier markers are omitted.

References: [1] Albanese A et al., https://doi.org/10.1002/mds.25475; [2] Delnooz CC et al., https://doi.org/10.1002/hbm.21464; [3] Odergren T et al., https://doi.org/10.1002/mds.870130321; [4] Carbon M et al., https://doi.org/10.1093/brain/awq017

CROSS-ACCURACY BETWEEN BAI X GAD-7 AND BDI X NDDI-E FOR DETECTION OF ANXIETY AND DEPRESSION SYMPTOMS IN PATIENTS WITH EPILEPSY

R. B. João[1]; M. H. Nogueira[1]; M. Morita-Sherman[1]; F. Cendes[1]; C.L. Yasuda[1]

[1]Neurology Department (Neuroimaging Laboratory), UNICAMP.

Introduction: Anxiety and Depression symptoms are more prevalent in patients with epilepsy (PWE) in comparison to the general population. Our aim was to compare the cross-accuracy between two classic screening tools for depression (Beck Depression Inventory [BDI]) and anxiety symptoms (Beck Anxiety Inventory [BAI]) with newer, brief inventories (Generalized Anxiety Disorder–7 [GAD-7] and Neurological Disorders Depression Inventory–Epilepsy [NDDI-E]) in a large group of PWE. **Materials and Methods:** We evaluated 610 PWE (360 women; median-age 40 years) at the outpatient Epilepsy Clinics – UNICAMP with the application of all 4 inventories. We used SPSS to obtain Kappa index (KI) values for comparisons between BAI / GAD7 (cut-off 6) and BDI/ NDDI-E (cut-offs 13 and 15). For both BAI/BDI we tested the following cut-offs: 12, 14, and 16 points. **Results:** Symptoms of anxiety (35.6% of patients) and depression (42.3% of patients) were frequently observed in PWE. The cross-accuracy evaluation between BAI and GAD-7 was represented by a KI=0.55 (BAI-12 points cut-off), KI=0.51 (BAI-14 points cut-off), and KI=0.48 (BAI-16 points cut-off). The cross-accuracy between BDI and NDDI-E (15 points cut-off) was represented by a KI=0.39 (BDI-12 points cut-off), KI=0.44 (BDI-14 points cut-off) and KI=0.49 (BDI-16 points cut-off). With an NDDI-E 13 points cut-off, we obtained a KI=0.53 (BDI-12 points cut-off), KI=0.60 (BDI-14 points cut-off) and a KI=0.60 (BDI-16 points cut-off) . We observed a moderate strength-of-agreement (KI=0.40-0.59) between BAI and GAD-7, and a better strength-of-agreement (KI=0.60-0.79) between BDI and NDDI-E. **Discussion/Conclusion**: The newer questionnaires (GAD-7 and NDDI-E) may be reliable and faster alternative screening tools for use in the neuropsychiatric evaluation of PWE, with better agreement associated with NDDI-E. **FUNDING -** FAPESP / CAPES

DEEP LEARNING ALGORITHM APPLIED TO CEREBELLUM SEGMENTATION IN MAGNETIC RESONANCE IMAGES

Leonardo Bernardes M. Roda[1], Livia Rodrigues[2], Marcondes Cavalcante França Jr[3], Thiago Junqueira R. de Rezende[3]

[1]IFGW, UNICAMP, [2]Medical Image Computing Lab, FEEC, UNICAMP, [3]Neurology Dept., FCM, UNICAMP.

Introduction: The segmentation of cerebellum is extremely useful to assess cerebellar damage in several diseases, especially spinocerebellar ataxias. Since manual segmentation is time consuming and shows lower levels of reprodu-

cibility due to the complex and irregular boundaries of cerebellum, hence, automated method of segmentation is required. The most used methods today are based in Bayesian algorithms. These methods show good results for healthy brains, after manual correction and long time of processing. In contrast, deep learning algorithms have been successfully used in medical imaging, especially those based in Convolutional Neural Networks (CNN). Therefore, this study proposes to automatically segment the human Cerebellum through Artificial Intelligence methods. **Materials and Methods:** We used 600 T1-weighted images from healthy controls previously acquired in a 3T scanner (Philips Achieva) and stored in our database. All images were processed using FreeSurfer software aiming to segment the cerebellum and use it as the ground truth (label) for our neural network. These 600 images were divided in training (~480 images) and validation datasets (~120 images). Some of these images were randomly submitted to a data augmentation (rotating and shifting) process in order to increase our training set and to increase the variability of the data. The algorithm was developed with Python 3.6, based on the U-net CNN that already presented excellent results for medical images, and we used free virtual GPUs from Google Collaboration in order to train the network in a reasonable amount of time. **Results:** The CNN are defined by some parameters as number of epochs, batch size, quantity of learning filters and convolutional layers. We developed 12 versions each one with different parameters. The best version took 5 hours to train the network with the training dataset and acquired a Dice of 84,50% for the validation dataset, the parameters used for this version were 35 epochs, batch size of 8 images and 368 filters split into 9 convolutional layers, the segmentation for each image was made in less than 5 seconds. We can see, in the figure 1, the result in two different views of a cerebellar segmentation with our deep learning algorithm in a healthy control imaging.

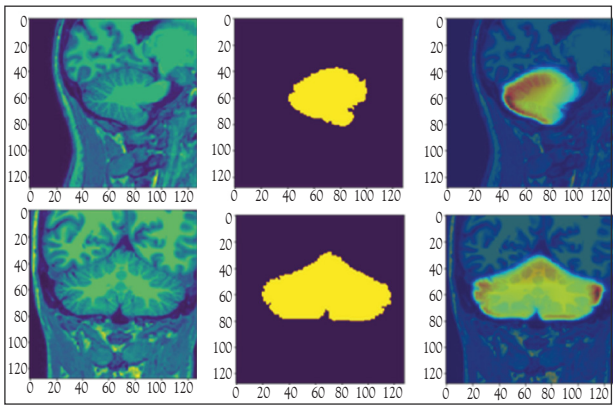

Figure 1. T1-weighted healthy brain image in first column. Ground truth/Label used for training in middle column, and the result as a probability distribution map in the last column.

Discussion/Conclusion: In conclusion the U-Net based CNN is a great alternative to segment the cerebellum. In order to increase the network performance, we are going to increase the dataset, feeding it with imaging of patients with spinocerebellar ataxia and refine the ground truth segmentations.

DEVELOPMENT OF AN OPTICAL DEVICE FOR CEREBRAL MEASUREMENTS IN HUMANS

G. A. Dollevedo[1], G. H. Scavariello[2], R.C. Mesquita[2]
[1]Institute of Physics, UNICAMP.

Introduction: Near-Infrared Spectroscopy (NIRS) is a safe, non-invasive optical technique capable of measuring brain activity based on cerebral hemodynamic changes. Compared to other neuroimaging approaches, NIRS offers the possibility to miniaturize its instrumentation and has a low application cost. Even with constant improvements around the technique, most commercially available NIRS systems are still relatively cumbersome, expensive, and make use of optical fibres. To address the low portability and high cost problem, we aim to build a fibreless, NIRS-based wearable optical device prototype. **Materials and Methods:** The prototype was built taking into account the latest advances towards wearable NIRS systems [1]. Briefly, a Silicon Photodetector (BPW-34) was used as light sensor. To amplify its signal output, a transimpedance amplifier with multiple gain setups was designed, where the electronic components were chosen based on their cost-efficiency and availability. As for light sources, a SMT735D/850D dual-wavelength (735/850 nm) LED was used. The device was powered through a regulated DC power supply (BK Precision 1550) for testing purposes. Data acquisition was made through a National Instruments DAQ board (NI USB-6251) and analyzed with homemade LabView codes and Matlab scripts. Characterization and pre-validation of the device were performed with optical phantoms and healthy subjects by strapping the optical sensor and light source with elastic bands at known distances in both cases. Circuit signal stability (employing the phantom) and dark current stability were both measured while isolating any external light sources over a two hour long experiment in a controlled temperature environment. **Results:** After testing the signal quality on a group of subjects, the system was designed to allow four different sets of gain (~470k, 5M, 10M, 20M). The variable gain enables measurements under several circumstances, and covers a wide array of source-detector distances. Circuit signal stability was determined for both wavelengths using least square regression. The measured signal drift is less than 1% per minute of the expected hemodynamic signal measured in typical subjects at rest. Dark current stability was also determined using least square regression, and a signal drift of less than 0.1% was measured. The total build cost of a 2-channel, multiple gain prototype was less than R$60.00, and the circuit board dimensions are approximately 59x36mm in a rectangular shape. **Discussion/Conclusion**: The device is able to detect physiological changes under less than ideal circumstances, at all the possible desired source-detector separations. The device is also robust enough to work properly in long-term experiments, since the voltage drift measured at both stability tests corresponds to less than 1% of the expected physiological signal amplitude that we measured. Although wireless communication has yet to be implemented, a communication protocol based on ESP-32 microcontroller is already under development. It will manage the circuit control and data transfer over Wi-Fi, ensuring that the device is able to work on a remotely manner. In conclusion, a low cost, efficient, portable NIRS prototype was designed. Our results support further developments of new alternatives to NIRS systems, which will certainly open new directions for neuroscience applications in natural environments.

References: [1] Zhao, H. et al., doi: 10.1117/1.NPh.5.1.011012

DIFFERENCES IN WHITE MATTER INTEGRITY IN TLE WITH AND WITHOUT HIPPOCAMPAL ATROPHY

L.f. Ribeiro[1], L.s. Silva[1], B.m. Campo[1], F. Cendes[1], C.l. Yasuda[1]
[1]Neuroimage Laboratory, UNICAMP.

Introduction: Temporal lobe epilepsy (TLE) is the most common focal epilepsy in adults. Hippocampus atrophy (HA) is the most common neuroimage abnormality seem in this group of patients. In this study we evaluated the white matter (WM) integrity in TLE patients with and without HA using diffusion-tensor imaging (DTI) and tractography. **Materials and Methods:** we acquired T1-weighted, and DTI images (32 directions) in a 3T MRI scanner from 158 TLE patients followed at the University of Campinas and 129 controls. Patients were divided into 4 groups: LEFT- HA (61), RIGHT- HA (45), BILATERAL- HA (21), and NEGATIVE (31). Tractography from DTI was processed with MainExploreDTI (http://www.exploredti.com/) running on MATLAB. We delineated two commissural (corpus callosum-CC and fornix-FX) and five bilateral tracts (corticospinal-CST, cingulum-CG, arcuate-ARC, inferior-frontal-occipital-IFO, and uncinate-UNC) and extracted diffusion parameters (Fractional Anisotropy (FA), mean diffusivity (MD), radial diffusivity (RD), and axial diffusivity (AD). We used SPSS with MANOVA's for commissural and REPEATED-MEASURES ANOVA's for bilateral tracts to compare the parameters among groups using age and sex as covariates ($p<0.05$, Bonferroni corrected). **Results:** groups were balanced for age and sex ($p>0.05$). All HA groups showed reduced FA/AD and increased MD/RD in CC and FX ($p<0.05$). LEFT-HA showed alterations in the CG, IFO, UNC (reduced FA and increased MD/RD), ARC, and CST (increased MD/RD). RIGHT-HA group presented alterations in the CG, UNC (reduced FA, and increased MD/RD), ARC (increased MD/RD), and IFO (increased MD). BILATERAL-HA group exhibited alterations in the CG, IFO, UNC (increased MD/RD), and CST (increased MD). NEGATIVE patients only showed increased MD and RD in UNC. **Discussion/Conclusion**: while all HA groups presented extensive abnormalities, the NEGATIVE group displayed minor WM alterations, suggesting different physiopathology and more benign disease.

EEG SIGNAL CONNECTIVITY FOR CHARACTERIZING INTERICTAL ACTIVITY IN PATIENTS WITH MESIAL TEMPORAL LOBE EPILEPSY

Leonardo Rodrigues da Costa[1], Gabriela Castellano[1]
[1]Neurophysics Group, IFGW, UNICAMP.

Introduction and Hypothesis: Though neuroscience and neurology have extensively researched and treated it, a full understanding of epilepsy and its roots is yet to be achieved. The electroencephalogram (EEG) is the flagship in epilepsy study and diagnosis, but its content analysis is still mainly performed visually by neurologists. This project will investigate the kind of information (and its usefulness) we can extract with methods such as graphs, machine learning, coherence and correlation analysis applied to EEG signals of epileptic patients. **Objective:** The goal of this project is to apply some recent computational methods such as graphs, motifs, coherence, Pearson correlation and machine learning to analyze the EEG of 128 epileptic patients and, hopefully, build tools to aid epilepsy characterization. **Materials and Methods:** The EEG signals were previously acquired from 128 adult epilepsy patients. These acquisitions were made along with fMRI images. Each acquisition was made with two *BrainAmp MRplus* (*BrainProducts GmbH*, München, Germany) amplifiers, *BrainVision Recorder* 1.20 program, the *BrainCap MR* EEG cap with 64 electrodes (including one ECG electrode), 10/20 positioning system, conductive gel and 5000Hz sampling rate, corresponding to 35-48 minutes of EEG-fMRI data. The data analysis will be made in *MATLAB* using the *EEGLab* pack. Methods include artifact removal, filtering, coherence/correlation measurements and graph characterization. The resulting profiles will be compared with the neurologists' visual analysis of the EEG, using machine learning algorithms. **Relevance:** Epilepsy is a chronic neurological disturb that affects 1-2% of the world population. It is estimated that, in Latin America, more than 50% affected by epilepsy don't receive treatment. Among those who do, only 70% are responsive to drug treatment, 10% are responsive to surgery and/or ketogenic diet and 20% are non-responsive to any type of treatment. Annually, 2 million new epilepsy cases are diagnosed around the world. New tools to help understand and analyze this condition are welcomed.

References: [1] Quintero-Quiroz, C. et al., DOI:10.1063/1.5036959; [2] Rangayyan , RM, DOI:10.1002/9781119068129; [3] SHAW, JC, DOI:10.1016/0167-8760(84)90045-X; [4] Goodfellow, et al. Deep Learning, MIT press, 2016.

EFFECTS OF AEROBICAL PHYSICAL TRAINING ON STRUCTURAL DAMAGE IN TEMPORAL LOBE EPILEPSY

Luciana R. P. Silva[1], Nathalia Volpato[1], Gabriela Scriptore[2], Mateus Henrique Nogueira[1], Clarissa Lin Yasuda[1], Fernando Cendes[1]
[1]Department of Neurology, FCM, UNICAMP, [2]Department of Cardiology, Clinic Hospital, UNICAMP.

Introduction: This study aimed to investigate the effects of an aerobic physical training on structural hippocampal atrophy in temporal lobe epilepsy. **Materials and Methods:** We included 25 patients divided into training (n=10) and control (n=15) groups. The training group performed an aerobic physical training program for six months. All individuals underwent the following exams before and after the six months period: maximum effort test on treadmill to evaluate cardiopulmonary capacity and MRI scan to obtain T1-weighted volumetric images in a 3T scanner (Philips Achieva). We analyzed volumetric images using the Freesurfer toolkit (version 5.3.0). Repeated-measures analysis of variance was applied to investigate the effects of the evaluation time and training program differences on hippocampal volumes (HVol, normalized for the intracranial total volume). We set $p<0.05$ as statistically significant. **Results:** For ipsilateral HVol, we found no effects of the training program ($F_{1,23}=0.11$, $p=0.7$) or evaluation time ($F_{1,23}=0.81$, $p=0.3$). For contralateral HVol, there were no isolated effect of the training program ($F_{1,23}=0.35$, $p=0.5$) or evaluation time ($F_{1,23}=0.03$, $p=0.8$), however, we found a significant training program *vs* evaluation time interaction ($p=0.02$). Analysis of combined effects showed a significant contralateral HVol reduction only in the control group after six months ($p=0.029$, mean ± standard deviation: pre-training 4006.8±541.2mm³, post-training 3914.1±470.7mm³). **Discussion/Conclusion**: Our data suggest that aerobic training might influence the disease course as shown by similar HVol before and after in patients who underwent aerobic physical training and reduced contralateral HVol after six months in patients who were not active. **Acknowledgments:** We thank FAPESP for financial support.

EFFECTS OF KINESIO TAPING TECHNIQUE ON THE BRAIN FUNCTION

Basilio F.B.[1], Campos, B.M.[2], Novi, S.L.[3], Quiroga, A.[3], Mesquita, R.C.[3], Coan A.C.[1]
[1]Child Neurology Discipline, Department of Neurology, FCM-UNICAMP.; [2]Neuroimaging Lab, UNICAMP.; [3]Neurophysics Group, IFGW, UNICAMP.

Introduction: Kinesio Taping (KT) is a promising and an effective method for motor rehabilitation. It is used to facilitate or inhibit muscle functions, stabilize joints and reduce pain. The fundamental mechanisms of the technique are not yet fully understood. **Materials and Methods:** Nine right-handed healthy adult volunteers (26 to 32 years) performed functional magnetic resonance imaging (fMR) with block motor experiments with and without the use of KT. The experiment was divided into a part without KT and another with KT in the left hand, according to the table below. All individuals underwent five minutes of baseline echo-planar images, followed by three blocks of motor activity for each hand composed by interleaved 20-seconds of activity and 20-seconds of rest. The experiment was repeated after placing the KT in the left hand. The fMRI images were analyzed with the SPM12 program. We performed one-sample T-tests for each condition and paired T-tests between sequences with or without KT for each hand ($p<0.001$, FDR 0.05, minimum of 40 contiguous voxels). **Results:** During hand activity, we observed activations in the contralateral pre-central gyrus for all conditions. Comparison of the left-hand movement test with or without KT revealed activation in more diffuse brain areas using KT, including additional activation of the medial frontal gyrus, posterior cingulate, and right calcarin area (Figure 1). **Discussion/Conclusion**: The use of KT altered cerebral hemodynamic response in healthy volunteers, with increased brain areas activated during motor tasks with the ipsilateral hand.

Table 1. Motor Experiment:

fRM – Motor Experiment						
Right hand without KT	Baseline	20s Activity	20s Rest	20s Activity	20s Rest	20s Activity
Left hand without KT	~~~	20s Activity	20s Rest	20s Activity	20s Rest	20s Activity
KT application						
Right hand with KT (on the left hand)	Baseline	20s Activity	20s Rest	20s Activity	20s Rest	20s Activity
Left hand with KT (on the left hand)	~~~	20s Activity	20s Rest	20s Activity	20s Rest	20s Activity

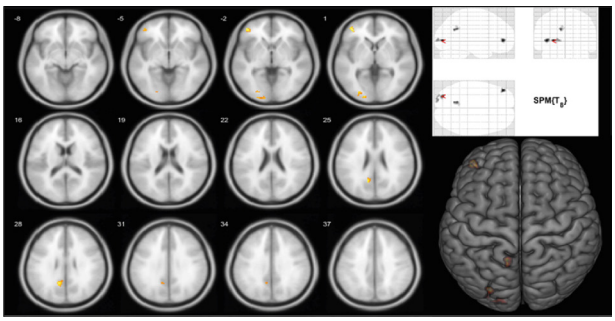

Figure 1. The use of KT revealed more diffuse brain areas activated during during motor activity of the ipsilateral hand.

EFFECTS OF THREE DIFFERENT CLASSES OF ANTIDEPRESSANTS IN THE PROTEOME OF A HUMAN OLIGODENDROCYTE CULTURE

L. R. da Silva[1], V. Almeida[1], D. Martins-de-Souza[1]
[1]Laboratory of Neuroproteomics, Biochemistry and Tissue Biology Dept., Institute of Biology, UNICAMP

Introduction and Hypothesis: Major Depressive Disorder (MDD) is a common and multifactorial psychiatric disease in which symptoms are mainly treated with antidepressants. The main targets of these drugs are neuronal cells, by modulating the monoamine system, which consists of the central hypothesis of the disorder. Strong evidence has shown that oligodendrocyte progenitor cells (OPC), oligodendrocytes (OLD) and myelination impairments can influence the pathophysiology of the disorder as well. Lesions of myelinated fibers in the white matter were associated with the severity of depression, and patients with

severe damage to myelinated fibers had a poor response to antidepressants. Therefore, we aim to know if these drugs could induce a protective effect in these cells. **Objective:** The objective of this study is to unravel, through a proteomic approach, the biological processes and metabolic pathways modulated by three classes of common antidepressants: Fluoxetine (Selective Serotonin Reuptake Inhibitor), Nortriptyline (Tricyclic) and Bupropion (Noradrenaline-Dopamine Reuptake Inhibitor) in human oligodendrocyte cell cultures (MO3.13). **Materials and Methods:** The concentrations of drugs to be tested have been standardized through MTT assays, which measure the cell viability. After this, the MO.313 cells will be cultured, and subsequently treated with fluoxetine (SSRI), nortriptyline (TCA) and bupropion (NDRI). Cells will be harvested after 8h and their proteins will be extracted and digested. These samples will be submitted to mass spectrometry-based shotgun proteomics, and the data will be processed by Progenesis software, where the proteins will be identified and quantified. The differentially expressed proteins between treatment and vehicle (p-value <0,05) will be analysed using bioinformatics tools available online; DAVID (https://david.ncifcrf.gov), Reactome (https://reactome.org) and String (https://string-db.org). **Relevance:** According to Worldwide Organization, MDD affects about 320 million people worldwide and represents a great burden for patients and society. Only about 30% of subjects affected by this disorder have a good response to a first-line treatment. Aside from that, it takes a long time to attain therapeutic benefit, and treatment-emergent side effect burden is significant. Moreover, the neurobiological basis of this illness isn't completely understood and the effects of antidepressants in OPC and OLD cells are poorly known. Elucidating how these drugs modulate biochemical pathways of these cells can improve the molecular understanding of the disorder and the mechanisms of action of these three kinds of antidepressants. In addition, a better understanding of these points may be helpful in order to develop more effective antidepressants.

EVALUATION OF STABILITY OF ^{31}P-FMRS MEASURES THROUGHOUT ACQUISITIONS

A. F. Nascimento[1,6], T. B. S. Costa[2,6], B. Foerster[3], R. C. G. Landim[4], E. L. Silva[5,6], G. Castellano[1,6]

[1]Neurophysics Group, IFGW, UNICAMP; [2]DSPCom, FEEC, UNICAMP; [3]FCI, IFSC, USP; [4]Technical University of Munich; [5]IF, UFMT; [6]BRAINN.

Introduction: Several studies have used the Phosphorus-31 functional Magnetic Resonance Spectroscopy (^{31}P-fMRS) technique in an attempt to understand high energy phosphate changes in the brain accompanying some form of brain stimulation (see, e.g., [1]). However, intersubject variability has made the results extremely controversial. The aim of this study was to evaluate the stability of ^{31}P-fMRS intrasubject data. **Materials and Methods:** Seven acquisitions of ^{31}P-fMRS data were made with the same individual (male, 27 years), approximately every 3 weeks, over 18 weeks, in a 3T MRI scanner, using an ISIS sequence (TR/TE = 3750/0.10ms, NSA=8, 8 phase cycles, 3000 Hz bandwidth, 1024 complex data points), with voxel size of 50×70×70 mm^3, placed on the occipital cortex. The fMRS paradigm was composed of 7 blocks interleaving rest and visual stimulus, the latter consisting of a checkerboard pattern reversing at 4, 8 and 16 Hz (in the 2nd, 4th and 6th block respectively). Spectra were quantified using the AMARES method [2] with the jMRUI software [3]. Metabolites assessed for each block were: glycerol-3-phosphorylcholine (GPCh), inorganic phosphate (Pi), phosphorylethanolamine (PE), glycerol-3-phosphorylethanolamine (GPE), phosphocreatine (PCr), nicotinamide adenine dinucleotide (NADH) and the three peaks of adenosine triphosphate (α, β and γ-ATP) (Figure 1). All quantification values were normalized to the first rest block, and coefficients of variation (CV) were calculated for rest, 4 Hz, 8 Hz and 16 Hz blocks, and also, for all blocks together. **Results:** Table 1 shows the CV for all quantified metabolites. **Discussion/Conclusion**: As seen in Table 1, most CVs are high, for all conditions and metabolites. This is possibly due to the low sensitivity of the technique, which prompted a large voxel, which in turn may englobe several metabolic processes. The lowest CVs were achieved for PCr (9%), which is the highest peak in the ^{31}P spectra, followed by α-ATP (18%). The CVs achieved for PE (115%) and NADH (73%) suggest that these metabolites should not be evaluated in ^{31}P-fMRS experiments; also, the α and γ peaks of ATP should be preferred to the β peak when evaluating this metabolite. Finally, our results suggest than in ^{31}P-fMRS experiments, PCr changes smaller than ~10%, ATP changes smaller than ~20%, and GPCh, Pi and GPE changes smaller than ~50%, should be disregarded.

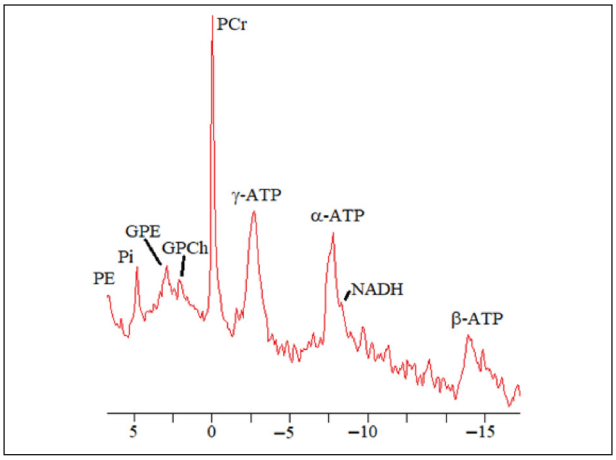

Figure 1. Example of ^{31}P-fMRS spectrum.

Table 1. Coefficient of variation (CV) over 7 ^{31}P-fMRS acquisitions. CV for Rest was computed over 3 blocks per acquisition, for stimuli (4, 8 and 16 Hz) over 1 block per acquisition, and for "All" over 6 blocks (3 rest + 3 stimulus) per acquisition.

	Condition				
Metabolite	Rest	4 Hz	8 Hz	16 Hz	All
GPCh	37 %	43 %	15 %	37 %	35 %
Pi	51 %	36 %	35 %	46 %	45 %
PE	155 %	119 %	54 %	42 %	115 %
GPE	40 %	63 %	40 %	51 %	46 %
PCr	9 %	9 %	10 %	10 %	9 %
NADH	63 %	94 %	53 %	76 %	73 %
α-ATP	17 %	24 %	17 %	14 %	18 %
β-ATP	39 %	40 %	44 %	16 %	40 %
γ-ATP	24 %	19 %	25 %	20 %	22 %

References: [1] Costa TBS et al., doi: 10.1007/s42600-019-00023-0. [2] Vanhamme L et al., J. Magn. Reson. 129(1): 35-43, 1997. [3] Stefan D et al., doi: 10.1088/0957-0233/20/10/104035.

EVALUATION OF TEXTURE PARAMETERS IN MUSCLE MRI OF DUCHENNE PATIENTS: A PILOT STUDY

D. L. Mendes[1,3], L. S. Souza[2,3], M. C. França Jr.[2,3], G. Castellano[1,3]

[1]Neurophysics Group, IFGW, UNICAMP, [2]Neurology Dept., FCM, UNICAMP, [3]BRAINN.

Introduction: Duchenne muscular dystrophy (DMD) is a degenerative and progressive genetic disease, which still has no cure and which affects the skeletal and cardiac striated muscles [1]. It is caused by mutations in the DMD gene [1]. Magnetic resonance imaging (MRI) has been used to monitor the evolution of this disease, but so far, only visual information has been extracted from the images. The aim of this work was to explore whether texture parameters extracted from muscle MRI of DMD patients could provide additional information regarding disease progression. **Materials and Methods:** MR images from the gastrocnemius were acquired in a 3T scanner (Philips Achieva) from five male DMD patients (mean age 14±6 years) in two instances, 13±5 months apart. The images were normalized to 128 gray levels; regions of interest (ROIs) were manually segmented in the images; and co-occurrence matrices [2] were computed for distances from 1 to 5 pixels, using the MaZda software [3]. From these matrices, nine texture parameters were computed: angular second moment, contrast, correlation, variance, inverse difference moment, sum average, sum variance, sum entropy, entropy, totaling 45 parameters. These parameters were compared individually between the two instances, using a t-test. **Results:** We found significant differences (p = 0.0288) among instances for the contrast parameter, for a co-occurrence matrix computed with a 3-pixels distance. **Discussion/Conclusion:** This was an exploratory work aiming to verify the feasibility of using texture parameters as markers of disease progression in DMD

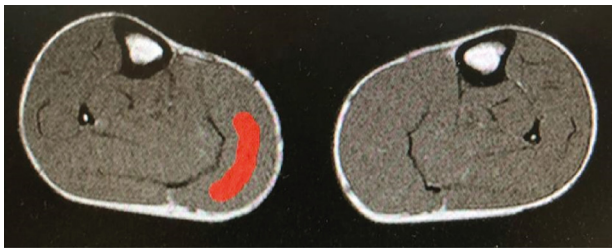

Figure 1. Example MRI of a patient's legs. The highlighted region in the gastrocnemius is the ROI used to calculate the texture parameters.

patients. The study has several drawbacks, which could be excused due to it being an exploratory/pilot study. In the first place, the sample (five patients) is too small to allow to state whether texture differences in a larger DMD population are really occurring over time. Also, the use of the t-test is not indicated for such a small sample, and a multiple comparisons correction should have been performed. Nonetheless, a proof of concept was made that it is possible to extract texture parameters from the given images and that they may carry some useful information. Next, we intend to increase the patients' sample and address all the aforementioned drawbacks; also, we will explore other texture features, as well as different normalization intervals of the MR images.

References: [1] Mah JK et al., doi: 10.1017/cjn.2015.311. [2] Haralick RM et al., IEEE Trans. Syst. Man Cybern., SMC-3(6): 610-21, 1973. [3] Strzelecki M. et al., doi: 10.1016/j.nima.2012.09.006.

GENETIC ALGORITHMS COMPARISON FOR FEATURE SELECTION IN A MI-BCI WITH THE DATASET 2A OF BCI COMPETITION IV

M. B. Kersanach[1,2], L. F. S. Uribe[1,2], R. Attux[1,2]

[1]FEEC/UNICAMP, [2]Brazilian Institute of Neuroscience and Neurotechnology (BRAINN).

Introduction: Usually a Brain-computer interface (BCI) have some steps that include extraction and selection of relevant features from the brain signal, followed by classification of the signals according to the task at hand. For our work the Motor Imagery (MI-BCI) was used and a signal processing was made to the EEG signal to obtain features related to power frequency information. Previous studies have shown the importance of feature selection when choosing channels (electrodes) and frequency bands [1], for example, wrapper-type forward selection (FS) techniques have advantages in that they optimize channel subsets for use by final classifier. Therefore, different genetic algorithm (GA) were used to compare the FS type selection to choose an effective feature subset measuring their impact on the classification gain accuracy. **Materials and Methods:** We used the dataset 2a of BCI competition IV to evaluate the performance of the proposed methods for the classification of two classes of MI - left and right hand. Pwelch was used to extract the energy power features for 4 frequency mu and beta sub-bands. Subsequently, the wrappers FS and four strategies based in evolutionary algorithms were compared included: CLONALG, Differential Evolution (DE) classical and with XOR function for mutation and finally a classic genetic algorithm. At the end, a classifier based on linear discriminant analysis (LDA) was used for classification. **Results:** The values presented in the Figure 1 show the average of the classification accuracy and the deviation over 5 executions performed for each method used. In relation to the average value of accuracy by method used among all subjects, the highest was 66.7% for EvoDiff. CLONALG and wrappers obtained both 64.7% being the lowest. Finally, the ANOVA test was performed between each evolutionary method in comparison to wrappers and only for two subjects the genetic methods were superiorly significant: 6 with $p < 0.1$ for EvoXOR, EvoDiff and Gen, and 2 with $p < 0.2$ for genetics. **Conclusion**: After the ANOVA test was carried out, it was found that superior results were only for 23% percent of the subjects, which shows that if there is a gain in the classification accuracy using evolutionary methods in this case except for CLONALG. **Acknowledgements:** The authors thank CNPq, CAPES and FAPESP for the financial support.

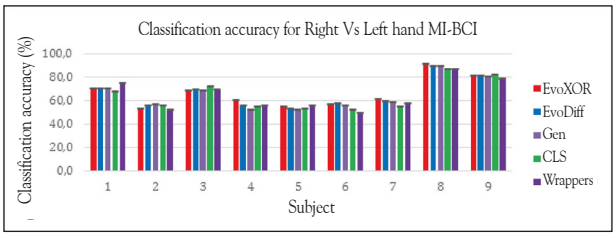

Figure 1. Average value of classification accuracy for the methods for selection of features tested.

References: [1] Islam, M. R. et al. https://doi.org/10.1088/1741-2552/aac313

GENOME-WIDE ASSOCIATION STUDY (GWAS) IDENTIFIES MULTIPLE LOCI FOR MESIAL TEMPORAL LOBE EPILEPSY

E. M. Bruxel[1], P. H. M. Magalhães[1], T. K. de Araujo[1], R. Secolin[1], F. Rogério[2], F. Cendes[3], I. Lopes-Cendes[1]

[1]Department of Medical Genetics, FCM, UNICAMP; [2]Department of Anatomical Pathology, FCM, UNICAMP; [3]Department of Neurology, FCM, UNICAMP.

Introduction: Mesial temporal lobe epilepsy (MTLE) is the most common form of focal epilepsy in the adult population, frequently associated with hippocampal sclerosis and, accounting for approximately 40% of all cases of epilepsy in this population [1]. The understanding of the underlying mechanisms, including genetic predisposition, leading to epilepsy, has grown rapidly in the last few decades; however, in complex inherited epilepsies, which are the most frequent forms, the genetic basis remains poorly understood. In the focal epilepsies, there has been suggestive evidence for a locus at chromosome (ch) 2q24.3 for all focal epilepsies combined, as well as two loci for temporal lobe with hippocampal sclerosis on chs 3q25.41 and 6q22.31 [2]. **Materials and Methods:** We studied a large cohort of patients with MTLE identified in different centers in Brazil and Portugal. All patients fulfilled the clinical diagnosis of MTLE proposed by the International League Against Epilepsy. We enrolled a total of 472 patients and 415 controls. Controls were ethnically matched with cases and were enrolled in the same clinical centers as patients. **Results**: Principal components analysis showed that there were no significant differences in the genomic composition of patients and controls and were used as covariates in the association analysis. After quality control, we performed a logistic regression using an additive model for the association. We confirmed two association signals previously reported with one SNP at ch 2q24.3 ($p_{Bonferroni}$ = 0.03) and two SNPs at ch 6q22.31 ($p_{Bonferroni}$ = 0.003 and $p_{Bonferroni}$ = 0.01). We also found a novel genome-wide significant association. **Discussion/Conclusion**: The SNPs found to be associated with the MTLE phenotype are located in introns, transcription factors binding site, intergenic regions, and regulatory regions of brain-related genes. Future steps on this project aim to integrate transcriptomic and epigenomic data in other to refine better the candidate regions identified.

References: [1] Engel J. Epilepsia 42: 796–803, 2001; [2] International League Against Epilepsy Consortium on Complex Epilepsies. Nat Commun 9(1): 5269, 2018.

GENOTYPE-SPECIFIC PATTERNS OF SPINAL CORD DAMAGE IN HEREDITARY SPASTIC PARAPLEGIA

KRS[1], RFC[2], TJRR[1], LPR[1],MCFJ[1]

[1]School of Medical Sciences (FCM), UNICAMP, Campinas, Brazil. [2]Seaman Family MR Research Center, University of Calgary, Calgary, Canada.

Introduction: This study focused on cervical spinal cord image in hereditary spastic paraplegias (HSPs). Spinal cord damage is a hallmark of HSPs, but it is still not clear whether specific subtypes of the disease have distinctive patterns of SC gray (GM) and white (WM) matter involvement [1-4]. **Objective:** We compared cervical cross-sectional, GM and WM areas in patients with distinct HSP subtypes. We also assessed whether these metrics correlated with clinical parameters. **Materials and Methods:** We analyzed 37 patients (17 men; mean age 47.3 ± 16.5 years) and 21 healthy controls (7 men; mean age 42.3 ± 13.2 years). There were 7 SPG3A, 12 SPG4, 10 SPG7 and 8 SPG11 patients. Image acquisition was performed in a 3T MRI scanner and T2*-weighted 2D images were assessed by the Spinal Cord Toolbox [5]. Statistical analyses were performed in SPSS using analysis of covariance and Sidak corrected p-values < 0.05. **Results**: Mean disease duration for the HSP group was 22.4 ± 13.8 years and SPRS was 22.8 ±. 11.0. We failed to identify SC atrophy in SPG3A and SPG7. In contrast, SPG4 and SPG11 had SC cross-sectional area reduction ($p < 0.03$ and 0.05, respectively). While SPG4 had both SC GM and WM atrophy, SPG11 had only GM atrophy. HSP-SPG4 showed strongly inverse correlation between GM area and disease duration ($\rho = -0.903$; $p < 0.001$). **Conclusion**: In conclusion, cervical SC atrophy is found in some, but not all HSP subtypes. Additionally, SPG4 and 11 present definite, but distinct patterns of SC damage.

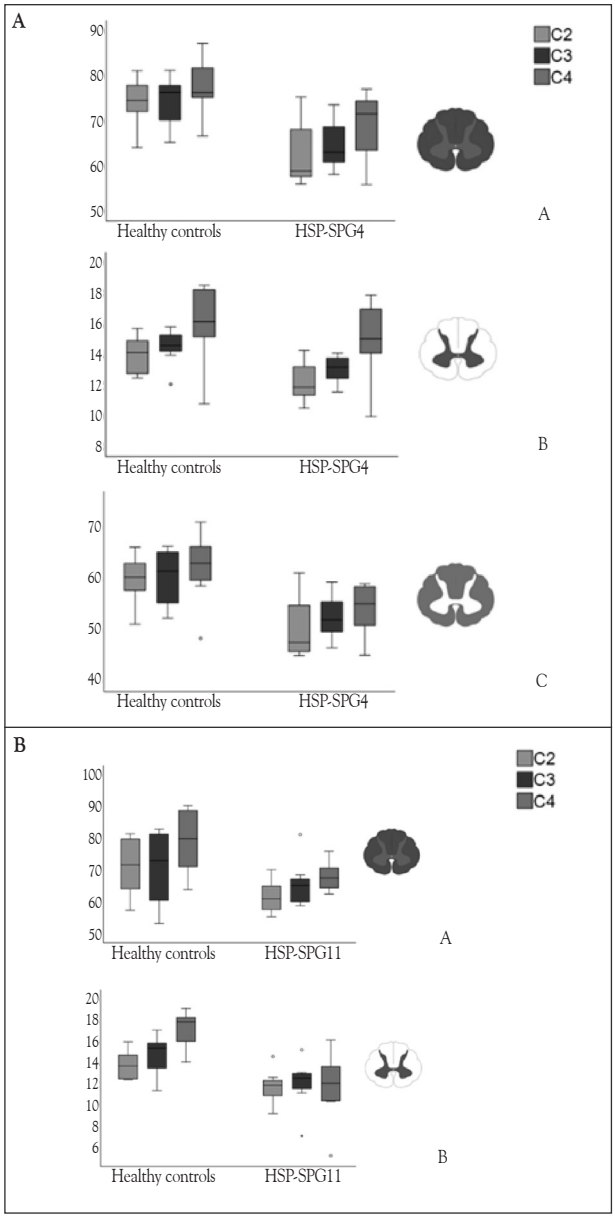

Figure 1. A: Box and whiskers plot showing the distribution of the SCA (upper lane), GM (middle lane) and WM (lower lane) areas of patients with HSP-SPG4 versus healthy controls along cervical levels C2, C3 and C4. B: Box and whiskers plot showing the distribution of the SCA (upper lane) and GM (lower lane) areas of patients with HSP-SPG11 versus healthy controls along cervical levels C2, C3 and C4.

References: [1] Parodi L, *et al.* doi:10.1016/j.neurol.2017.03.034. [2] DeLuca GC, *et al.* doi:10.1111/j.1365-2990.2004.00587.x. [3] List J, *et al.* doi:10.3390/brainsci9100268. [4] Hedera P, *et al.* doi: 10.1007/s00234-005-1415-3. [5] De Leener B, *et al.* http://dx.doi.org/10.1016/j.neuroimage.2016.10.009.

HEMODYNAMIC RESPONSES IN PREFRONTAL CORTEX DURING PREFERRED AND FAST WALKING SPEED OF YOUNG AND OLDER PEOPLE

Belli, V[1], Orcioli-Silva, D[1], Vitório, R[1,2], Beretta, V. S[1], Zampier, V. C[1], Gobbi, L. T. B[1]

[1]São Paulo State University (Unesp), Institute of Biosciences, Rio Claro. [2]Oregon Health & Science University, Department of Neurology, Portland, Oregon, United States.

Introduction: Older people have increased prefrontal cortex (PFC) activity during walking, which has been considered a compensatory mechanism due to loss of gait automaticity. In more demanding situations, such as fast walking speed, older people further increase PFC activity. However, PFC activity while fast walking has been investigated only over treadmill, which may be a limitation since gait modulation is externally guided. Therefore, the aim of this study was to analyze the hemodynamic activity in PFC during preferred and fast walking overground in young and older people. **Materials and Methods:** Twelve young and 15 older people walked in a 26.8m circuit in two conditions: preferred walking speed and fast walking speed. Five trials were performed for each condition, starting with the preferred walking speed for all participants. The total duration of each trial was 60s, being 30s of standing quietly (baseline) and 30s of the experimental task. An 8-channel mobile functional near-infrared spectroscopy (fNIRS) system was positioned over the left and right forehead following the international 10-20 system. Oxyhemoglobin (HbO_2) concentration was used as a marker of hemodynamic response in PFC. HbO_2 analysis was divided into 'baseline' period, experimental task. Baseline HbO_2 concentration was subtracted from the experimental task to evaluate the relative change in HbO_2 concentration in each experimental condition. ANCOVAs and ANOVAs, with group and condition as factors, were used for statistical analysis of HbO_2 level and gait parameters, respectively ($p \leq 0.05$). The difference between preferred and fast walking speed was used as covariate. **Results:** ANCOVA indicated a main effect of group, showing that older people presented higher left ($p=0.003$) and right ($p=0.013$) PFC activity compared to the young people. There were no main effect of condition and interaction between group and condition. **Discussion/Conclusion**: It can be concluded that the older people have increased PFC activation during overground walking, suggesting that older people need to use executive-attentional resources to control gait. However, fast walking speed not require greater PFC activity compared to preferred walking speed.

Support: FAPESP 2017/23476-1, 2016/21499-1; CNPq 309045/2017-7 and CAPES Code 001.

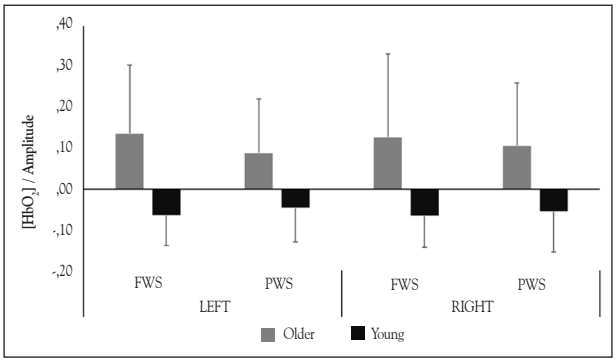

Figure 1. Means and standard errors of Oxyhemoglobin (HbO_2) in prefrontal cortex during preferred (PWS) and fast walking speed (FWS) of the older and young people.

HEMODYNAMIC RESPONSES OF THE INTERICTAL EPILEPTIFORME ACTIVITY IN BENIGN EPILEPSY WITH CENTROTEMPORAL SPIKES

Cavalcante, C. M[1]; Campos, B. M[2]; Coan, A. C[1,2]

[1]Child Neurology Service, FCM– UNICAMP; [2]Neuroimaging Laboratory, FCM – UNICAMP.

Introduction: Benign childhood epilepsy with centrotemporal spikes (BECTS) is a self-limited childhood epilepsy with good prognosis. However, some patients with BECTS might have a larger number of seizures as well as cognitive comorbidities. While interictal epileptiform discharges (IEDs) in all children with BECTS have similar topographical distribution on the scalp EEG, different patterns of spike-related neuronal network activation or deactivation may justify such different outcomes. Therefore, we aimed to evaluate the patterns of IEDs-related hemodynamic responses of children with BECTS and their association with different seizure control and cognitive outcomes **Materials and Methods:** We selected 12 consecutive children with BECTS from four different child neurology services. Up to this moment, eight of them (four girls and four boys) were submitted to concomitant electroencephalography and functional MRI (EEG-fMRI). All images were acquired in a 3 Tesla scanner (Philips Achieva) with concomitant 64-channel EEG electrodes compatible with the MRI environment. The patients were instructed to remain still, with eyes closed and they were allowed to sleep during the two runs of 24 minutes of eco-planar images. The EEG was post-processed and the IEDs were visually marked with Brain Analyzer software. MRI images were analyzed with SPM12 software. The instants of the IEDs were convolved with the three cannonical

hemodynamic response functions (HRFs) (instants -2, zero and +2 from the IEDs marker) and used to look for blood oxygen level dependent (BOLD) changes. A merged map of the maximum T-value of each HRF was considered as the result map for each individual ($p<0.001$, minimum of 40 contiguous voxels). We then performed a second level analysis comparing the IED-related hemodynamic responses of: i) children with BECTS with more than or up to ten seizures; ii) children with BECTS with or without learning disabilities (Two-sample T-tes, $p<0.001$, minimum of 40 contiguous voxels). **Results:** All patients presented perirolandic discharges,which resulted in positive BOLD changesin the ipsilateral supplementary motor area, postcentral gyrus, rolandic opercular region, inferior temporal gyrus, and fusiform gyrus; contralateral precentral gyrus; bilateral precuneus and medium occipital gyrus. Negative BOLD changes were observed in the ipsilateral medial temporal gyrus, inferior frontal gyrus, fusiform gyrus, anterior and medial cingulate gyrus, calcarine gyrus, medial occipital gyrus; contralateral superior frontal gyrus, medial superior frontal gyrus, supramarginal gyrus, bilateral precentral gyrus and medial frontal orbital gyrus. Compared with those with learning disabilities, children with BECTS without learning disabilities showed positive BOLD changes in the bilateral perirolandic regions. There were no differences of IEDs-related BOLD changes in children with BECTS with more or less than ten seizures. **Discussion/Conclusions**: Distinctly from a previous study[1], we observed a more diffuse brain network activation related to the perirolandic IEDs in children with BECTS. This difference might be due to the study population. Since the present study was conducted in secondary and tertiary child neurology services, we were able to evaluate a high proportion of children with BECTS and worse clinical outcomes related to the number of seizures and cognitive profile. IEDs in children with BECTS are usually very frequent and the diffuse IEDs-related BOLD changes detected might contribute to the worse clinical and cognitive outcome. We also observed that in children with BECTS without learning disabilities, IEDs-related BOLD changes are more pronounced in the peri-rolandic area, as previously described[1].

References: [1] Lengler U, Kafadar I, Neubauer BA, Krakow K. fMRIcorrealtes of interictal epileptiactivity in patients with idiopatic benign focal epilepsy of childhood: A simultaneous EEG-functional MRI study. Epilepsy Research, 2006.

HISTOPATHOLOGICAL ANALYSIS OF HETEROTOPIC NEURONS AND OLIGODENDROCYTE-LIKE CELLS IN THE WHITE MATTER OF PATIENTS WITH EPILEPSY

Bruna Cunha Zaidan[1], Vítor Henri Baldim[1], Marina Koutsodontis Machado Alvim[2], Enrico Ghizoni[2], Helder Tedeschi[2], Fernando Cendes[2], Fabio Rogerio[1]

[1] Pathology, FCM, UNICAMP, 2 Neurology, FCM, UNICAMP.

Introduction and Hypothesis: Epilepsy, the most common neurological disease, can result from several pathological conditions. Approximately 25% of epilepsy patients are refractory to drugs and may be candidates for surgery. However, in 2-26% of surgical cases, the histopathological findings do not allow a conclusive diagnosis of cortical alteration, despite the approach of the region previously identified as epileptogenic. In this context, the contribution of the white matter, including the oligodendroglial population, to epileptogenesis has been investigated. In the present study, we assessed histological features of the white matter of epilepsy patients who underwent surgery for different etiologies. We aimed to verify whether such patients presented microscopic white matter changes associated with epilepsy in comparison with non-epileptic individuals. **Materials and Methods:** Retrospective analysis of histological sections of temporal or frontal surgical specimens from epilepsy patients with hippocampal sclerosis, ganglioglioma or mild malformation of cortical development (n = 20) and specimens from individuals who were necropsied for non-neurological causes (controls; n = 20). Photodocumentation of microscopic fields (40x) from the superficial and deep white matter (within 500 μm and 500 μm from the gray/white matter boundary, respectively) was performed for cell counting in Hematoxilin and Eosin (HE) sections by using the ImageJ® software. Additionally, immunohistochemical analyses were performed for neuronal (MAP2 and NeuN) or oligodendroglial cells (Olig2). Immunostained cells were counted by using the same protocol described for HE-stained sections. **Results:** We found a significantly ($p<0.05$) higher oligo-like cell count in the epilepsy (E) group *versus* controls (C), both in the superficial and deep white matter (E:167.22±23.24 *vs* C:92.25±16.96 and E:154.06±25.62 *vs* C:90.05±14.92, respectively). Corroborating the morphological findings, a significantly higher number of Olig2-labeled cells were also found in the superficial and deep white matter (E:136.11±24.99 *vs* C:40.98±14.92 and E:107.06±22.66 *vs* C:32.22±11.96, respectively). In addition, we identified a significantly higher number of heterotopic neurons only with the immunohistochemical markers both in the superficial (MAP2 = E:1.81±0.79 *vs* C:0.70±0.51; NeuN = E:1.46±0.51 *vs* C:0.50±0.31) and deep white matter (MAP2 = E:1.08±0.71 vs C:0.34±0.31; NeuN = E:0.53±0.25 vs C:0.21±0.26). **Discussion/Conclusion**: Our data are original for the Brazilian population and demonstrate that epilepsy patients present with changes in the white matter, that is, increased number of oligodendroglial cells and heterotopic neurons. Our future investigations are focused on understanding oligodendroglial hyperplasia in the context of epilepsy.

References: [1] Schur et al., doi: 10.1111/bpa.12347; [2] Gibson et al., doi: 10.1126/science.1252304.

HLA ALLELES AND CUTANEOUS ADVERSE DRUG REACTIONS TO AROMATIC ANTIEPILEPTIC DRUGS

T. K. de Araujo[1], M. K. M. Alvim[2], C. L. Yasuda[2], F. R. Torres[1], F. Cendes[2], I. Lopes-Cendes[1]

[1]Department of Medical Genetics and Genomic Medicine, [2]Department of Neurology; School of Medical Sciences, University of Campinas (UNICAMP), Campinas, SP, São Paulo, Brazil; and the Brazilian Institute of Neuroscience and Neurotechnology (BRAINN), Campinas, SP, Brazil.

Introduction. Aromatic antiepileptic drugs (AEDs) such as carbamazepine (CBZ), lamotrigine (LTG) and phenytoin (PHT) are among the most common causes of cutaneous adverse drug reactions (cADRs). About 3% to 5% of the population is susceptible to develop a wide-ranging spectrum of cADRs, including mild maculopapular eruption, drug hypersensitivity syndrome, Stevens-Johnson syndrome (SJS) and toxic epidermal necrolysis (TEN) [1]. Since the human leukocyte antigen (HLA) B*15:02 allele was identified as a genetic marker for CBZ-induced SJS/TEN in the Chinese Han population [2], different association studies between varied AEDs-induced cADRs and the HLA alleles provided some guidelines for the safe use of AEDs in that specific population. Therefore, we aimed to determine if there is a genetic association between AEDs-induced cutaneous adverse drug reactions and HLA variants in the Brazilian population. **Materials and Methods:** This is a case-control study (30 patients with temporal lobe epilepsy with AEDs-induced cADRs and 200 AEDs-tolerant epilepsy patients as controls). The HLA genes were sequenced using the NGSgo® panel (GenDx, Utrecht) (Illumina), which provides an assay to obtain ultrahigh-resolution sequencing of 12 HLA Loci (HLA-A, -B, -C, -DRB1, -DQB1, -DPB1, -DQA1, -DPA1, -DRB3/4/5 e –G). The DNA libraries were loaded onto a MiSeq Sequencer (Illumina), and the data were analyzed with the NGSengine v. 2.15.0 software (GenDx). To date, we have completed sequencing of 12 patients with cADR (seven CBZ-cADRs, two CBZ and LTG-cADRs, two LTG-cADRs, and one PHT-cADRs) and 70 controls. Statistical analysis of relative allele frequencies was performed using an Excel spreadsheet; p-value and odds ratio (OR) were calculated using the R studio. We reported the HLA in the high-resolution system of 3-field. **Results and Discussion:** Initially, we found a difference between the frequencies of the alleles in HLA-B*38:01:01, HLA-C*02:02:02 and HLA-DQB1*06:03:01 between the group of patients and controls. However, after Bonferroni correction for multiple comparisons, this difference was not statistically significant ($p>0.05$). Furthermore, our findings do not confirm previous studies showing a clear association between cADR with CBZ and HLA-B*15:02 [2] and HLA-A*31:01 [3]. Indeed, these alleles were not found in our cohort of Brazilian individuals (cases and controls). Thus, indicating that the previous association results between specific HLA alleles and cADR in Asian individuals for HLA-B*15:02, and Europeans for HLA-A*31:01 may not be present in the Brazilian population. **Conclusion:** Although still preliminary, our results are relevant, since they indicate that recommendations for HLA testing which have been issued for other populations may not apply to Brazilian patients. In addition, as we complete the study in additional individuals, we may find other associations with different HLA alleles in our population. Our results are an important reminder that findings of genetic association for complex traits are influenced by ethnic characteristics and are not always transferable to individuals of distinct origins.

Supported by FAPESP

References: [1] Błaszczyk B et al., http://dx.doi.org/10.1016/j.pharep.2014.11.009; [2] Chung W et al. doi:10.1038/428486a; [3] McCormack M et al., doi: 10.1056/NEJMoa1013297.

IDENTIFICATION OF A 76,000 BP REGION IN CHROMOSOME 18 ASSOCIATED WITH A FAMILIAL FORM OF MESIAL TEMPORAL LOBE EPILEPSY

M.C.P. Athié[1], R. Secolin[1], A.S. Vieira[3], T.K. Araujo, M.E. Morita[2], C. Maurer-Morelli[1], M. Alvim[2], C.L. Yasuda[2], F. Cendes[4], I. Lopes-Cendes[2]

Department of Medical Genetics and Genomic Medicine, 2. Department of Neurology; School of Medical Sciences; 3. Department of Structural and Functional Biology, Institute of Biology; University of Campinas – UNICAMP, and 4. The Brazilian Institute of Neuroscience and Neurotechnology (BRAINN), Campinas, SP, Brazil.

Introduction: For more than 20 years our group study a familial form of mild epilepsy with most likely autosomal dominant inheritance. The family symptoms and neuroimaging findings are consistent to a mesial temporal lobe type of epilepsy (MTLE) with mesial temporal sclerosis (MTS), which is the most frequent focal epilepsy in the adult population and is characterized by epileptic discharges and histological abnormalities in the mesial structures of the temporal lobe. Although MTLE +MTS were classically considered as sporadic, in which environmental factors seemed to play a more relevant role, a linkage study of such family previously made by our group identified a candidate locus on the chromosome (ch) 18p11.31 [1]. Since 2016, with the rapid advancement of techniques for high-throughput genetic studies, we are revisiting this family (F-10) in order to identify more accurately the region possibly associated with MTLE and, perhaps, a causative genetic element. **Materials and Methods:** We performed a DNA SNP Array study of 25 members of F-10 family using Genome-Wide Human SNP Array 6.0 microarray chips (Thermo Fisher Scientific, USA). Quality control (QC) of SNP Array data was carried by the Genotyping Console software version 4.2 (Thermo Fisher Scientific, USA), using chips contrast as measure of QC after filtering against Homo sapiens (human) genome assembly GRCh37 (hg19). The chips data considered *In Bounds* were then analyzed for (ch) 18p11.31 region phasing and putative region identification. SNP array data was transformed by PLINK software [2], phased by SHAPEit software [3] and final analysis carried inside R environment, using pegas [4] and vcfR [5] packages for chromosome region visualization and comparison between groups. Chromosome Analysis Suite (ChAS) Software version 4.0 (Thermo Fisher Scientific, USA) was used for Copy Number Variation (CNV) analysis using non-affected family individuals as background and manufacturer filters for segment gain and loss. **Results:** Phasing of locus 18p11.31 showed a segregating chromosomic region spanning ≅ 76,000 base pairs (chr18: 4,770,146 – 4,846,270) among Familial MTLE and some family individuals with clinical history of seizures. The aforementioned region comprises a gene, regulatory sites and CNV spots. Subsequent CNV analysis showed no segment gain or loss segregating in family individuals with Familial MTLE in chromosome 18 and all other chromosomes. **Discussion/Conclusion:** The use of more advanced genetic techniques confirmed the presence of a region in the locus 18p11.31 that segregates in Familial MTLE individuals as well as some family members with clinical history of seizures. In this chromosomic region there is the sequence of a long non-coding RNA gene, AP005203.1, whose expression was detected in several neural regions in different transcriptomic studies deposited in public databases [6]. Also, such location might present some regulatory importance since it presents evidence of open chromatin, and diverse regulatory domains as enhancers biding sites, and CCCTC-binding factor (CTCF) biding sites. This way, the candidate region presents interesting characteristics that deserve to be explored further, once it could have had an impact in neuronal development and, therefore, some influence in the occurrence of Familial MTLE in the F-10 family.

References: [1] Maurer-Morelli C et al., doi: 10.3389/fneur.2012.00124; [2] Purcell S et al., doi: 10.1086/519795; [3] Delaneau O et al., doi: 10.1038/nmeth.2307; [4] Paradis E, doi: 10.1093/bioinformatics/btp696 [5] Knaus BJ et al., doi: 10.1111/1755-0998.12549.; [6] https://www.ebi.ac.uk/gxa/genes/ENSG00000266268?bs=%7B%22homo%20sapiens%22%3A%5B%22ORGANISM_PART%22%5D%7D&ds=%7B%22kingdom%22%3A%5B%22animals%22%5D%7D#baseline

IDENTIFICATION OF HAND GESTURES USING PATTERN RECOGNITION OF ELECTROMYOGRAPHY SIGNALS ACQUIRED WITH MYOARMBAND

Bruno G.Sgambato[1], Gabriela Castellano[1]

[1]Neurophysics Group, IFGW, UNICAMP.

Introduction: Identification of hand gestures is important in many fields, since this information can be easily integrated to already existing technologies as well as provide ground for novel applications' development. Together with pattern recognition systems, the electromyography (EMG) biosignal has been shown to be capable of providing enough information for high gesture recognition rates. This study aimed at reproducing these rates using classical (linear discriminant analysis - LDA, support vector machine - SVM, k nearest neighbors - K-NN) methods and neural networks (convolutional neural network - CNN, long short-term memory network - LSTM). **Materials and Methods:** Data were acquired using the MyoArmband system (www.support.getmyo.com). The device is worn like an armband below the elbow and has8 EMG detectors evenly spaced. It records the signal with a limited 100 Hz bandwidth and sends it via Bluetooth Low Energy (BLE) to a nearby capable device. Data from 8 participants were collected (CAAE 58592916.9.1001.5404). Each subject performed 10 times each of 5 hand gestures in random order. Subjects were instructed not to hold the gestures and to perform these naturally. The data were collected with a variable length window with no overlap; in the neural network approach it was scaled to a 420-points window. Accuracy was computed using k-fold cross validation with 8 folds. The folds were created in two different ways. In the first each fold was composed using individual subjects so the validation would be done on a previously unseen subject; we labeled this "Without Bias". In the second all data were shuffled so the same subjects appeared both in training and testing, labeled "With Bias"; this is the most prevalent method in the literature. For the classical approaches, features from the literature [1] were selected and fed to three classifiers: LDA [2], SVM and K-NN. The features chosen were root mean square (RMS), mean absolute value (MAV), slope sign change (SSC), waveform length (WL), zero crossings (ZC), Willison amplitude (WAMP) and cardinality (CARD), sample entropy (SampEn) and approximate entropy (ApEn) [2]. All possible combinations of features were tested. For the neural network approach, we used 1D-CNN and LSTM. The initial structured for both was based on the literature [3]. Most hyperparameters (convolution layers, polling and dense layers, filters, dropout, batch size, optimizers, weights, loss functions, enveloping points, windowing and data augmentation) were tested as possible, considering the used hardware limits.

Results:

	Accuracy (%) ± std of k folds				
	Classic methods			Neural Networks	
	LDA	SVM	K-NN	CNN	LSTM
With Bias	95 ± 2	95 ± 3	97 ± 2	95 ± 3	83 ± 3
Without Bias	75 ± 11	76 ± 11	73 ± 15	75 ± 12	70 ± 12

Discussion/Conclusion: We were successful in replicating the high accuracy rates found in the literature using the first validation approach despite the small and very natural dataset with little preprocessing. However, we recognize that the real challenge lies in achieving these same accuracy rates in never seen subjects. Nonetheless, the results showed that the classifiers were still able of high generalization of the contractions with results in the upper 70% for the second approach. Future work will be conducted to improve these approaches and propose new ones.

References: [1] Laezza, R.Master's Thesis, Chalmers University of Technology, Gothenburg, Sweden, 2018. [2] Sgambato, BG, Rev. Trabalhos de IC da UNICAMP, Campinas, SP, n.27, 2019. [3] Chen, X. et al. Biomedical Signal Processing and Control, 8(2), 184–192, 2013.

IDENTIFYING BIOMARKERS IN PATIENTS WITH ISCHEMIC STROKE: A METABOLOMIC PROFILE

D. C. Rosa [1], A. Donatti [1], F. S. Oliveira [1], A. B. Godoi [1], A. Canto [1], A. Sousa[2], W. M. Avelar [2], M. Q. Escobar [3], L. Tasic [3], I. Lopes-Cendes [1]

[1] Dpt. of Medical Genetics and Genomics Medicine, School of Medical Science, University of Campinas, Brazil; [2] Dpt. of Neurology, School of Medical Science, University of Campinas, Brazil, and the Brazilian Institute of Neuroscience and Neurotechnology (BRAINN); [3] Dpt. of Organic Chemistry, Institute of Chemistry, University of Campinas, Brazil.

Introduction: Stroke is caused by a blockage of the blood flow, resulting in neurological deficits [1]. Ischemic stroke (IS) is the most prevalent type, as it affects almost 85% of all stroke patients, whose most frequent subtype is atherosclerosis of large vessels [1- 3]. The effects of ischemia on the neural tissue worsen with the increase of the injured area, while tissue recoveries strategies, as vase recanalization, have a pivotal role to avoid the increase of ischemic events at the penumbra and to prevent further neural injuries [4]. Despite all clinical knowledge, there are no biomarkers to determine whether a given patient will

follow to the recanalization process, thus leading to clinical improvement, or he/she will get worse. One of the best ways to identify molecules present in a complex biological sample is the application of proton nuclear magnetic resonance (^{1}H NMR) in conjunction with the use of references in a databank and specific statistical strategies [5; 6]. Therefore, the present study aims to use ^{1}H NMR to determine the metabolomic profiles of plasma samples from patients in the acute and chronic stages of large vessels IS, and compared it with the profile of patients with as severe internal carotid stenosis, but no stroke, and healthy individuals. **Materials and Methods:** We used a 600 MHz^{1}H nuclear magnetic resonance to create a metabolomic profile of plasma samples from 20 control subject (with no stroke cases relatives and aged 50-plus), 20 patients with severe internal carotid stenosis, 20 patients in the acute and 20 patients in the chronic stages of large-vessel IS. The standardization of the ^{1}H NMR spectra is made using MestReNova (© 2014 Mestrelab Research S. L.) software and the statistical analysis is made on MetaboAnalyst (Xia Lab at McGill University) platform. The results of the metabolomic profiles will also be correlated with the NIH (National Institute of Health) stroke score variation, a measure of clinical evolution and prognosis. **Results:** To date, we have acquired ^{1}H NMR spectra from 19 patients with large vessel IS at the acute stage, 18 patients with large vessel IS at the chronic phase, 16 healthy individuals and 12 patients with severe internal carotid artery stenosis. The principal component analysis of the data indicated that the groups present similar structures and can be compared to each other. Furthermore, the partial least squares discriminant analysis has shown a good prediction for IS and the severe internal carotid artery stenosis group. We are currently working on the identification of specific metabolites, which could be used as biomarkers for the different groups. **Discussion/Conclusion:** This is a still ongoing study and to date we have observed qualitative and statistical differences in the metabolomic profile of patients in different stages of IS when compared with control subjects, which could be related to key metabolic pathways involved in the pathophysiological process. However, further analyses are still necessary to confirm which metabolites are included in each profile identified.

References: [1] Caplan LR, Stroke, NY: AAN, 1 ed., 2006; [2] Markus HS, doi: 10.1186/1741-7015-10-113; [3] Adams HP et al, doi: 10.1161/01.str.24.1.35; [4] Kunz A et al,doi: 10.1016/j.bpa.2010.10.001; [5] Puchades-Carrasco L et al, doi: 10.1016/j.copbio.2015.04.004; [6] Pavia, DL et al, Introdução à Espectroscopia, SP: CL, 4 ed., 2010.

IMPACT OF THE METHYLENE BLUE ON BEHAVIORAL AND MOLECULAR PATTERNS IN THE EMBRYOS MAINTENANCE AND ZEBRAFISH-SEIZURE MODEL

L.B.G. Ramos[1], J.A.A. Fernández[1], V.C. Fais[1], C.V. Maurer-Morelli[1]

[1]Zebrafish Laboratory, Department of Medical Genetics and Medical Genomics, FCM, UNICAMP.

Introduction and Hypothesis: Animal models of epilepsy and seizures are essential approaches to shed light on mechanisms underlying epilepsy in humans. Today, *Danio rerio*, popularly named as zebrafish, is recognized for modeling human diseases, and drug screening. Methylene Blue (MB) is often used as an antifungal in aquariums worldwide, and routinely incorporate in the embryo medium to maintain zebrafish safe. It is known that MB exerts an antioxidant and neuroprotective action. However, there is no study on whether MB can modify responses of experimental protocols, especially those involving oxidative stress response. Therefore, this study aims to investigate if MB can modify the behavioral and molecular pattern of the zebrafish induced to seizures. **Objective:** To investigate whether: (i) MB exposure, 24h prior to seizure-induced, can modify the behavior and molecular response of the zebrafish larvae; (ii) embryos raised in embryo medium with MBshow different response when submitted to seizures-induction; (iii) MB modify mRNA expression of *sod2, bcl2a, casp3*, and *c-fos* genes. **Materials and Methods:** To evaluate the influence of MB on seizures protocols:- Wild type larvae zebrafish at 6 days post-fertilization (dpf) will be randomly divided into (n=25 each group) - 1. MB AS – larvae exposed to 0.5μM MB for 24h before seizure-induced by pentylenetetrazole (PTZ) 15mM for 20 minutes (acute seizure protocol); 2. MB AS CG, animals, will be handled in the same manner as MB AS but in MB-water free; 3. MB SE- larvae exposed to 0.5μM MB for 24h before seizure-induced by pentylenetetrazole (PTZ) 15mM for 3h (status epilepticus protocol); 4. MB SE CG, animals, will be handled in the same manner as MB SE but in MB-water free; 5. MB CG - larvae exposed to 0.5μM MB for 24h but not exposed to the PTZ. *To evaluate the influence of MB on embryos maintenance*: Embryos will be raised in E3 medium + 0.1μM MB from fertilization to 7dpf prior to 15mM PTZ exposure. Larvae will be divided into (n=25 each group) -1. AS- larvae at 7 dpf will be exposed to PTZ 15mM for 20 minutes; 2. SE- larvae at 7dpf will be exposed to PTZ for 3h; Control groups for AS e SE will be handled in the same manner, but animals in these control groups will raise in E3 medium free of MB. At 7dpf larvae from CG AS and CG SE will be exposed to PTZ 15mM.For all groups described above, behavior patterns will be monitored using the Danio Vision System and evaluated by the Ethovision Software. Animals will be euthanized, and their heads collected for total RNA extraction. RT-qPCR (n=5 each group) will run in triplicate to investigate genes related to different molecular pathways: *sod2* – antioxidant; *casp3 and bcl2a* – apoptosis, and *c-fos* – as a marker for neuronal activity. The mRNA transcript levels of the target genes will be normalized by the housekeeping gene *eef1a1a*. The relative quantification (RQ) will be calculated by the equation RQ=2 –ΔΔCT. Statistical analyses will be performed by Mann-Whitney test and significance considered when $p \leq 0.05$. **Relevance:** MB is commonly used to maintain the zebrafish colony, especially embryos and larvae. Due to its antioxidant and neuroprotective capacity, the MB may alter the cellular responses, mainly those related to oxidative stress. Today, none studies indicate if MB can modify experimental responses. **Support:** FAPESP- BRAINN 2013/07559-3 and PIBIC-CNPq.

IN VIVO NONINVASIVE DETERMINATION OF OPTICAL AND DYNAMICAL PROPERTIES OF TISSUE WITH DIFFUSE OPTICAL SPECTROSCOPY

G. G. Martins[1], R. C. Mesquita[1]

[1]Institute of Physics, UNICAMP.

Introduction and Hypothesis: Light scattering in biological tissue is predominant over absorption for near-infrared radiation. One can characterize such highly scattering media by their optical and dynamic properties, related to the concentration and the mean square displacement of the medium constituents that interact with the radiation, respectively. In the near-infrared range (~650-900 nm), absorption is mainly due to hemoglobin molecules. Thus, diffuse optical spectroscopy (DOS) techniques are able to measure hemoglobin concentration, therefore quantifying tissue oxygenation, as well as the mean square displacement of red blood cells, which can be associated with blood flow [1]. This capability allows DOS to be widely used for *in vivo* applications. However, the accuracy in determining optical and dynamic parameters has limitations, which may lead to misinterpretation based on unreliable results with high uncertainty. The techniques obtain the optical parameters by modeling the scattered light intensity with approximations about the medium. Such approximations, mostly related with the geometry or the composition of the medium, are not always experimentally accurate, which results in innacurate optical parameters estimation [2,3]. In this context, it is desirable to increase the accuracy of the estimated optical parameters in order to increase the confidence and the range of clinical applications of DOS in the medical sciences. **Objective:** The goals of this research project are: *i)* to develop standard optical properties as reference for several tissues (*i.e.,* brain and muscle) under healthy conditions, and *ii)* to quantify the sensitivity of the optical parameters to diagnose vascular diseases. We will achieve these goals by developing novel methods through more detailed modeling of light propagation in tissue and with machine learning algorithms. **Materials and Methods:** The first step of the project is to study analytical models to obtain the optical parameters based on the collected light intensity. We will study the models available in the literature, test them with data collected in previously calibrated phantoms, and improve their reliability on extracting meaningful information from the biological tissue. Then, we will choose the most stable model that best fits test data and use this model to collect biological information in volunteers. We will collect all data with a commercial system (Imagent, ISS, Inc.) with 8 near-infrared light sources and 4 detectors. In the second stage, we will collect optical properties of different biological tissues (several regions of head and muscle) on 200 healthy subjects during resting state and classify these values according to age, gender and ethnicity, checking the dependency of the properties according to these cofactors. In the final step, we will use the values from these *optical atlas* to quantify the sensitivity of the optical properties to detect carotid stenosis. To this, we will collect data on 50 carotid stenosis patients and compare the obtained optical parameters with optical atlas values. **Relevance:** Diffuse Optical Spectroscopy techniques are noninvasive, affordable, portable and can provide physiological information with high temporal resolution [1]. However, the techniques heavily depends on its accuracy to obtain optical and biological parameters [2], which

currently is not good enough. This work proposes to develop novel methods based on light propagation and machine learning to improve the estimation of these parameters, and test its usefulness as potential biomarkers in a vascular disease.

References: [1] T. Durduran et al., doi:10.1088/0034-4885/73/7/076701; [2] A. Kienle et al., Applied Optics, 37(4): 779-791, 1998; [3] L. Gagnon et al., Optics Express, (16)20: 15514-15530, 2008.

INCREASED NUMBER OF FUNCTIONAL CONNECTIONS DURING RESTING-STATE REVEALED BY COMPLEX NETWORKS ANALYSIS FOLLOWING HANDS MOTOR IMAGERY PRACTICE

C. A. Stefano Filho[1,3], R. Attux[2,3], G. Castellano[1,3]

[1]Neurophysics Group, IFGW, UNICAMP, [2]Lab. if Signal Process. for Communications, FEEC, UNICAMP, [3]BRAINN.

Introduction: Motor imagery (MI) has been increasingly employed in brain--computer interfaces and in motor rehabilitation applications [1]. Although it has been assumed that MI and motor execution share activation sites on the primary sensorimotor cortex (PMC), recent studies have revealed that the participation of other areas, such as the parietal and even prefrontal cortices, may be important as well [2,3]. Nevertheless, MI training protocols are usually restricted to features from the PMC. To deepen the understanding of this issue, we investigated functional connectivity (FC) alterations following MI practice in resting-state functional magnetic resonance imaging (RS-fMRI) data of participants that underwent extensive MI practice, aiming to analyze where such alterations occurred. **Materials and Methods:** Ten healthy subjects (mean age 22 ± 3 years old; 8 men) underwent 12 hands MI practice sessions with no feedback, having their brains scanned through MRI before the first session and after the last. In each session, participants executed both right- and left-hand MI tasks guided through a graphical interface, alternating task and rest blocks, with each session lasting for 640 s split into five 128 s-runs. RS-fMRI data were modeled as a graph based on the functional atlas introduced by Power *et al.* [4]. Pre- and post-MI sessions adjacency matrices (AMs) were calculated through Pearson's correlation, maintaining only the 30% strongest connections for each participant. Group AMs were estimated by considering only common connections across subjects. Each node's degree was calculated from these matrices, and its variation between fMRI scans was investigated. **Results, Discussion and Conclusion:** Statistically significant degree variations ($p < 0.05$, t-test) were found for the parietal (PL) and occipital (OL) lobes (Fig. 1A). A graphical representation over the cortex (Fig. 1B) shows that this increased number of connections was bilateral and more spread for the OL, whereas, for the PL, it was more localized. Although MI is commonly linked to the PMC, our study suggests that an increased number of connections occurred at other cortical sites: visual integration is reinforced by the results for the OL, and parietal participation (agreeing with [3]) also was present in MI practice. Therefore, when designing MI experimental protocols, information from areas beyond the PMC should not be overlooked. These results question the well-established approach of restraining the useful MI information to the primary motor areas.

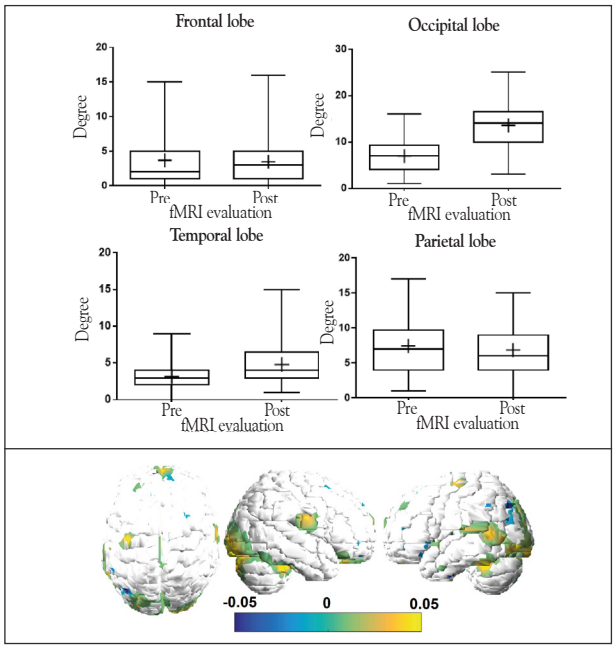

Figure 1. (A) Boxplot for the degree in the pre- and post-fMRI evaluations, per lobe. (B) Degree variations plotted over the cortex. The color scale indicates a percentage scale in relation to the first evaluation (i.e., 5 % increases or decreases).

References: [1] Mokienko OA et al., doi: 10.1007/s11055-014-9937-y; [2] Castro MCF et al., doi: 10.1109/BRC.2014.6880972; [3] Oostra KM et a., doi: 10.3389/fnbeh.2016.00005; [4] Power JD et al., 10.1016/j.neuron.2011.09.006.

INFLUENCES OF JOINT ANGLE AND VISUAL FEEDBACK ON MUSCLE FORCE CONTROL

E. P. Zambalde[1,2], C. M. Germer[2,3], L. A. Elias[1,2]

[1]DEEB, FEEC, UNICAMP [2]Neural Engineering Research Laboratory, CEB, UNICAMP [3]DEBM, UFPE.

Introduction: Many factors influence how the motor system controls force generation, and the analysis of muscle force variability is of paramount importance to understand the neurophysiological control of movement. For instance, it is well known that low-frequency fluctuations of the neural drive to the muscle (i.e., the discharge times of a population of motor units) largely influence force steadiness [1]7.5% and 10% of the maximal force. Spike trains of a total of 222 motor units were identified from the EMG recordings with decomposition algorithms. Principal component analysis of the smoothed motor unit discharge rates indicated that one component (first common component, FCC. Also, visual feedback [2]and visual feedback may be processed differently based on the body effector where feedback-based corrections are used. This study compared the effect of changes in visual gain on the control of steady-state force at the elbow and ankle. Ten subjects produced steady-state isometric force to targets at 5 and 40% of their maximum voluntary contraction at seven visual gain levels. Visual gain was used effectively at both joints to reduce variability of the force signal and to improve accuracy, with a greater effect of visual gain at the elbow than the ankle. Visual gain significantly decreased the regularity of force output, and this effect was more pronounced at the elbow than the ankle. There were accompanying changes in the proportion of power in the 0-4, 4-8, and 8-12 Hz frequency bins of the force signal across visual gain at the elbow. Changes in visual gain were accompanied by changes in both agonist and antagonist electromyographic (EMG and joint angle [3]isometric, plantarflexion contractions, physiological tremor increases as the ankle joint becomes plantarflexed. Modulation of physiological tremor as a function of muscle stretch differs from that of the stretch reflex amplitude. Amplitude of physiological tremor may be altered as a function of reflex pathway gains. Healthy humans likely increase their γ-static fusimotor drive when muscles shorten. Quantification of physiological tremor by manipulation of joint angle may be a useful experimental probe of afferent gains and/or the integrity of automatic fusimotor control. Abstract: The involuntary force fluctuations associated with physiological (as distinct from pathological can alter force variability, since they change both the presynaptic signals that command the motoneurons and the configuration of the controlled biomechanical system. The present study aims to investigate the combined effect of joint position and visual feedback on the force control of an intrinsic hand muscle at different contraction intensities. **Materials and Methods:** Fourteen subjects (29±2.84 yrs., 6 males) were recruited to the experiment, which was approved by ethics committee. The index finger abduction force was recorded using a three-axis force transducer. At the beginning of the experiment, the maximum voluntary contraction (MVC) was estimated at three different joint angles: 0° (i.e., fully extended), +15°, and -15°. In the subsequent trials, each subject was asked to perform isometric abduction contractions at six submaximal force targets (5-75% MVC). Isometric contractions were performed with and without visual feedback (random order) in the same trial. Each block of six submaximal contractions were performed at the three joint angles described above. Joint angles and force levels were randomly presented to the subject. Force variability was measured as the standard deviation (SD). A relation between force SD and the mean force (referred to as the signal dependent noise, SDN [4]a model was constructed and its output compared with the empirical data. SDN was evident in voluntary isometric contractions as a linear scaling of force variability (SD) was estimated for each joint angle and visual feedback condition. An analysis of covariance (ANCOVA) was performed to evaluate the statistical significance of the SDN results, while an analysis

of variance (ANOVA) was applied to MVC data. Multiple comparisons were corrected with Bonferroni post-hoc test. The significance level was 0.05 for all statistical analysis. **Results:** Significant difference was found between the MVC produced at three joint angles ($p<0.001$). When the index finger is adducted (-15°), the force produced is higher (21.04±1.87N) than when it is fully extended (15.16±1.38N) or abducted (11.49±0.90N). SDN analysis showed that force SD depends on the mean contraction intensity. The ANCOVA showed a statistical significance in the SDN for both visual feedback ($p<0.001$), and joint angles, so that the scaling of force SD with the mean force is different between +15° and -15° ($p=0.010$). **Discussion/Conclusion**: When a muscle is stretched a higher force is produced due to either the elastic passive property of muscle fibers or the increased afferent inflow from stretched muscle spindles. Conversely, when muscular fibers are shortened the force is reduced as a result of a low interaction between myosin and actin molecules. The difference in the SDN observed for the two joint angles and visual feedback conditions might be due to changes in presynaptic signals impinging into the motor nucleus, but the neural determinants should be further evaluated by recording the activity of a population of motor units.

References: [1] Negro F et al., doi: 10.1113/jphysiol.2009.178509. [2] Prodoehl J et al., doi: 10.1007/s00221-009-1966-3. [3] Jalaleddini K et al., doi: 10.1113/JP274899. [4] Jones KE et al., doi: 10.1152/jn.2002.88.3.1533.

INTEGRATIVE TRANSCRIPTOMICS AND PROTEOMICS ANALYSIS OF DIFFERENT HIPPOCAMPUS REGIONS FROM THE PILOCARPINE MODEL OF MESIAL TEMPORAL LOBE EPILEPSY

Amanda M. do Canto[1,2], Alexandre H. B. de Matos[1,2], Alexandre B. Godoi[1,2], André S. Vieira[2,3], Beatriz B. Ayoama[2,3], Cristiane S. Rocha[1,2], Barbara Henning[1,2], Benilton S. Carvalho[2,4], Diogo F. T. Veiga[5], Rovilson Gilioli[6], Fernando Cendes[2,7], Iscia Lopes-Cendes[1,2]

[1.] Department of Medical Genetics and Genomic Medicine, School of Medical Sciences. [2.] University of Campinas – UNICAMP and the Brazilian Institute of Neuroscience and Neurotechnology (BRAINN), Campinas, SP, Brazil; [3.] Department of Structural and Functional Biology, Institute of Biology. [4.] Department of Statistics, Institute of Mathematics, Statistics and Scientific Computing; [5.] The Jackson Laboratory for Genomic Medicine, CT, USA; [6.] Laboratory of Animal Quality Control; University of Campinas – UNICAMP, Campinas, SP, Brazil; [7.] Department of Neurology, School of Medical Sciences.

Introduction: Mesial temporal lobe epilepsy (MTLE) is a chronic neurological disorder characterized by the occurrence of seizures and by histopathological abnormalities in the mesial temporal lobe structures, mainly hippocampal sclerosis (HS). We used a multi-omics approach to determine the profile of protein and gene expression in the dorsal and ventral hippocampus dentate gyrus (DG) and *Cornu Ammonis* 3 (CA3) in an animal model of temporal lobe epilepsy induced by pilocarpine. **Materials and Methods:** *Label-free* proteomics (LC-MS/MS – Cetics Butantan Institute) and RNAseq (*TruSeq Stranded Total RNA* (Illumina®)) were performed from laser-microdissected tissue isolated from the pilocarpine-induced male Wistar rats 15 days after epilepsy induction ("latent phase"). The DG and CA3 were divided into dorsal and ventral and the four subfields were analyzed independently. We performed a data integration analysis that evaluated the enriched signaling pathways and the integrated networks generated based on the gene ontology processes. **Results:** We found differences between the proteomic and the transcriptomic profiles of the DG and the CA3 portions of the hippocampus. In addition, DG and the CA3 profiles also differ from each other. Moreover, our data reveal that the epileptogenesis processes are predominantly occurring in the CA3 region, which shows more abnormalities in both RNA and protein levels. In addition, our results suggest the involvement of several mechanisms in the epileptogenesis of the pilocarpine model, including **i)** regulation of the excitatory imbalance in the neurons through NMDA receptors, **ii)** changes in the serotonin signalling, **iii)** neuronal activity controlled by the CamKs regulation, **iv)** the LRRK2/WNT signalling pathways, and **v)** the involvement of a set of non-coding RNAs that have never been associated with epilepsy. **Discussion/Conclusion**: This is the first multi-omics study addressing the mechanisms underlying the epileptogenesis of the pilocarpine model. Our results highlight the benefits of high-throughput omics techniques in the study of complex disorders and the advantage of obtaining tissue from delimitated areas to fully appreciate the large biological heterogeneity of different cell populations within the central nervous system. In addition, we obtained evidence suggesting that the epileptogenesis processes in the pilocarpine model is highly enhanced in the CA3 region.

INTERVENTION FOR VIRTUAL REALITY AND PHYSICAL EXERCISE IN BALANCE, MOBILITY AND COGNITION IN ELDERLY

Thaís Sporkens Magna[1,4], Alexandre Fonseca Brandão[2,3], Paula Teixeira Fernandes[1,3,4]

[1]College of Medical Sciences, State University of Campinas- UNICAMP, Campinas, São Paulo, Brasil. [2]Institute of Physics Gleb Wataghin, UNICAMP, Campinas, São Paulo, Brasil. [3]Brazilian Institute of Neuroscience and Neurotechnology – BRAINN, Campinas, São Paulo, Brasil. [4]Sport's Psychology and Neurosciences Study Group – UNICAMP, Campinas, São Paulo, Brasil.

Introduction: Physical exercise (PE) associated with virtual reality (VR) is an innovative method in the rehabilitation process, is safe and feasible. This study aims to show if there is a significant improvement in balance, gait, cognitive function and functional performance of the elderly with PE and VR therapy. **Methodology**: 31 elders divided in 3 groups Group 1 - VR; Group 2 - Virtual Reality and Physical Exercise (VRPE); Group 3 - Physical Exercise (PE). The groups with VR performed procedures with the virtual puzzle software GesturePuzzle [1], and the groups with PE performed a walking activity. Instruments for evaluation: Dynamic Gait Index, Clinical Sensory Interaction and Balance Test, Memory Pictorial Test and Alternate Attention Test. **Results:** In the attention variable [F time (1, 28) = 77.75 points], all groups increased the mean score after the intervention period. For memory [F time (1, 28) = 17.85 points], confidence intervals demonstrated that statistically significant differences occurred in the VR and VRPE groups. Regarding balance [F time (1, 28) = 135.00 seconds], all groups increased the score after the intervention period. Finally, the confidence intervals revealed that the PE and RVEF groups improved gait after the intervention period [F time (1, 28) = 17.86 points]. **Discussion:** VR has a good acceptance by the elderly, who are more motivated during the intervention, breaking the barriers of technology use, reducing social isolation and increasing the autonomy for technological devices. There is good acceptance and greater motivation on the part of the elderly when they come into contact with VR, breaking down the barriers of technology, indicating that they can use it for other purposes [2]. **Conclusion:** The interventions by VR and FE proved to be effective for the improvement of balance, gait, attention and memory. Therefore, we can conclude that the intervention by VR associated with PE improves the functional physical performance in the elderly. **Keywords:** elderly, virtual reality, physical exercise.

References: [1] BRANDÃO, AF; DIAS, DRC; GUIMARÃES, MP; TREVELIN, LC; PARIZOTTO, NA; CASTELLANO, G. GestureCollection for Motor and Cognitive Stimuli: Virtual Reality and e-Health prospects. J. Health Inform. 2018, 10(1): 9-16. ISSN 2175-4411 http://www.jhi-sbis.saude.ws/ojs-jhi/index.php/jhi-sbis/article/view/544/325 [2] ROBERTS, AR; De SCHUTTER, B; FRANKS, K; RADINA, ME. Older adults' experiences with audiovisual virtual reality: Perceived usefulness and other factors influencing technology acceptance. Clinical gerontologist, 2019; 42(1), 27-33. https://doi.org/10.1080/07317115.2018.1442380.

INVESTIGATION OF TRANSCRIPTOME CHANGES IN VENTRAL HIPPOCAMPAL NEURONAL POPULATIONS FOLLOWING ACUTE SEIZURES GENERATED IN ANIMALS WITH DEPRESSIVE BEHAVIOR INDUCED BY SOCIAL DEFEAT

G.G; Zanetti[1], E. V. Dias [1], I. Lopes-Cendes[2], A. Vieira[1]

[1]Department of Structural and Functional Biology, [2]Department of Medical Genetics, School of Medical Sciences, University of Campinas (UNICAMP); and the Brazilian Institute of Neuroscience and Neurotechnology (BRAINN), Campinas, SP, Brazil. [4]Multidisciplinary Center for Biological Investigation (CEMIB); University of Campinas (UNICAMP), Campinas, SP, Brazil.

Introduction and Hypothesis: Depression is a very common and recurrent mental disorder nowadays, impairing the daily life and well-being of the individual. Induction of depressive behavior through social stress is already well established in the literature, highlighting the social defeat stress model (EDS) in rodents, using social interaction to analyze depressive behavior. The ventral hippocampus is one of the most studied structures in depression, due to its neuroplasticity and key role in the limbic system. In addition, the ventral hippocampal cell layers show different functions when related to behavior, making their separation very important. Another disease that commonly affects the hippocampus is epilepsy, being noteworthy its frequent association with depression. The hypothesis is that with RNAseq and laser microdissection of specific hippocampus cell populations we can find molecular mechanisms related to depression, resilience, and mechanism related to depression and epilepsy. **Objective:** To investigate biological processes and the respectives molecular componentes in different ventral hippocampus subregions, associated to depression condition and resilience (animals that suffer from social defeat, but does not demonstrate depressive behavior), and the effect of seizures um

both conditions. **Materials and Methods:** To accomplish this, the protocol of social defeat, laser microdissection and RNAseq will be used for the analysis of the transcriptome, which can quantify and analyze the heterogeneity of the hippocampal layers. **Relevance:** The relevance is to outline a transcriptomic profile of different ventral hippocampus subregions in stress induced depression, and resilience, noting that such data collection has never been done in the neural circuit, separating the different neuronal layers in this model or in other models of depression. Moreover, the generated data would indicate genes related to resilience, possibly suggesting mechanisms responsible for the resistance to depressive behavior, and also the relation of epilepsy and depression.

KINECT ONE MOTION CAPTURE IN SUPPORTING REHABILITATION OF PATIENTS AFTER STROKE

L. R. Scudeletti[1], D. R. C. Dias[2], A. F. Brandão[3,4], J. R. F. Brega[5]

[1]Master Program, São Paulo State University, UNESP; [2]Computer Science Dept, Federal University of São João del-Rei, UFSJ; [3]Neurophysics Group, University of Campinas, UNICAMP; [4]Brazilian Institute of Neuroscience and Neurotechnology, BRAINN; [5]Interfaces and Visualization Laboratory, São Paulo State University, UNESP.

Introduction and Hypothesis: Cerebrovascular accident (CVA) also known as stroke is one of the diseases that most kills and disables people in the world, affecting men, women and children of all ages. Among the challenges faced by specialists in the rehabilitation process is the difficulty in obtaining accurate data on the evolution of the patient and the monotony of rehabilitation sessions, which causes some patients to give up or not to undergo rehabilitation sessions with the necessary attention [1]. Thus, this study aims to support specialists in obtaining more accurate information about the patients' stages of evolution, also motivating patients to perform the exercises, applying challenges and goals in the activities that will be performed in rehabilitation. **Objective:** This study proposes the projection and development of a system that includes the following functionalities: i) capture the movements generated by the patient and perform the transposition, in real time, to a virtual skeleton; (ii) enable the specialist to capture only specific members or groups of members; iii) measure the amplitude (ROM) of the movements performed; iv) and calculate the percentage of successes and mistakes of movements performed by the patient in relation to movements performed by the specialist. **Materials and Methods:** The motion capture is performed using the Kinect One device, which allows tracking without the use of markers, because it projects a grid of infrared points through the space in front of it and captures the reflections of these points when they collide with objects, calculating how long each point emitted takes to be reflected back to the device, allowing the tracking of up to 25 joints coordinates in 3D space [2]. To build the system will be used the C# language, which is the same language whose Kinect SDK is developed, which enables greater compatibility with the device, and allows the use of Windows Presentation Foundation (WPF) in the construction of layouts and visualizations, allowing the construction of a system with modern design, responsive and good usability [3]. **Relevance:** Data from the World Stroke Organization (WSO) [4] show that every year around the world 13.7 million people have a stroke, about 5.5 million of them die and another 5 million have some sort of disability. In addition, it is estimated that one in six people in the world will have a stroke during their lifetime. Due to these alarming data and the difficulties encountered, it is reasonable the interest in the development of new applications to assist stroke treatment, aiming to support specialists in decision-making about the appropriate treatment, as well as motivating patients to attend regularly rehabilitation sessions.

References: [1] Langhammer, B. Physiotherapy after stroke, 2017, ISBN 978-3639071337; [2] RODRIGUES, J. et al, 2016, DOI: 10.4018 / 978-1-5225-0435-1; [3] Microsoft, 2017, available at <https://docs.microsoft.com/en-us/dotnet/csharp/>; [4] WSO Annual Report 2019, available at <https://www.world-stroke.org/about-wso/annual-reports>.

LASER CONTRAST SPECKLE IMAGING (LCSI) FOR FUNCTIONAL STUDIES IN THE ZEBRAFISH BRAIN

I. C. Galvão[1], T. C. de Moura[1], G. H. Scavariello[2], R. C. Mesquita[2], C. V. Maurer-Morelli[1]

[1] Zebrafish Laboratory, Department of Medical Genetics, School of Medical Sciences – UNICAMP, [2]Neurophysics Group, IFGW, UNICAMP.

Introduction and Hypothesis: Zebrafish is an animal model with many advantages in research, including high fecundity, external development, high genetic homology to humans, and embryo/larvae transparency allowing direct observation of organs/tissues. This model has been widely used for seizures studies and also for the study of cerebrovascular diseases, like stroke. The Laser Contrast Speckle Imaging (LCSI) is a technique that can monitor the motion of scattering particles by measuring the blood flow, thus representing an important tool for investigation of spatial and temporal changes in the brain. In light of this, we expect to adapt and implement this system to detect possible changes in zebrafish brain blood flow associated with seizures. This project is an exploratory study that may provide a functional tool for identifying changes after genetic manipulation or for screening for seizure suppression compounds. **Objective:** to adapt and implement a new tool for functional studies in the zebrafish brain. **Materials and Methods:** In the LCSI, briefly, a high coherence laser is guided to the sample, and the reflection pattern, which changes according to the movement of the light-shattering particles (red blood cells for an infrared laser), is detected with a CCD camera. Therefore, it is possible to associate the light intensity variation. For the optical apparatus, which is being developed in IFGW, we will use as a light source a high coherence (> 3 m) diode laser at 830 nm and an optical lens to homogenize the light over the region of interest of the sample. The detection is done by a low-cost webcam, remotely controlled by a computer. Images are taken in a field of view of up to 20 mm x 20 mm, distributed over a set of 1080 x 1080 pixels (each pixel is approximately 0.02 mm). At first, larvae immobilization will be with agarose, but alternatives include glass slides. For this, zebrafish larvae at 5 to 7 days post-fertilization will be anesthetized with 0.02% tricaine and immobilized with d-tubocurarine (10μM) and allocated to the immobilization platform, which must contain maintenance solution (water or convulsive agent solution). For the functional experimentation, the larvae will be divided into a seizure group, which will be exposed to pentylenetetrazole (PTZ) 15mM (convulsing agent), and the control group, which will be manipulated in maintenance water without PTZ (n=5 each group). **Relevance:** LSCI is a tool to monitor spatial and temporal changes in the brain using blood flow. Therefore, it has the potential to step forward our studies in seizures and screening of new compounds for seizure suppression. Besides, the LSCI adapted to the zebrafish brings new perspectives of investigations, considering that this little fish is a valuable model for studying many other human brain diseases such as stroke. **Support:** FAPESP- BRAINN 2013/07559-3 and PIBIC-CNPq.

LINEAR CLASSIFIER VS. MLP FOR FOUR-CLASS DISCRIMINATION IN EEG SIGNALS

Larissa R. Azevedo[1], Victor D. Nascimento[1], Harlei M. A. Leite[1,2], Sarah N. Carvalho[1,2]

[1]Federal University of Ouro Preto (UFOP) – Brazil. [2]Brazilian Institute of Neuroscience and Neurotechnology (BRAINN) – Brazil.

Introduction: Brain-computer interface (BCI) is a closed-loop system that establishes communication between a brain and an application of control or communication, making this innovative human-computer interaction useful in the development from assistive technologies to entertainment. In this study, we have analyzed and compared the performance of a BCI based on steady state visually evoked potentials (SSVEP) employing two approaches of classification - a linear discriminant and a neural network. **Materials and Methods:** The brain signal was acquired by electroencephalography (EEG) from 32 health subjects, with 8 repetitions for every visual stimuli of 12 s each. Four visual stimuli were projected by a monitor at frequencies 6, 10, 12 and 15 Hz [Leite *et al.*, 2018]. The preprocessing consisted of application of a notch filter at 60 Hz, a passband filter (5 – 100Hz) and a digital filter based on Common Average Reference (CAR). The features of the EEG were extracted in windows of 2 s without overlap employing the Fast Fourier Transform (FFT) algorithm, considering the magnitude of signal at frequencies of stimulation. The classification was realized by a linear classifier based on the least squares (LC) and a Multi-Layer Perceptron (MLP) with two hidden layers, each with 512 neurons and the output layer with four neurons. **Results:** Tables 1 and 2 show the average hit rate applying the 10-cross-fold validation for each subject using the BCI system

Table 1. Accuracy employing the LC.

Subject	1	2	3	4	5	6	7	8	9	10	11	12	13	14	15	16
Accuracy (%)	86	19	27	49	36	37	28	83	35	62	65	88	29	53	24	58
Subject	**17**	**18**	**19**	**20**	**21**	**22**	**23**	**24**	**25**	**26**	**27**	**28**	**29**	**30**	**31**	**32**
Accuracy (%)	55	40	57	64	45	25	31	39	33	43	69	53	53	92	40	91

Table 2. Accuracy employing the MLP.

Subject	1	2	3	4	5	6	7	8	9	10	11	12	13	14	15	16
Accuracy (%)	84	24	27	47	35	36	31	79	40	67	67	88	29	52	26	60
Subject	**17**	**18**	**19**	**20**	**21**	**22**	**23**	**24**	**25**	**26**	**27**	**28**	**29**	**30**	**31**	**32**
Accuracy (%)	56	51	48	70	60	29	47	43	32	53	75	43	44	91	43	89

with the linear classifier and the MLP, respectively. The average accuracy was 50.3±17.2 % for the LC and 52.1±16.4% for the neural network. **Discussion/Conclusion**: The results show that both classifiers are able to discriminate the four classes of visual stimuli with an accuracy of about 50%. The average performance employing the MLP is slightly higher than employing the linear classifier. However, the difference of accuracy is within the standard deviation presented. The high standard deviation is due to the large variation in performance among subjects, ranging from over 90 for Subject 30 to practically the randomization rate for the Subject 2. But, the performance of the subjects between the techniques was practically the same, the subjects with the highest variability (9 or more) were: 18, 21, 23 and 26 (with better performance with MLP) and 19, 28 and 29 (with better performance using linear).Thus, the simplicity of the linear classifier and its low computational cost make this approach more attractive for BCI-SSVEP systems. **Acknowledgements:** The authors thank CNPq, Fapesp and UFOP for the financial support.

Reference: [1] LEITE, H. M. A., et al. Analysis of user interaction with a brain-computer interface based on steady-state visually evoked potentials: case study of a game. Computational intelligence and neuroscience, v. 2018, 2018.

MEASURING BRAIN ACTIVITY IN NATURAL SETTINGS WITH A WEARABLE OPTICAL SYSTEM

G. H. Scavariello[1], G. A. Dollevedo[1], R.C. Mesquita[1]
[1]Institute of Physics, UNICAMP.

Introduction and Hypothesis: Near-Infrared Spectroscopy (NIRS) is a safe, non-invasive optical technique which can continuously measure cerebral oxygenation using near-infrared light. NIRS allows for both miniaturization as well as uses outside of controlled environments, and the development of wearable NIRS devices is considered a big step in functional neuroscience [1]. Wearable systems allow functional experiments to be performed in settings which do not restrict the subject and thus provide results which can be more representative of a real, or natural, setting. In addition, there are no mainstream wearable NIRS systems developed in Brazil as of today. Our lab has pioneered the development and application of NIRS in Brazil and, in the spirit of continuing in this position, we propose to build and validate an inexpensive wearable NIRS system in the country. **Objectives:** The project's objectives can be divided into two phases. In phase 1, we plan to construct a working prototype of a wearable system. This phase consists of the selection and integration of optical and electronic components, and the prototype characterization. Phase 2 is focused on validating the characterized prototype by comparing the results obtained from simultaneous measurement with a commercial system. In this phase, we also plan to perform a proof of concept by collecting data in a natural setting. **Materials and Methods:** A NIRS measurement consists of shining light into biological tissue and collecting the scattered light a certain distance away. Since biological tissue is highly scattering, the light will be diffusively spread through the tissue, and eventually comes back towards the surface. The collected light retains information regarding the tissue's oxygenation, and the distance between the source and the detector determines the depth penetration of light. Although wearable NIRS systems have been built elsewhere, most of them share common disadvantages such as being expensive and not having short-separation channels [2]. These channels are essential to understanding NIRS signals because they allow for the removal of extra-cortical contaminations. The essence of this project is to build a truly wearable NIRS system, *i.e.*, a system in which the subject does not carry any extra weight such as heavy laptops. For that, we will build a modular system where each module will have a set of LED light sources and Silicon Photodiode detectors in a range of distances that should allow for brain measurements and for short separation channels. Each module will be able to either work as a standalone version or as a group of several channels and will have an array of adjustments to fit most types of subjects. A wireless microcontroller will manage data acquisition and adjust the modules via Wi-Fi as necessary through a clinical-friendly graphical user interface. **Relevance:** Most functional neuroscience experiments impose physical/spatial constraints on the subject. As a consequence, results regarding real-life situations obtained in these settings can be limited. Despite the growing need in functional neuroscience for means of measuring subjects in natural environments, there are no mainstream wearable systems developed in Brazil as of today. By constructing an inexpensive system, we plan to trail a path for the growth of functional neuroscience in the country, which will impact studies in social, behaviour and cognitive sciences.

References: [1] Ferrari, M. et al; doi:10.1016/j.neuroimage.2012.03.049; [2] Zhao, H. et al; doi:10.1117/1.NPh.5.1.011012

MICROFLUIDIC SETUP FOR EEG AND ECG ANALYSIS USING ZEBRAFISH LARVAE

[1]Parolari T.G, [3]Gomes V.P, [1]Fais V.C, [2]Peixoto N, [3]Panepucci R.R, [1]Maurer-Morelli C.V
[1]Zebrafish Laboratory, Department of Medical Genetics and Medical Genomics, FCM, UNICAMP, [2]Electrical and Computer Engineering Department - George Mason University, Fairfax, VA, [3] The Center for Information Technology Renato Archer, Campinas-SP.

Introduction and Hypothesis: Animal models have been contributing to the development of new drugs and compounds, toxicity tests, and trials for innovative treatments (1). Zebrafish is a well-accepted model for human disease modeling, genetic assay, preclinical studies, and drug screening with many advantages over other models, especially for the capacity to provide multi-sample studies due to its small size. Therefore, experimental setups using parallel systems can increase data collection while reducing the time to reach the results. Zebrafish is an advantageous model for electrographic studies since it resembles many electrical aspects found in mammals in physiological or pathological conditions. This is an exploratory study. **Objectives:** 1. to implement a scalable and simplified electrophysiological setup for simultaneous neuronal and cardiac data (EEG / ECG) data collection. 2. to validate the setup by applying it to the zebrafish seizure-model. **Materials and Methods:** Wild-type zebrafish will be maintained according to standard patterns (2). Zebrafish larvae anatomical metrics will be measured for the correct dimensioning of the proposed setup. This study will run using larvae ranging at 120 to 168 hpf; thus, the channel design should respect the size of the animals over time by aligning the plate design according to animal development. The microfluidic unit design will consist of different layers. The plate will be 3D-printed on polydimethylsiloxane (PDMS) followed by an electrical and chemical treatment for further multi-channel electrical modules incorporation. These electrical modules will contain exposing areas to contact anatomic regions for the recordings, as the *tectum opticum* in the brain and cardiac chamber (Figure 1). The electrical signal will be processed with 10-fold preamplification and a 1 to 1000Hz filter and amplified for the last time by the RhD2000 Evaluation System. The frame rate will be 10,000 per second, then stored digitally and further processed in mathematical data extraction software. **Relevance:** The proposed multifunctional electrographic setup can maximize studies and data collection in the zebrafish model. Especially, our setup will contribute to leveraging drug screen studies in zebrafish, since the setup will support testing

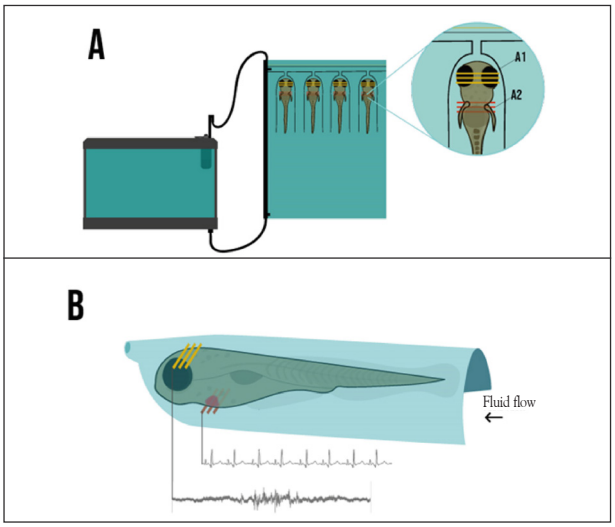

Figure 1. Design of the proposed zebrafish multifunctional electrographical recording. A: setup overview; head (A1) and heart (A2) electrodes. B: Side view of the microfluidic system.

different drugs and concentrations, besides to measure EEG and ECG changes at the same time. **Support:** FAPESP- BRAINN 2013/07559-3 and CAPES.

References: [1] Lieschke GJ et al., doi: 10.1038/nrg2091; [2] Westerfield M., The Zebrafish Book. isbn: 9994860577.

MODELING LAFORA DISEASE IN THE *ZEBRAFISH*: A PLATFORM FOR INVESTIGATING NEURODEGENERATION IN EPILEPSY

Cintra, L.N[1], Maurer-Morelli, C.V[1]

[1]Zebrafish Laboratory, Department of Medical Genetics and Medical Genomics, FCM, UNICAMP.

Introduction and Hypothesis: Lafora Disease (LD) is a severe and progressive myoclonic epilepsy associated with mutations in the *EPM2A* and *EPM2B* genes, which encodes the Laforin and Maline proteins, respectively. These proteins play a role in glycogen metabolism and the alternative physiological pathway, such as the stress response of the endoplasmic reticulum. The symptoms onset usually occurs in early adolescence, and course with refractory seizures, neuropsychiatric disorders, psychosis, dementia, cerebellar ataxia, leading to the patient's death around ten years from the early symptoms. Zebrafish is a suitable model for modeling human diseases since this little fish has an extensive (70%) genomic homology with humans, transparency, and external fecundity and development, allowing easy genetic manipulations. The CRISPR/Cas9 system has been successfully applied to the zebrafish to create genetically modified models, such as knockout zebrafish. Thus, this study aims to model Lafora Disease in zebrafish by targeting the epm2a gene using the CRISPR/Cas9 system. **Objective:** 1. to create a Lafora Disease *zebrafish* model. 2. to characterize the model by analyzing electrographic, histological, and behavior changes in the zebrafish brain. **Materials and Methods:** Wild type zebrafish embryos up to 4 cells stage will be injected with a CRISPR/Cas9 system targeting the *epm2a* gene, to create an *epm2a -/-* animal as described previously by our group (1). The efficiency of the CRISPR/Cas9 will be assessed by sequencing the gDNA of F1 embryos. Embryos and larvae behavior will be monitored daily. At 7dpf larvae will be investigated for swimming behavior (quantitative speed and distance traveled) assessed by Danion Vision System and Ethovision software. Neuronal activity will be investigated by the whole-mount immunofluorescence using antibodies for *cfos*. EEG patterns will be assessed in immobilized larvae at 7 and 15 by placing a 125um diameter 316L stainless steel electrode in the tectum opticum. Electrical signs will be amplified by the Intan RhD2000. **Relevance:** A zebrafish model for LD will allow new insights into the pathologic process underlying this devastating neurodegenerative disease and create a very affordable and fast platform for drug screening, leveraging a further treatment/intervention approaches with translational potential. **Support:** FAPESP- BRAINN 2013/07559-3 and CAPES

Reference: Digital Repository http//repositorio.unicamp/jspui/handle/REPOSIP/333749

MONITORING PATIENT REHABILITATION USING A GESTURE RECOGNITION DEVICE

S. A. Godoy[1,2], A. Brandao[3], D. Dias[6], S. R. M. Almeida[4], G. Castellano[3], M. P. Guimarães[1,5]

[1]Computer Dept, UNIFACCAMP; [2]Computer Dept, IFSP-Registro; [3]Neurophysics, IFGW, UNICAMP; [4]School of Medical Sciences, FCM, UNICAMP; [5]Federal University of São Paulo, Reitoria, UNIFESP, [6]Federal University of São Carlos.

Introduction: The development of new technologies for monitoring and quantifying rehabilitation treatments is achieved using devices that allow the tracking of patients' movements. These devices have inertial measurement units and depth sensors, allowing the combination of kinematic variables to build computational systems to assist therapists during physical rehabilitation sessions. This study aimed to develop a system for tracking the upper and lower limbs of patients to quantify their physical rehabilitation sessions, creating a range of motion measurement (ROM) environment without the use of markers, sensor clothing, or three-dimensional motion capture devices. We use solely optical methods and computer vision techniques to track the movements. **Materials and Methods:** The motion tracking system created was based on the device Microsoft Kinect® [1, 2], which quantifies the ROM. The solution executes the following steps: 1. Skeleton detection; 2. Angle calculation of each joint, video and data recording (x, y, and z position of each joint); 3. The movements are compared with the pattern created previously by the therapist, and the patient progress of each movement is shown in real-time; 4. The final results are shown. **Results:** The developed tool allows the therapist to configure patient session data and create a personalised exercise session. It also offers the patient the opportunity to perform the proposed exercises and view the number of errors and hits in real-time (visual feedback). It further records and stores ROM information and video files (RGB and/or depth images) of each session in a database for further expert analysis. **Discussion/Conclusion**: Other studies [3, 4] present similar solutions, but without measuring ROM. In our solution, the therapist records exercise patterns for each patient, using the angle and velocity of movement for further analysis and follow-up of the evolution of the patient's condition. These data are analysed to verify the percentage of correct movements performed by the patients and provide evidence of their improvement during rehabilitation. This solution encourages the execution of the exercises by the patients, providing feedback and treatment parameters to the therapist in real-time.

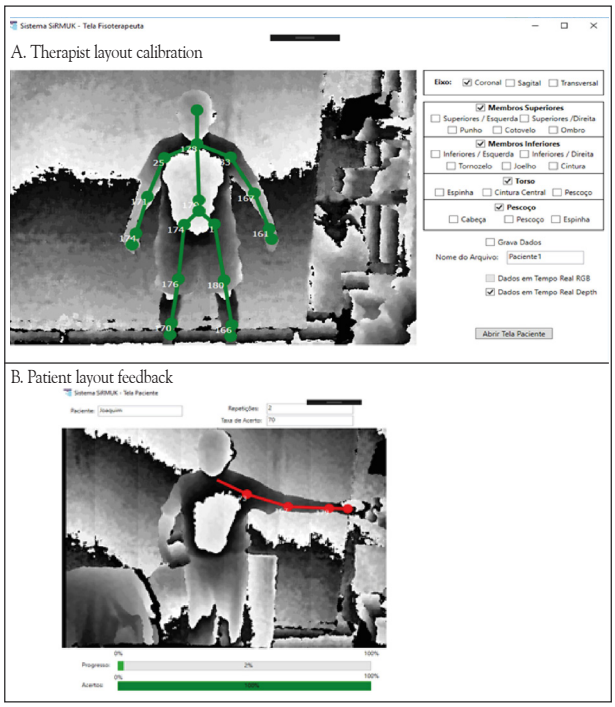

Figure 1. Software for measuring the range of motion (ROM) of lower and upper limbs.

References: [1] Shotton J. et al., (2011). Microsoft Research Cambridge & Xbox Incubation https://www.microsoft.com/en-us/research/wp-content/uploads/2016/02/BodyPartRecognition.pdf; [2] Microsoft Kinect (2019). https://msdn.microsoft.com/en-us/library/hh438998.aspx; [3] KinectSpace (2019). https://code.google.com/archive/p/kineticspace/; [4] FAAST (2019). http://projects.ict.usc.edu/mxr/faast/.

NEURODEGENERATION WITH BRAIN IRON ACCUMULATION: T2 RELAXOMETRY AS A DIAGNOSTIC TOOL

A. M. Mecê[1], M. C. F. Júnior[2], T. J. R. de Rezende[3]

[1]Neurology Department, Neuromuscular Division, University of Campinas (UNICAMP), Campinas, São Paulo, Brazil. [2]Neurology Department, Neuromuscular Division, UNICAMP, [3]Neurology and Neuroimaging Department (UNICAMP), Campinas, São Paulo, Brazil.

Introduction and Hypothesis: The deposition of iron in the central nervous system is a physiological event, however, higher brain iron deposits (BIDs) are associated with neurodegeneration. Magnetic Resonance Image (MRI) can be used in many clinical situations, including the detection of brain iron deposits (BID) with T2 relaxometry (RT2) proven specially useful in the assessment of neurodegeneration related to brain iron accumulation diseases (NBIAs) and other movement disorders. In this context, the development of softwares capable of estimate BIDs can be helpful as a diagnostic tool of theses diseases, which Aftervoxel representing an important example.**Objective:** This study aimed to compare RT2 values (obtained from the software Aftervoxel) from four brain regions of interest (ROIs) in healthy controls with individuals with four neurodegenerative diseases, including Friedreich's Ataxia (FA), Parkinson's Disease (PD), Machado-Joseph Disease (MJD) and Amyotrophic Lateral Sclerosis (ALS), aiming to determine patters of brain iron deposition according to age and

gender. **Materials and Methods:** We selected 3T multiecho brain MRI obtained from 207 healthy controls and 191 patients (32 FA, 48 MJD, 58 ALS and 53 PD). For each image, we selected eight ROIs (including right and left thalamus, dentate nucleus, pallidum and substantia nigra), determined the RT2 values and compared the healthy group against the pathological population. **Relevance:** There was significant increase of BID according to age in the healthy controls, also, higher BIDs levels were measured in left dentate nucleus in FA ($p = 0,03$), right substantia nigra in MJD ($p = 0,01$) and left thalamus in ALS ($p = 0,01$), compared to group control, inferring areas of neurodegeneration. In conclusion, these data suggest that relaxometry is an useful technique not only as a diagnostic tool, but also in the follow up of patients with neurodegenerative diseases.

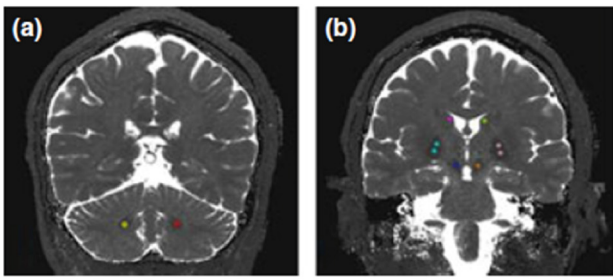

Figure 1. Brain MRI images showing the delimitation of ROIs using the software Aftervoxel. (a) Denatate nucleus; (b) Pallidum, substantia nigra, caudate nucleus.

References: [1] Silva CB, *et al. European Journal of Neurology* 2014; 21 (8): 1131-6; [2] Schenck JF. *Journal of Neurological Sciences* 2003; 207: 99-102.

NORMATIZATION OF CORTICAL THICKNESS VALUES

Pereira, F.O.[1] , França Jr[1] , MC, Cendes, F.[1], Rezende, T.J.R.[1]
[1]Neurophysics Group, IFGW, UNICAMP.

Introduction: This study aimed to propose normative values of cortical thickness of different parts of the brain based on MRI scans from 573 healthy individuals aged 10 to 70 years, considering gender and age effects and total intracranial volume. Such study will allow us to evaluate the true extent of gray matter damage in several diseases as well as the frequency of this damage in patient groups. This information can assist the search for image biomarkers, which might be useful in clinical trial. **Materials and Methods:** All images were acquired in a 3T scanner (Philips Achieva) and segmented using FreeSurfer software. We separated the individuals into 6 age groups (10-20 yrs, 21-30 yrs, 31-40 yrs, 41-50 yrs, 51-60 yrs and 61-70 yrs), then using the MATLAB software, we built a linear regression model for each FreeSurfer region in each age group [1]. In order to evaluate fit quality and, hence, the normative cortical thickness computed, we calculated for each region the normative effect size (Z_{op}) [2]. **Results:** We found that most normative cortical thickness presented Z_{op} small than 0.2 for all age groups. Regions that showed Z_{op} greater than 0.2 also present smaller reliability in general [3]. Indeed, such regions are known to be affected by movement and susceptibility artifacts [4]. As a sanity check, we found that cortical thickness decreases linearly with age as expected. **Discussion/Conclusion**: In conclusion, despite the small sample size, we were able to determine a normative value of cortical thickness from different brain areas for healthy individuals of different age groups. However, the sample size must be improved to remove effect size in some regions. The study shows a reduction in cortical thickness value according to age and its results may be of great importance in studies of neurological diseases, helping to identify brain atrophies.

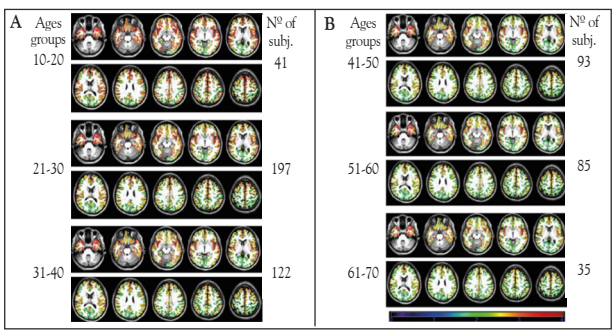

Figure 1. Results of mean values of cortical thickness. A) Ages groups 1,2 and 3. B) Ages groups 4,5 and 6.

References: [1] Fischl B et al., doi: 10.1073/pnas.200033797; [2] Potvin et al., doi: 10.1016/j.neuroimage.2017.05.019; [3] Kim HY, doi:10.5395/rde.2015.40.4.328; [4] Rezende et al., doi: 10.1002/brb3.1363.

P-BTX-I AS A CANDIDATE FOR SEIZURES SUPPRESSION: A STUDY IN ZEBRAFISH-SEIZURE MODEL

T. C. de Moura[1], J.A.A. Fernandes[1], C. V. Maurer-Morelli[1]
[1]Zebrafish Laboratory, Department of Medical Genetics, School of Medical Sciences – UNICAMP, Campinas, SP- Brazil.

Introduction: Most patients with epilepsy may have seizures controlled by available drugs. However, 30% of patients do not respond to antiepileptic drugs, becoming refractory to drug treatment. Thus, searching for therapeutic targets and new compounds seizures suppression may impact the life quality of individuals with epilepsy. Zebrafish (*Danio rerio*) is a popular model for investigating molecular mechanisms underlying epilepsy and seizures, offering several advantages compared to other animal models. Among the cellular events associated with seizures, the activation of inflammatory, apoptosis, and oxidative stress pathways has been receiving significant attention. In this study, we investigate the potential activity of the synthetic snake-venom-based peptide p-BTX-I (Glu-Val-Trp) isolated from *Bothrops atrox* venom in the inflammatory pathway, as well in the neuronal activity and zebrafish larvae behavior. **Materials and Methods:** Larvae at 6 days post fertilization (dpf) were randomly separated into 4 groups: Control (CG), PTZ, p-BTX-I Treatment 50 μl/ml (T50), and p-BTX-I Treatment 10 μl/ml (T10), with 25 larvae each. After this, larvae from treatment groups were exposed to the tripeptide for 24h. In the next day, at 7 dpf, larvae from PTZ and treatment groups were exposed to 15mM of pentylenetetrazole (PTZ) for 20 minutes. Larvae from the control group were handled identically, however, in PTZ-free water. The number of seizures and latency to reach a complete seizure was measured during the PTZ exposure. Immediately after the PTZ exposure, animals were crioanesthetised, and their heads collected. Total RNA was extracted using Trizol® following the manufacture's protocol. cDNA was obtained by RT-PCR using a high capacity kit. The qPCR was performed using the SYBR® Green method. The housekeeping gene *eef1a1a* normalized the mRNA transcript levels of the target gene *il1b* and the neuronal activity marker, c-*fos*. Relative gene expressions (RQ) were calculated by the equation described in Livak and Schmittgen (2001) [1]. Seizures behavior was visually monitored for the evaluation of seizure onset latency and the number of seizures during PTZ exposure. Statistical analyses were performed by ANOVA using GraphPad v. 6.0 with significance ($p \leq 0.05$). **Results:** We found that *il1b* mRNA expression was down-regulated in both groups, T50 and T10, compared to the PTZ group ($p \leq 0.01$). However, the treatment with the lower concentration (T10) presented the most significate reduction in the *il1b* transcript profile. No statistical significance was found in the *c-fos* mRNA expression, as well as in the number of seizures. Despite these statistical data, we observe that animals treated with p-BTX-I showed a tendency to present a smaller number of seizures and swimming, both behaviours, when increased, are associated with seizures. Notably, there was an increase in latency in the T10 group ($p \leq 0.05$), showing that animals in this group were less responsive to the PTZ-seizure induction. **Discussion/Conclusion**: In 2016, we described that seizure could increase inflammatory cytokines, as *il1b* in the zebrafish larvae brain [2], as seems in other animal seizure/epilepsy models. In the present study, we showed a positive effect of p-BTX-I on *il1b* gene downregulation, and on seizure attenuation. Although the peptide did not reduce the neuronal activity, determined by the *c-fos* mRNA expression, and showed little effect on seizure behavior, it was notable that animals treated with T10 increased the seizure latency and promoted a significant reduction of the *il1b* mRNA expression. These results might indicate that a lower dose of the p-BTX-I may have a protective effect on the zebrafish brain. **Support:** FAPESP- BRAINN 2013/07559-3 and CAPES.

References: [1] Livak KJ et al., doi: 10.1006/meth.2001.1262 [2] Barbalho PG et al., doi: 10.1186/s12868-016-0246-y

PHARMACORESISTANCE ASSOCIATES WITH CEREBELLAR ATROPHY IN GENERALIZED GENETIC EPILEPSY

R Brioschi[1], J. C. V. Moreira[1], L. F. Ribeiro[1], M. K. M. Alvim[1], M. E. Morita[1], F. Cendes[1], C. L. Yasuda[1]

[1]Laboratory of Neuroimage – University of Campinas.

Introduction: Generalized genetic epilepsies (GGE) are a group of epilepsy syndromes that seems to present better seizure outcome than most focal epilepsies [1]. This patient group, however, also show specific brain structural abnormalities [2]. In our study, we investigated cerebellar abnormalities in patients with Genetic Generalized Epilepsy, according to seizure control. **Materials and Methods:** Sixty-eight patients with GGE from UNICAMP's Epilepsy Clinic were recruited: 38 SEIZURE-PERSISTENT (patients with current seizures during the previous year of MRI, 25 women, median 33 years); 30 SEIZURE-FREE (free of any type of seizures for at least one year before MRI, 20 women, median 33 years)], compared to 68 controls matched for age (p=0.96) and sex (p=1). High-resolution T1-weighted scans acquired on 3T PHILIPS were segmented with SUIT protocol (http://www.diedrichsenlab.org/imaging/suit.htm). After extracting individual maps of the cerebellum with SUIT, we investigated areas of atrophy with T-tests (between groups of patients and controls), on SPM12/MATLAB 2014. SPM results were displayed with a minimum T-statistic of 3.2, p<0.05 (FDR corrected). Clinical data were analyzed with SPSS20. **Results:** While we did not identify cerebellar atrophy in the SZ-free group, there was significant atrophy in the SZ-persistent group, compared to controls. Most of the atrophy was located in the posterior regions of the right cerebellar hemisphere. **Discussion/Conclusion**: As these patients did not use phenytoin, we can infer that cerebellar atrophy may be associated with recurrent seizures and possibly with the cerebellar diaschisis phenomenon.

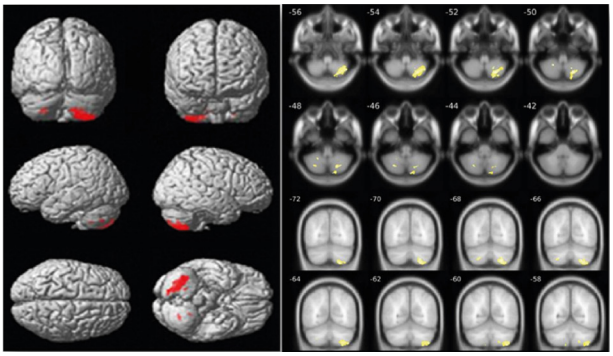

Figure 1. Regions of cerebellar atrophy in SEIZURE-PERSISTANT group.

References: [1] Camfield CS et al. doi: 10.1212/WNL.0b013e3181b9c86f; [2] Nuyts S et al. doi: 10.1111/epi.13928.

PREDICTION OF GENERAL INTELLIGENCE FROM FUNCTIONAL CONNECTIVITY AND NEUROANATOMICAL DATA

S. A. Silva[1], E. A. de Souza[1], B. H. Vieira[1], C. E. G. Salmon[1]

[1]InBrain Lab, Universidade de São Paulo, Ribeirão Preto, Brazil.

Introduction: There has been increased interest in understanding the neural substrates of general intelligence that could be used to account for its variability across individuals. Machine learning can be utilized to predict general intelligence from neuroimaging data, providing understanding of which information contributes more for predictions. We used Elastic Net regression to predict intelligence scores using functional connectivity (FC) matrices, brain area and brain thickness. **Materials and Methods:** Data were provided [in part] by the Human Connectome Project (HCP), WU-Minn Consortium (1U54MH091657); and by the McDonnell Center for Systems Neuroscience at Washington University [1]. We obtained general intelligence scores through factor analysis using R package *stats*, from the HCP 1200 data release subjects. We used subject-specific sets of 50 node timeseries (components) as provided by the HCP9000-PTN release to obtain FC matrices. 812 subjects had complete imaging, intelligence and demographic data, and were eligible for further analyses. Our prediction model was a 10-fold cross-validation Elastic Net regression choosing alpha and lambda parameters among 10 possible values (0.10-1.00), repeated 100 times, using R package *caret*. Folds were separated based on family ID, due to several subjects in the HCP dataset being genetically related, and we removed confoundings effects of the variables gender, age, handedness and total brain volume using multiple linear regression. Predictions used brain area, brain thickness and resting-state FC matrices, separately. Predictions based on FC matrices were also done with a fixed value for alpha=0.01, as in [2], choosing a lambda parameter among 100 possible values and being repeated 100 times; predictions were made from all 50 components, from 49 components (removing the edges of one component each time), and from one component (selecting only the edges of one component, that is, its connectivity to all other components). **Results:** We obtained an average $R^2 = 0.136$ for the prediction of general intelligence from FC matrices, $R^2 = 0.005$ from brain area, and $R^2 = 0.008$ using brain thickness when modeled through the 10-fold cross-validation Elastic Net. When setting a fixed alpha=0.01, we obtained an average $R^2 = 0.149$ for the prediction using complete FC matrices. The highest R^2 obtained using only one component was $R^2 = 0.115$ for component number 24, followed by component 29 with $R^2 = 0.105$. Results considering 49 components showed a lowest $R^2 = 0.135$ when component 11 is excluded, followed by component 13 with $R^2 = 0.138$. We also tested the prediction without components 24 and 29, which showed high predictive power by themselves, and obtained a significant difference $R^2 = 0.135$ ($p < 0.0004$) compared to the result with complete FC matrices. **Discussion/Conclusion**: Our results show that functional connectivity holds a moderate relationship with general intelligence, accounting for 13.6%-14.9% of the variance, aligned with other studies [2, 3]. A higher average R^2 obtained with alpha=0.01 may support that using almost all edges contributes to better predictions. The use of total brain volume as a confounding variable likely had an effect in the low R^2 obtained with brain area and thickness data, once these properties are correlated. Components that showed high predictive power correspond roughly to Brodmann areas (BAs) 45 and 22 in the right hemisphere, while components that led to a lower R^2 when removed correspond to areas in the frontal and occipital lobes, roughly BAs 7, 19, and 44, which are all amongst areas that show significant relationship with intelligence in the frontoparietal network [4]. In conclusion, functional connectivity information was more relevant than anatomical data to predict general intelligence, with emphasis to areas included in the frontoparietal network.

References: [1] Van Essen DC et al., doi:10.1016/j.neuroimage.2013.05.041; [2] Dubois J et al., doi:10.1098/rstb.2017.0284; [3] Finn ES et al., doi:10.1038/nn.4135; [4] Jung RE et al., doi:10.1017/s0140525x07001185

PRELIMINARY APPLICATION OF AUTOENCODERS FOR FEATURE EXTRACTION IN BCI-SSVEP

R. A. Granzotti[1], M. A. Chinelatto[1], G. V. Vargas[1], L. Boccato[1]

[1]School of Electrical and Computer Engineering (FEEC) – University of Campinas (UNICAMP) – Brazil.

Introduction: A Brain-Computer Interface (BCI) is a system that enables the transmission of information from the brain to a computer by recording and interpreting the electrical activity of the brain to produce a command for an application [1]. One of the BCI paradigms is based on Steady-State Visually Evoked Potential (SSVEP). In a BCI-SSVEP, the individual should focus their attention on different visual stimuli, which are exposed in different frequencies. The challenge is to identify the frequency corresponding to the visual stimulus at which the user is concentrated based on electroencephalography (EEG) recordings. To perform this activity, it is necessary to process the EEG signals, which involves four main stages: (1) preprocessing, to mitigate artifacts, (2) extraction and (3) feature selection, to obtain a compact representation of the signals, and (4) classification, in order to identify the visual stimulus selected by the user. Autoencoders constitute promising alternatives due to the nonlinear processing capability of the underlying neural network structures, as well as due to efficient training and regularization strategies [2]. This work aims at investigating whether the use of autoencoders [2] to extract features from the EEG signals can lead to a better discrimination of the visual stimuli and improve the performance of the system. **Materials and Methods:** The brain signals were acquired by EEG with 16 electrodes placed on the occipital, parietal and central zones. The visual stimulation consisted of two squares that alternated the colors black and white on a monitor, with frequencies of 12 and 15 Hz. Each individual focused on each visual stimulus for 12s, being this process repeated eight times. The BCI-SSVEP analyzed in this work consisted of: (1) CAR filtering; (2) an

autoencoder, whose architecture is depicted in Fig. 1, for feature extraction; and (3) an SVM-based classifier. The 368 samples available were split applying the holdout technique: 75% of the samples for training and 25% for validation. **Results:** Fig. 1 exhibits the information extraction potential of autoencoders in a BCI application considering only two visual stimuli (12 and 15 Hz). In this experiment, the neural network was trained to reconstruct the EEG samples of 1s time windows from Oz electrode; internally, it was forced to create a representation with only three features in the bottleneck. Interestingly, the use of such features in the BCI system led to a classification accuracy close to 95%.

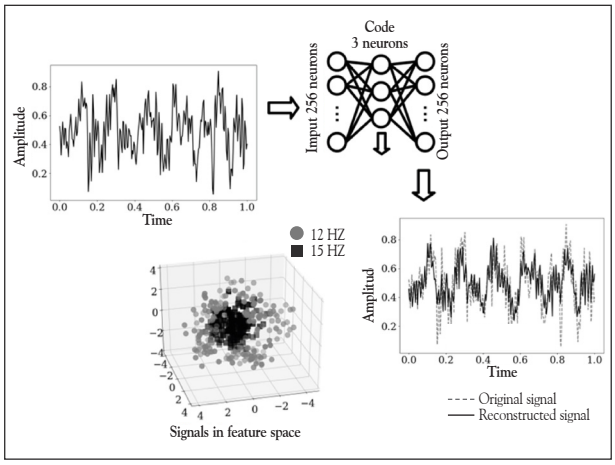

Figure 1. Design of the proposed zebrafish multifunctional electrographical recording. A: setup overview; head (A1) and heart (A2) electrodes. B: Side view of the microfluidic system.

Discussion: The studied autoencoder with a 3-neuron bottleneck layer was capable of creating a representation for the EEG signals with an adequate class separability, allowing an SVM-based classifier to achieve an accuracy of 95%. This result, albeit considering in a simple scenario, highlights the potential of using autoencoders and motivates further investigations.

References: [1] Wolpaw, J. R. , doi: 10.1016/S1388-2457(02)00057-3; [2] Goodfellow et al., Deep Learning, MIT Press, 2016.

PROPOSING A NEW APPROACH FOR THE ANALYSIS OF CELL-FREE DNA METHYLATION AS A POTENTIAL BIOMARKER IN NEUROLOGICAL DISORDERS

D. C. F. Bruno[1], W. Souza[1], B. S. Carvalho[2], F. Cendes[3], I. Lopes-Cendes[1]

[1]Department of Medical Genetics and Genomic Medicine, [2]Department of Statistics, Institute of Mathematics, Statistics and Scientific Computing; [3]Department of Neurology; School of Medical Sciences. University of Campinas (UNICAMP) and the Brazilian Institute of Neuroscience and Neurotechnology (BRAINN), Campinas, SP, Brazil.

Introduction: DNA methylation is essential for many regulatory processes occurring in the cell [1]. The ability to accurately identify methylated genomic regions, contribute to a better understanding of normal gene regulation as well as the mechanisms underlying different disorders. Whole-genome bisulfite sequencing (WGBS) has long been the gold standard for genomic methylation analysis (methylome) [2transcription factor binding, and suppression of transposable elements. The use of whole genome bisulfite sequencing (WGBS]; however, the chemical reaction of bisulfite damages and degrades DNA, resulting in fragmentation and consequent loss of methylation information [3used widely for both fundamental and disease-oriented research. Library preparation methods benefit from a variety of available kits, polymerases and bisulfite conversion protocols. Although some steps in the procedure, such as PCR amplification, are known to introduce biases, a systematic evaluation of biases in WGBS strategies is missing.\n\nResults\nWe perform a comparative analysis of several commonly used pre- and post-bisulfite WGBS library preparation protocols for their performance and quality of sequencing outputs. Our results show that bisulfite conversion per se is the main trigger of pronounced sequencing biases, and PCR amplification builds on these underlying artefacts. The majority of standard library preparation methods yield a significantly biased sequence output and overestimate global methylation. Importantly, both absolute and relative methylation levels at specific genomic regions vary substantially between methods, with clear implications for DNA methylation studies.\n\nConclusions\nWe show that amplification-free library preparation is the least biased approach for WGBS. In protocols with amplification, the choice of bisulfite conversion protocol or polymerase can significantly minimize artefacts. To aid with the quality assessment of existing WGBS datasets, we have integrated a bias diagnostic tool in the Bismark package and offer several approaches for consideration during the preparation and analysis of WGBS datasets.\n\nElectronic supplementary material\nThe online version of this article (10.1186/s13059-018-1408-2]. In addition, DNA sequencing libraries tend to have a high GC bias and are enriched for methylated regions[3used widely for both fundamental and disease-oriented research. Library preparation methods benefit from a variety of available kits, polymerases and bisulfite conversion protocols. Although some steps in the procedure, such as PCR amplification, are known to introduce biases, a systematic evaluation of biases in WGBS strategies is missing.\n\nResults\nWe perform a comparative analysis of several commonly used pre- and post-bisulfite WGBS library preparation protocols for their performance and quality of sequencing outputs. Our results show that bisulfite conversion per se is the main trigger of pronounced sequencing biases, and PCR amplification builds on these underlying artefacts. The majority of standard library preparation methods yield a significantly biased sequence output and overestimate global methylation. Importantly, both absolute and relative methylation levels at specific genomic regions vary substantially between methods, with clear implications for DNA methylation studies.\n\nConclusions\nWe show that amplification-free library preparation is the least biased approach for WGBS. In protocols with amplification, the choice of bisulfite conversion protocol or polymerase can significantly minimize artefacts. To aid with the quality assessment of existing WGBS datasets, we have integrated a bias diagnostic tool in the Bismark package and offer several approaches for consideration during the preparation and analysis of WGBS datasets.\n\nElectronic supplementary material\nThe online version of this article (10.1186/s13059-018-1408-2]. More recently, cell-free DNA methylation pattern (met-cfDNA) has been proposed as a potential biomarker for different diseases, as it can be noninvasively analyzed and quantified and carries information specific to the disease and/or affected tissue[4,5]. However, cell-free DNA (cfDNA) is highly fragmented (~160-180 bp) and poorly concentrated in circulation [5]. To overcome these limitations, we aim to find a new approach to accurate determine met-cfDNA pattern. Thus, we tested the enzymatic Methyl-seq (EM-seq) method and compared the results with the current gold standard, WGBS. **Materials and Methods:** DNA sequencing libraries were prepared using the bisulfite (Pico Methyl-Seq Library Prep Kit, Zymo Research) and EM-seq (NEBNext Enzymatic Methyl--seq) methods. Assays were generated with 10 ng cfDNA from the plasma of a patient with mesial temporal lobe epilepsy. The libraries were sequenced in a HiSeq X Illumina and the reads were trimmed to remove the adapter sequence using TrimGallore software. Filtered reads were aligned to the reference human genome (GRCh38) using Bismark. The duplicated reads were removed from the alignments to avoid amplification bias. The methylation percentage was calculated with the Bismark software and analyzed with the R statistical environment using the bsseq from the Bioconductor package. **Results and Discussion:** WGBS and EM-seq alignment generated 432.5 and 431.6 million reads, respectively. Although they are the same samples and have similar sequencing read quantities, the raw data obtained showed clear differences. In the WGBS assay, 60% of reads were unique without duplicates and contained 34% of GC. In the EM-seq, the number of uniquely aligned reads was higher, 82%, and with lower GC content, 22%. After sequence trimming, 7.5% (32.2 million) WGBS reads were removed and only 0.2% (0.9 million) in the EM-seq, indicating a better use of EM-seq sequencing data. EM-seq was also better in sequencing alignment, with 83.9% of unambiguous alignments, whereas WGBS aligned only 51.5% of the reads. In addition, EM-seq had a lower number of deduplication levels (17%) compared to WGBS (60.9%). Most importantly, MS-seq had a lower methylation bias (M-Bias of approximately 75% in WGBS and 35% in EM-seq). Furthermore, it was possible to access a higher number of C's sites in the EM-Seq assay (9,308.5 compared 1,295.7 in the WGBS). These results are summarized in Table 1. Finally, by implementing the BSmooth algorithm (bsseq package) to estimate methylation levels, we found a total of 58,690,664 methylation loci. We also noticed that the average CpGs coverage for EM-seq was 6X higher than that obtained in the WGBS assay (table 2).

Table 1. Quality and comparison assessment of cfDNA methylation (met-cfDNA) sequencing of the whole genome using the current gold standard, whole-genome bisulfite sequencing (WGBS) using bisulfite for convert DNA methylation, and enzymatic methylation sequencing (EM-seq), which does not use bisulfite.

Raw Data	WGBS	EM-seq
Total reads (Millions)	432.5	431.6
Average of GC content (%)	54.7	34.0
Unique reads_R1	236,404,092 (54.7%)	354,544,157 (82.1%)
Unique reads_R2	298,512,368 (69.0%)	352,414,166 (81.6%)
Duplicate reads_R1	196,070,541 (45.3%)	77,101,943 (17.9%)
Duplicate reads_R2	133,965,265 (31.0%)	79,231,934 (18.4%)
Trimming Data	**WGBS**	**EM-seq**
Total reads (Millions)	400.3	430.7
Total base pairs (Millions)	32.2 (7.5%)	0.9 (0.2%)
Aligned uniquely	206,369,153 (51.5%)	361,225,216 (83.9%)
Deduplicated reads remaining	80,606,072 (39.1%)	299,941,894 (83.0%)
Deduplicated reads removed	125,763,037 (60.9%)	61,283,320 (17.0%)
Average M-Bias CpG (%)	75	35
Total C's analyzed (Millions)	1,295.7	9,308.5
mCpG (%)	77.7	35.2
mCHG (%)	1.2	3.8
mCHH (%)	1.6	4.0

Table 2. Statistical data of CpGs coverage comparing both methods whole-genome bisulfite sequencing (WGBS) using bisulfite for convert DNA methylation, and enzymatic methylation sequencing (EM-seq), which does not use bisulfite.

Variable	WGBS	EM-seq
Minimum	0.0	0.0
1st Quart	0.0	4.0
Median	1.0	7.0
Mean	1.2	7.2
3rd Quart	2.0	10.0
Maximum	184.0	8,990.0

Conclusion: We found that cfDNA EM-seq libraries have lower duplication levels, a higher percentage of mapped reads, and less GC bias compared to bisulfite converted libraries. Also, EM-seq has higher average CpGs coverage, thus clearly indicating that EM-seq is superior to the current used WGBS to identify met-cfDNA analysis. We are currently applying EM-seq in our projects aiming to discover biomarkers in different neurological disorders.

References: [1] Breiling A and Lyko F, https://doi.org/10.1186/s13072-015-0016-6; [2] Stuart T et al., https://doi.org/10.1007/978-1-4939-7774-1_17; [3] Olova N et al., https://doi.org/10.1186/s13059-018-1408-2; [4] Cheuk IWY et al., https://doi.org/10.4048/jbc.2017.20.1.12; [5] Elshimali YI et al., https://doi.org/10.3390/ijms140918925.

SIMULATING MOTION CORRUPTED MRI DATA TO FACILITATE DEEP LEARNING TRAINING

I. Fantini[1], L. Rittner[1], C. Yasuda[2], R. A. Lotufo[1]

[1]Medical Image Computing Lab, FEEC, UNICAMP, [2]Neuroimaging Laboratory, FCM, UNICAMP.

Introduction: Currently, Deep Learning (DL) is the best method for performing imaging tasks, such as classification, segmentation, and detection. DL is being used on medical images, allowing the research progress on several diseases. Nonetheless, it requires a large amount of data, and the data must be annotated, which usually is performed manually, hence is tiresome and costly. This study aims to detect Magnetic Resonance (MR) images corrupted by motion artifacts. Since low-quality MR images are discarded the amount of data for DL training is not sufficient. Based on the knowledge of MR image acquisition we propose to simulate motion artifacts on good-quality MR images, train the model on the simulated and real data, and evaluate the model using real motion corrupted data. **Materials and Methods:** The MRI data were acquired at the University of Campinas, on a 3T Philips Achieva scanner from 68 healthy volunteers as approved by the local ethics board. The T1-weighted volumetric 3D sequence was acquired in the sagittal plane (isotropic voxels). The motion corrupted class has 34 acquisitions. From the 68 acquisitions we separated 20 acquisitions (10 from each class) for testing purposes. The motion was simulated on the control group by performing rotation and translation on the images, following 3 steps: applying the geometric transformation to the image; transforming the images to frequency domain where the lines from multiple images (original and geometric transformed) are combined, and then transforming back to image domain [1]. The DL architecture InceptionV3[2] was used to perform the transfer learning experiments. Two models were generated: fine-tuned with real motion-corrupted data, and fine-tuned with both, real and simulated motion data. **Results:** To assess our results, we checked the False Positive (FP) and False Negative (FN) curves, as well as the accuracy. All models were tested using the same dataset (real images only). Due to the training dataset size, we used a three-fold training strategy. **Discussion/Conclusion**: The curves stand for the classes' errors related to the classifier threshold, and the best threshold is where the lines cross. The curves from the models trained using both data present less variability between folds and smaller error for the best threshold when compared to models trained using only real data (Fig. 1). The average accuracy confirms that the models trained using both motion simulated and real corrupted data performed slightly better than the one trained with real corrupted data only, 94% and 93% respectively (Tab.1).

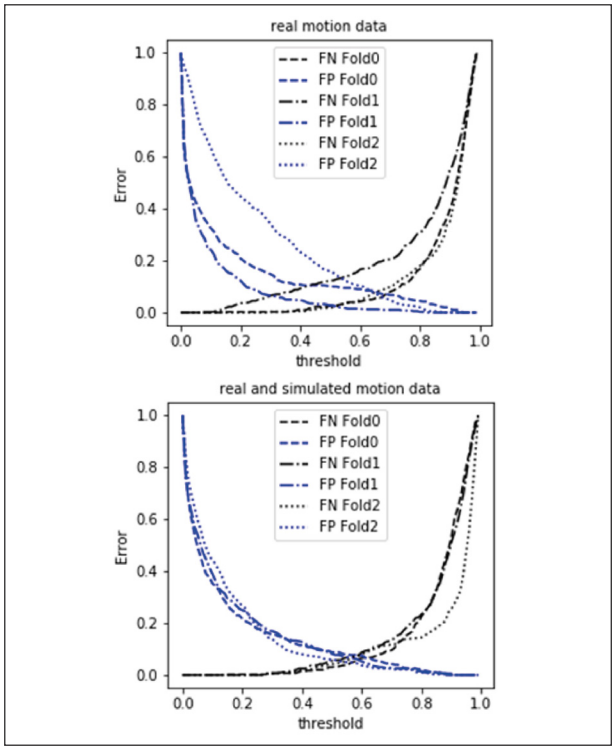

Figure 1. False Positives and False Negatives curves for models trained using real motion only data or real and simulated motion data.

Table 1. Accuracies (in percentage) per fold for models trained using real data or both, real and simulated motion data. The test data is real data only and is the same for all folds.

Motion corrupted data	Fold 1	Fold 2	Fold 3
Real	93%	94%	92%
Real and simulated	94%	94%	95%

References: [1] Loktyushin, A. et al., DOI: 10.1007/978-3-319-27929-9_1; [2] SZEGEDY, C. et al., DOI: 10.1109/CVPR.2016.308

STNFR2 PLASMA LEVEL AS A POTENTIAL EPILEPSY BIOMARKER

MKM Alvim[1], ME Morita[1], MH Nogueira[1], L Ramalho[1], NP Rocha[2], EL Vieira[2], AL Teixeira[2], CL Yasuda[1], F Cendes[1]

[1] University of Campinas, [2]Federal University of Minas Gerais.

Introduction: We aimed to investigate the association of inflammatory markers associated with epilepsy and pharmacoresistance, given the important role of inflammation in the epilepsy pathogenesis and neuronal hyperexcitability. **Ma-**

terials and Methods: Explorative study with 446 consecutive patients (18-70 y.o) with epilepsy, and 166 controls. The patients were classified according *i.* **Frequent seizures**: at least 6 impaired awareness seizures or 2 bilateral/generalized tonic-clonic-seizures in 1 year and *ii.* **Infrequent seizure**: less seizures than group *i.* The plasma analysis of BDNF, CTNF, NGF, GDNF, NT3, NT4/5, TNF and its soluble receptors, sTNFr1 and sTNFr2 was performed by ELISA and interleukine (IL)1β, IL-2, IL-4, IL-6, IL-10, IL-17, TNFα and IFNγ by CBA. The analysis was blinded. **Results:** The interleukins, TNF, sTNFr1, CNTF and IFNγ levels were lower and sTNFr2, BDNF, CTNF, NGF and NT3 were higher in patients than controls. IL1, NT4/5 and GDNF were similar between the two groups.sTNFr2 was the only marker to present significant difference to discriminate patients from controls (AUC=0.857, p<0.001), in ROC analysis (Fig 1), and according seizure frequency, being higher in frequent seizures group (p=0.027). **Discussion/Conclusion**: TNF and its receptors present the membrane and the soluble forms. Some studies suggests that soluble form are good plasma markers of TNF activity and TNFr2 mediates anti-ictogenic effects and reduces the sensitivity for seizures. We demonstrated, in a large cohort of patients, that sTNFr2 plasma levels present good accuracy to discriminate people with and without epilepsy and it is related to seizure frequency. sTNFr2 could be a potential good biomarker for epilepsy.

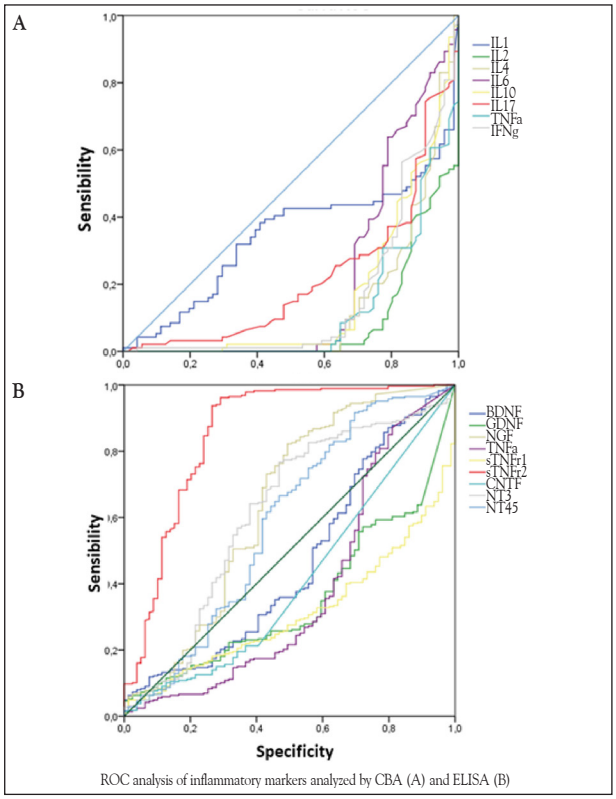

Figure 1. ROC analysis of plasma level of inflammatory markers comparing epilepsy patients and controls.

TEXTURE-BASED NETWORKS FOR DMN REGIONS: A PILOT STUDY

R. V. Silveira[1,3], B. M. Campos[2,3], L. L. Min[2,3], G. Castellano[1,3]

[1]Neurophysics Group, IFGW, UNICAMP; [2]Neuroimage Laboratory, FCM, UNICAMP; [3]BRAINN.

Introduction: Magnetic resonance imaging (MRI) has become the main modality for assessing the brain, allowing harmless non-invasive studies in both patients and healthy individuals. However, the increasing number of MR exams generates a tremendous amount of data. Therefore, we need tools to extract relevant information. Texture analysis [1] is an image processing technique, which extracts texture parameters based on the image gray-level distribution. This study proposes to verify structural similarities between the default mode network (DMN) regions of structural brain MR images using texture parameters. **Materials and Methods:** T1-weighted MR images from 10 healthy male subjects (mean age 39±14 years) were used. The images were preprocessed on the SPM12 software. A brain parcellation was performed on the PickAtlas software, using the Automated Anatomical Labeling (AAL) atlas [2]. The co-occurrence matrix [3] was calculated for each of the 14 DMN regions (as defined in [4]), using a proprietary algorithm, for a 1-pixel distance. From these co-occurrence matrices, three texture parameters were extracted: contrast, uniformity and correlation. For each texture parameter, we set the node as the vector containing all 10 subjects' values of that parameter for that brain region. The similarity measure to compute the links was the inverse of the Euclidean distance between every pair of nodes, normalized to the 0 to 1 interval. A threshold of 0.25 was set to obtain binary networks. **Results:** Figure 1 shows the three texture networks, plotted using the BrainNet Viewer software [5]. **Discussion/Conclusion**: Different texture parameters showed different relationships among DMN regions. The nodes with highest degrees for each network were: contrast – left (L) dorsolateral superior frontal gyrus (SFG); correlation – L angular and right (R) anterior cingulate and paracingulate gyrus (ACPG); uniformity – R medial SFG and L inferior temporal gyrus. Common connections between the three networks were all relating homologous (L and R) regions: ACPG, dorsolateral SFG and medial SFG. In future work, we intend to increase the number of analyzed subjects, as well as examine the relationship between our findings and resting-state fMRI networks.

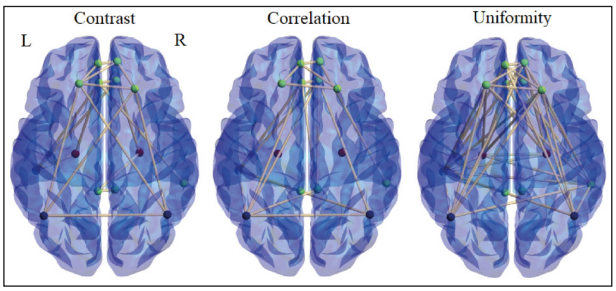

Figure 1. Texture networks for 10 healthy subjects.

References: [1] Castellano G et al., doi: 10.1016/j.crad.2004.07.008. [2] Tzourio-Mazoyer N et al., doi: 10.1006/nimg.2001.0978. [3] Haralick RM et al., IEEE Trans Syst Man Cybern, SMC-3(6): 610-21, 1973. [4] Wang Y et al., doi: 10.4236/jbbs.2017.713044. [5] Xia M et al., doi: 10.1371/journal.pone.0068910.

THALAMUS SEGMENTATION USING CONVOLUTIONAL NEURAL NETWORK

G. R. Pinheiro[1], L. Brusini[2], G. Menegaz[2], L. Rittner[1]

[1]Medical Image Computing Laboratory (MICLab), School of Electrical and Computer Engineering (FEEC), UNICAMP [2]Department of Computer Science, University of Verona.

Introduction: Parkinson Disease (PD) is a progressive nervous system disorder that can cause tremors or stiffens the movements of the patient. PD cannot be cured, however, there are treatments for the symptoms with medication and surgery in more severe cases. In those cases, there are two main structures that are targets to the procedure, Thalamus and Globus Pallidus [1]. In order for doctors to correctly target them and plan the surgery, there is a need to acquire CT or MRI and process the images to reliably segment the structures. Since most of the software's take many hours to process those types of data, and have some issues on sub-cortical structures processing, we propose a method based on Convolutional Neural Networks (CNNs) to extract the needed information. Previous work [2] has already accomplished the segmentation of the Globus Pallidus using this approach, thus, in the work, we are focusing on Thalamus segmentation. **Materials and Methods:** The dataset is a subset of 50 subjects from Human Connectome Project (HCP) [3] and it is composed of diffusion maps, computed using Dipy [4] (FA, MD, RD, and λ1) and structural maps (b0 and T1). The dataset was already preprocessed but we have normalized the data regarding the voxel values and voxels sizes (1.8x1.8x2mm). The annotation of the data was done on FSL and we used the label of 8 structures; Ventricle, Thalamus, Caudate, Putamen, Pallidum, Hippocampus, Amygdala, and Accumbens. The CNN model used in the project was the U-Net [5] as it is still the state-of-the-art in medical image segmentation and has shown good performance in other subcortical structures [2]. We have tested the CNN

using only diffusion maps, only structural data, and the combination of them. **Results:** The quantitative results were computed by using the DICE coefficient between the CNN prediction and the automatic segmentation. We achieved an average DICE of 0.80 for the Thalamus when using both diffusion and structural indices, 0.78 when using only diffusion, and 0.76 when using only structural data. A visual inspection in the test data (Fig. 1) shows that the segmentation was qualitatively very similar to the target. **Conclusion**: Even with a relatively small dataset and automatic segmentation as targets, the results were promising. The combination of diffusion and structural data has increased the results when compared to each of them separately. Since we are using automatic segmentation as labels, our results are limited by the quality of the labels. The inclusion of manually segmented data would certainly increase the segmentation quality to above automatic segmentation results. Future work will use this trained model and fine tune to a manually segmented dataset to improve the quality of the segmentation.

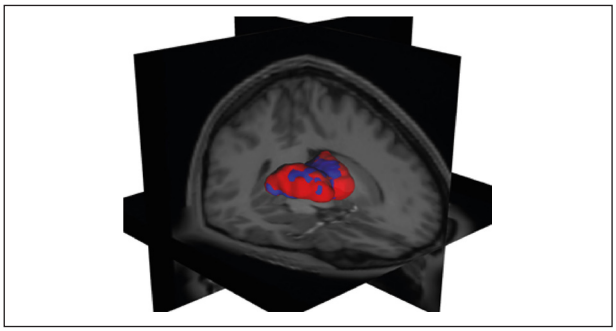

Figure 1. Thalamus segmentation over T1 weighted image: target from FLS (red) and CNN prediction (blue).

References: [1] Espinoza Martinez, J.A. et al., Neurosurg Rev 38, 753–763, 2015. [2] Pinheiro, et al., CDMRI MICCAI, 2019. [3] Essen, et al., NeuroImage 80:62-79, 2013. [4] Garyfallidis E, et al., Frontiers in Neuroinformatics, vol.8, 2014. [5] Ronneberger, O. et al., LNCS, vol. 9351, pp. 234–241, 2015.

THE EFFECT A SIX MONTHS PHYSICAL ACTIVITY PROGRAM IN A SMALL GROUP OF PARKINSON'S DISEASE PATIENTS

M. F. Sattolo[1], L.D. Rodrigues[1], L.C. de Lima[1], M. Diogo[1], P.C. Azevedo[1,2], L.G. Piovesana[1,2], F. Cendes[2,3]; R.P. Guimarães[1,2,3]

[1]Movement Disorders Group, UNICAMP, [2] Neurology Dept., UNICAMP, [3]Neuroimaging Laboratory, UNICAMP.

Introduction: PD is one of the most common disorders in the world. It is a progressive neurodegenerative disease. The progression of symptoms may lead to disability, impairing daily activities 2. Physical activity may influence disease onset, severity and progression.3 There is increasing scientific evidence on the effectiveness of physical therapy and physical activity as adjunctive treatments for dopaminergic replacement focusing on controlling motor and non-motor PD symptoms, and, consequently, improving quality of life, regardless the stage of the disease. **Materials and Methods:** Fourteen patients diagnosed with PD, according to the London brain bank criteria, who could walk independently or using assistive devices were included. All patients belonged to the Parkinson Ativo group, which consists of specific exercises for PWP. Activities were performed twice a week, with one hour duration. The UPDRS, Time UP and Go (TUG) and H&Y scales were applied at baseline and after 6 months. During the six months, different domains were trained, such as mobility, gait, balance, conditioning and motor coordination. **Results:** 11 patients (mean age 62,5 years, + 15.52) were assessed at baseline and after 180 days. Patients who attended to less than 10 sessions during the 180 days were excluded (n=3). The mean number of sessions was 20.37 (min 13, max 29). Mean UPDRS at baseline was 35.25 + 10.79. The mean UPDRS-III score at baseline was 16.85 + 10.23, and at 180 days were 13.62 + 7.04. Decrease of UPDRS part III (motor) score of greater than or equal to 5 points is considered clinically significant after six months 1. Although there was no significant difference between the two assessments, six of 11 patients demonstrated clinically significant decrease at six months. Schulman et al.28 reported that a difference of 2.5 in the UPDRS motor score, represents a minimal clinically important difference (CID), with 5.2 for moderate and 10.8 for large CID. At 180, only 2 patients exhibited an increase in UPDRS motor score of more than 2.5, while eight patients exhibited a decrease in UPDRS motor score of more than 2.5. Five out of 8 patients had better performance at the TUG test on the second assessment, after 180 days, and 3 patients took more time to complete the test, however, these differences were not statistically significant. **Discussion/Conclusion**: Despite not being statistically significant, our results suggest that physical activity is a valuable tool to improve patient's motor limitations. It should always be considered as a treatment for PWP.

References: [1] Schrag, A, Sampaio, C, Counsell, N Minimal clinically important change on the unified Parkinson's disease rating scale. Mov Disord 2006; 21: 1200–1207.

THE EFFECTIVENESS OF NEUROFEEDBACK AS A NONINVASIVE AND NON-DRUG ALTERNATIVE IN THE TREATMENT OF PSYCHOPATHOLOGIES: AN INTEGRATIVE REVIEW

J. O. F. Pigatto[1]

[1]Universidade São Francisco, Campinas.

Introduction: Neurofeedback is a brain training technique that allows the self-regulation of brain electrophysiological activity through operant conditioning of electrical signals captured in the cerebral cortex by electroencephalography (EEG) [1]. As a therapeutic resource, it has been increasingly used in the field of psychology not only because of its noninvasive and non-drug nature, but also for its effectiveness in improving various parameters of physical and mental well-being [2]. **Materials and Methods:** To evaluate how the effectiveness of neurofeedback in the treatment of several psychopathologies has been reported in recent scientific researches, this integrative literature review [3] selected twelve empirical studies works published in the last ten years on PubMed platform, using keywords related to the use of neurofeedback focused on the following disorders: obsessive compulsive disorder (OCD), anxiety disorders, depression, post-traumatic stress disorder (PTSD) or generalized anxiety disorder (GAD). **Results:** Although the corpus of this integrative review was not broad enough for in-depth conclusions, within the scope of undergraduate final project [4] it was possible to observe that even though all the studies have shown positive results for symptom reduction, methodological flaws were also reported by all of them, what can be an obstacle to neurofeedback validation in the scientific field. **Discussion/Conclusion**: In conclusion, we can assume the scientific investigations on neurofeedback effectiveness on psychology clinic requires both strong statistical power and better controlled and randomized studies. New research methodologies are probably the better way to produce reliable data that supports the use of neurofeedback in the treatment of the psychopathologies in question.

Tabel 1. Methodology compative board [4].

Study number	Total of subjects	Trainning group	Control group	Psychopathology	Diagnostic criterion
01	20	10	10	OCD	DSM-IV
02	36	36	-	OCD	DSM-IV
03	77	77	-	Depression / Anxiety	DSM-IV
04	10	10	-	Elderly Depression	Sensitive to depression
05	20	20	-	Major Depression	DSM-IV
06	24	12	12	Depression and fatigue in Multiple Sclerosis	McDonald
07	60	40	20	Major Depression	DSM-IV
08	9	9	-	Major Depression	DSM-IV
09	24	12	12	Depression	DSM-IV
10	28	14	14	GAD	DSM-IV
11	21	21	-	PTSD	DSM-IV
12	21	21	-	PTSD	DSM-IV

References: [1] Robbins J, A Symphony in the Brain, Grove Press, 2008; [2] Dias AM, Psicologia em Estudo, 15(4): 811-820, 2010; [3] Beyea SC et al., AORN J, 67(4): 877-880, 1998. [4] Pigatto JOF (final paper), Universidade São Francisco, Campinas, 2018.

THE EFFECTS OF TRANSCRANIAL DIRECT CURRENT STIMULATION (TDCS) IN THE TREATMENT OF REFRACTORY EPILEPSY

M. M. Pereira-Novo[1], S. E. Ferreira-Melo[1], B. Guedes[1], L. L. Min[1]

[1]Neuromodulation Group, Dept of Neurology, FCM, UNICAMP.

Introduction and Hypothesis: Epilepsy is the most common neurological disorder globally, affecting approximately 50 million people worldwide. Around 20% of these present with intractable or refractory epilepsy, where the frequency of seizures cannot be controlled adequately with anti-epileptic drugs

(AEDs), leading to great neurobiological, cognitive, psychological and social consequences[1,2]. Transcranial Direct Current Stimulation (tDCS) is a non-invasive brain stimulation (NIBS) technique that can effectively modulate (up- or down-regulate) cortical excitability of targeted brain regions[3]. In the present work, we aim to evaluate the effects of tDCS in the management of seizure control in refractory epilepsy and its impact on cognitive function and quality of life. **Objective:** The main aim of this randomized controlled trial is to determine if cathodal tDCS is effective in reducing the frequency of seizures in refractory epilepsy and secondly, to evaluate its impact on cognition and quality of life. **Methods:** This is a prospective, randomized, placebo-controlled, double-blind, single-center study. The participants in the study will be randomized to either the intervention – tDCS group or sham group. Each individual will undergo 15 consecutive sessions of real cathodal tDCS stimulation or sham-stimulation. The primary outcome measure will be the frequency of seizures, measured by a seizure diary; changes in interictal epileptiform discharges on the Electroencephalogram (EEG); and functional connectivity changes in the epilepsy focal area, measured by resting-state Functional Resonance Image (rs-fMRI). Secondary outcomes include quality of life and cognition. Outcome measures will be done prior to intervention; immediately after intervention, at 1 month-follow up and again at 3-months follow up. **Relevance:** Refractory epilepsy is a common disorder with significant negative impact on an individual's life. Increasingly there has been growing interest in the search for new, non-invasive treatment strategies that can remediate some of these negative consequences. Non-invasive brain stimulation techniques can be a promising therapeutic technique to manage the frequency of seizures in these patients. This study seeks to further investigate whether cathodal-tDCS stimulation can be effective in reducing seizures frequency am improving quality of life of people with refractory focal epilepsy.

References: [1] International league against Epilepsy. ILAE Commission Report The Epidemiology of the Epilepsies: Future Directions. *Epilepsia*. 1997;38(5):614-618. [2] Epilepsy IOF. Global burden of epilepsy and the need for coordinated action at the country level to address its health, social and public knowledge implications Report by the Secretariat BURDEN AND IMPACT OF EPILEPSY. 2014;(December):1-8. [3] Nitsche MA, Cohen LG, Wassermann EM, et al. Transcranial direct current stimulation: State of the art 2008. *Brain Stimulation*. 2008;1(3):206-223. doi:10.1016/j.brs.2008.06.004

THE GENETIC BASIS OF FOCAL CORTICAL DYSPLASIA

V.S. de Almeida[1], S.H. Avansini[1], M. Borges[1], F.R. Torres[1], F. Rogerio[2], B.S. Carvalho[3], A. M. Canto[1], E. Ghizoni[4], H. Tedeschi[4], A.C. Coan[4], M.K.M. Alvim[4], C.L. Yasuda[4], F. Cendes[4], I. Lopes-Cendes[1]

[1]Department of Medical Genetics and Genomic Medicine, School of Medical Sciences, [2]Department of Anatomical Pathology, School of Medical Sciences, [3]Department of Statistics, Institute of Mathematics, Statistics and Scientific Computing, [4] Department of Neurology, School of Medical Sciences; University of Campinas, UNICAMP, Campinas, SP, Brazil and the Brazilian Institute of Neuroscience and Neurotechnology (BRAINN), Campinas, SP, Brazil.

Introduction: Malformations of cortical development (MCD), including focal cortical dysplasia (FCD), can cause epilepsy and are often associated with the occurrence of refractory seizures [1]. FCD is characterized by alterations in the cytoarchitecture also observed in other MCDs, such as tuberous sclerosis (TS) and hemimegaloencephaly (HME) [2,3]. Recently, mosaic mutations were identified in TS, HME and FCD [4]. We aim to investigate the genetic basis of FCD in a large cohort of patients. **Materials and Methods:** Genomic DNA was extracted from brain tissue resected by surgery (BTRS) and blood leucocytes from 12 patients with FCD. These samples were submitted to deep sequencing of mTOR and GATOR pathway genes. Capturing and enrichment were performed with the SeqCap EZ Choice Library (NimbleGen, Roche). Samples were sequenced in a Miseq (Illumina), to achieve at least 600X of coverage. Mosaicism was evaluated using the following tools: Mutec, VarScan, and Strelka. Variants were classified as mosaic mutations when less than 10% of reads were not aligned to the reference human genome and are present only in BTRS. Variants were filtered prioritizing frameshift, missense, nonsense and splicing site mutations. Copy number variants (CNVs) were also evaluated in 17 patients with FCD using the CytoScanHD (Affymetrix®) microarray. The analysis was performed with *Chromosome Analysis Suite (Chas)* software (Affymetrix®) and CNVs were classified according to their deleterious effect using databases such as *Database of Genomic Variants (DGV)* and *OMIM® (Online Mendelian Inheritance in Man)*. In addition, overlapping with CNVs previously described were assessed using UCSC (https://genome.ucsc.edu/index.html). **Results:** A total of 11 mosaic mutations, localized in 10 genes, were identified in 67% of patients (n=8/12). Five mutations (*MTOR* n=2, *DEPDC5* n=1, *TSC2* n=1 and *RPTOR* n=1) had already been described in the literature; however, we identified additional six novel mutations (*RPS6KA1* n=1, *ULK1* n=1, *MAPK3* n=1, *PIK3CD* n=1, *WDR59* n=1 and *WDR24* n=1. These mutations were not found in the Exome Aggregation Consortium (ExAC) and a Brazilian database of genomic variants (www.BIPMed.org). Microarray analysis identified 37 CNVs, 10 are probably pathogenic and five have uncertain significance (VUS). **Discussion/Conclusion:** We identified somatic mutations in genes of the mTOR and GATOR pathways. Furthermore, somatic mutations in mTOR genes seem to be relatively common in patients with FCD since they are present in 67% subjects of our cohort. However, these preliminary data should be confirmed by Digital PCR. In addition, several potential candidate genes affected by CNVs were identified in our patients. Nevertheless, a more detailed analysis of each CNV is still needed to confirm if these structural changes are relevant to the etiology of FCD. Currently, our cohort of patients was submitted to very deep whole-exome sequencing (>1000x coverage). We believe that data from this experiment will allow more accurate identification of somatic mutations and CNVs in patients with FCD.

References: [1] Kuzniecky, RI. Epilepsia. 35 Suppl 6: S44-5 6, 1994. [2] Fauser S et al., Brain 129:1907-16, 2006. [3] Mühlebner A, et al., Acta Neuropathol 123:259-72, 2012. [4] Baldassari S et al., Acta Neuropathol 138: 885–900, 2019.

THE SEVERITY OF CORTICAL DYSFUNCTION DIFFERS IN TEMPORAL LOBE EPILEPSY PATIENTS WITH UNILATERAL AND BILATERAL HIPPOCAMPAL ATROPHY

L. S. Silva[1], L. F. Ribeiro[1], G. Artoni[1], F. Cendes[1], C. L. Yasuda[1]

[1]Neuroimaging Laboratory, FCM, UNICAMP.

Introduction: to compare Grey Matter (GM) changes in TLE patients with unilateral, bilateral and without hippocampal atrophy (HA) using voxel and surface based morphometry (VBM and SBM). **Methodology:** we acquired T1-weighted images (3T) of 146 TLE patients and 167 controls. Patients were divided into 4 groups: LEFT-HA (37), RIGHT-HA (34), BILATERAL-HA (28), and NEGATIVE (47). We processed all images with CAT12/SPM12/MATLAB(http://www.neuro.uni-jena.de/cat/). We performed the conventional VBM pipeline and also extracted Cortical Thickness (CT), Sulcal Depth (SD), Gyrification Index (GI), and Fractal Dimension (FD) with SBM. We used full factorial models on SPM to compare groups with age and sex as covariates. **Results:** The VBM analysis showed typical ipsilateral GM atrophy for unilateral HA and bilateral atrophy for the BILATERAL-HA group. The BILATERAL-HA group presented hypertrophy of cingulate areas, while the other groups presented bilateral hypertrophy of anterior thalamus-hypothalamus region and lentiform nuclei ($p < 0.001$). In SBM analysis, BILATERAL-HA/LEFT-HA/RIGHT-HA presented a thinner cortex in the posterior regions and a greater SD in the right cingulum. BILATERAL-HA also showed a reduced SD in the bilateral insula and a widespread increase of GI associated with lower GI in the bilateral insula. The RIGHT-HA/LEFT-HA presented lower GI in the ipsilat-

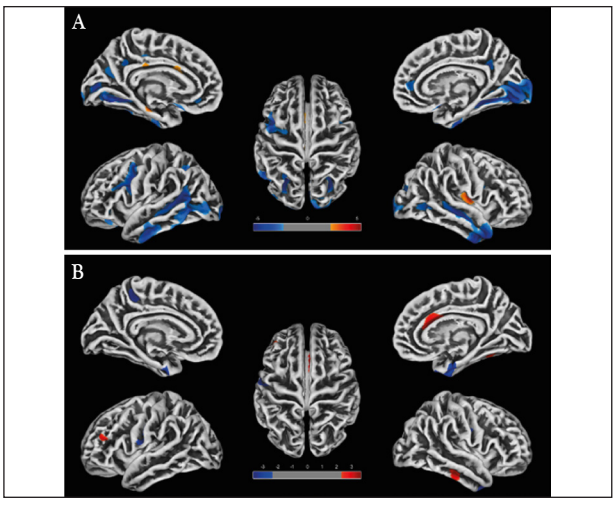

Figure 1. Cortical Thickness of BILATERAL-HA group (A) and NEGATIVE group (B).

eral insula ($p < 0.01$). The NEGATIVE group only showed higher FD in right middle frontal gyrus ($p < 0.05$). **Conclusion:** The four groups presented distinct patterns of GM abnormalities (with both VBM/SBM), with more severe alterations in patients with HA. Limbic involvement in the NEGATIVE/LEFT-HA/RIGHT-HA focused in the basal ganglia and thalamus-hypothalamus, while BILATERAL-HA had changes in the cingulum. **Funding:** FAPESP / CAPES

TRANSCRIPTOMIC ANALYSIS OF SUBICULUM REGION IN ANIMAL MODEL OF MESIAL TEMPORAL LOBE EPILEPSY (MTLE) INDUCED BY ELECTRIC STIMULATION

B. B. Aoyama[1],G.G Zanetti[1], E.V. Dias[1], A. S. Vieira[1]

[1]Department of Structural and Functional Biology, Institute of Biology; University of Campinas (UNICAMP); and the Brazilian Institute of Neuroscience and Neurotechnology (BRAINN), Campinas, SP, Brazil.

Introduction: Mesial temporal lobe epilepsy (MTLE) is the most frequent type of Temporal Lobe Epilepsy (TLE) and it is characterized by damage in the mesial temporal structures such as the hippocampus. The subiculum is an important structure because it forms the transition that connects the hippocampus with the entorhinal cortex, which allows for high amplification and modulation of the neuronal response, and it is involved in the recovery short-term memory and spatial memory codification. This study aims to understand the molecular changes in the subiculum after the induction of acute seizures by electrical stimulation of the Perforant Pathway (PP) in rats. **Materials and Methods:** For this study we used 8 sham-control and 8 electrical stimulated rats (CEMIB-UNICAMP). For all rats, stimulation electrodes were implanted in the PP and recording electrodes in the Dentate Gyrus, after 7 days rats from the stimulated group received an electric stimulation of the PP for 30 minutes in 2 consecutive days. After 24h, 5 sham and 5 stimulated rat brains were collected, frozen, histologically processed and the dorsal (dSub) and ventral subiculum (vSub) were laser microdissected using a PALM (Zeiss system). RNA was isolated from microdissected samples cDNA libraries were produced using Truseq (Illumina) library preparation kit according to manufacturer instructions. Sequencing was performed in an Hiseq 4000 platform, producing an average of 10 million paired-end 100bp reads per sample. Reads were aligned to the Rat genome using the STAR aligner. For immunolabeling, 3 sham and 3 stimulated rats were transcardially perfused with 4% formaldehyde 24h after stimulation. Brains were processed for histology and immunolabeling using fluorescent secondary antibodies were performed for NeuN and GFAP. Images were acquired in a confocal microscope (Leica). **Results:** Using the DESEq2 statistics package, we found 972 differential expression genes in ventral subiculum when comparing SHAM to Stimulated samples, which 399 genes were down-regulated and 573 genes were up-regulated. While in dorsal subiculum, we found 203 differential expression genes, which 71 genes were down-regulated and 132 genes were up-regulated. The gene ontology enrichment analysis was performed using DAVID, REACTOME and Wikipathways, the most significant common enrichment pathways with up-regulated genes in dorsal and ventral subiculum were *Steroid metabolism, Cholesterol Metabolism* e *Cholesterol Biosynthesis*, while the enrichment pathway using down-regulated genes in ventral subiculum was *axon guidance*. Moreover, we found *GFAP* up-regulated in dorsal and ventral subiculum, and also observed an increase in the immunolabeling of GFAP in both subiculum regions. **Discussion/Conclusion**: In conclusion, our data indicates that upregulation of cholesterol biosynthesis in dorsal and ventral subiculum may be related to the astrogliosis observed in both regions in which the cholesterol would be used to reconstruct astrocyte's membrane.

TRANSCRIPTOMIC PROFILE OF THE TISSUE RESPONSE TO DIFFERENT DEVICES IMPLANTED INTO THE BRAIN: ARE WE RECORDING HEALTHY NEURONS?

E. V. Dias[1], J. P. D. Machado[1] , R. Panepucci[2], R. Covolan[3], I. T. Lopes-Cendes[4], F. Cendes[5], A. S. Vieira[1]

[1]Dept of Structural and Functional Biology, IB, UNICAMP; [2]CTI Renato Archer; [3]Neurophysics Group, IFGW, UNICAMP; [4]Genetics Dept., FCM, UNICAMP; [5]Neurology Dept, FCM, UNICAMP.

Introduction: Neural probes are essential neuroscience investigative tools. They allow stimulating and recording the activity from a single neuron as well as from neuronal populations. Neural probes can also be used as clinical tools in different neurological diseases. However, once they are invasive devices, their insertion into the neural tissue causes a local inflammatory response changing the balanced neuron-glia interaction which, in turn, can lead to axonal retraction or even neuronal loss. In addition, glial cells form a capsule around the device, in an attempt to shield the affected area from the surrounding tissue, which impairs the probe performance. This study analysed for the first time the transcriptomic profile of the tissue response to three different neural probes implanted into the brain, in order to evaluate the impact of the probe implant on the tissue feasibility for recording. **Materials and Methods:** Stereotaxic surgery for implantation of recording neural probes was performed in Fischer 344 male rats. Rats received recording neural probes developed in BRAINN projects, or commercial silicon probes, or stainless steel micro wires. Recording probes were implanted into the dentate gyrus of the hippocampus (AP -3.0; L ±2.0; V -3.5). After a period of 2 or 28 days, rats were euthanized and the brains were removed. Laser microdissection of the regions proximal to probe implantation was carried out and the material was subjected to transcriptome analysis by RNA-seq using Illumina HiSeq platform. Neural tissue was also analyzed with immunofluorescence labeling for markers for foreign body reaction astrocyte marker (GFAP) and microglia marker (CD68), and for neuronal marker (NeuN). All procedures were approved by the Ethics Committee for Animal Research at the Unicamp (protocol 4438-1). **Results:** We found around 8000 genes differentially expressed, when comparing samples from any probe type to control samples, 2 days after neural probes implantation and 7000 genes differentially expressed 28 days after implantation. Most enriched pathways are involved in inflammatory process which changes over time. From those genes, 3506 are shared between the two time points and are mostly involved in enriched pathways related to inflammation. Surprisingly, we found approximately 2000 genes differentially expressed at 250-500um from the implanted probe. Most of these genes are involved with inflammatory pathways which determine a different response profile over distance. From those genes, 797 were also found at 0-250um from the probe and take part in the enriched pathways related to the inflammatory process. **Discussion/Conclusion**: Our results demonstrate a severe inflammatory response in the tissue surrounding neural probes. All three types of neural probes composed of three different materials induced similar changes of gene expression, with enrichment of pathways related to inflammation. However, this inflammatory response presents different profiles of gene expression when time and space are considered. Regarding time, the inflammatory response changes from 2 to 28 days after device implantation and two phases can be defined: an acute phase with prominent presence of microglia (CD68), and a chronic phase with an increase of astrocytes (GFAP) and oligodendrocytes (Cldn11), and a decrease of neurons (NeuN). Considering the spatial pattern, the adjacent tissue (0-250um) and the distant tissue (250-500um) present different changes in gene expression. The inflammatory response decreases over the distance but surprisingly it can be observed even at 250-500um from the probe, with an increase of microglia, astrocytes and oligodendrocytes. In conclusion, after the neural probe implantation, a severe inflammatory process in the tissue surrounding the device is observed, regardless of the probe composing material. Our findings allows a better understanding of the tissue response to neural probes implanted into the brain and may contribute to the development of probes more biocompatible which in turn will have a better performance in recording of the electrical neuronal activity.

UNDERSTANDING HYPOTHALAMIC VOLUME VARIATION IN THE LITERATURE

Livia Rodrigues[1], Thiago Rezende[2], Marcondes França[2], Letícia Rittner[1]

[1]MicLab - School of Electrical and Computer Engineering (FEEC), Unicamp, Brazil. [2]Department of Neurology, School of Medical Sciences, Unicamp, Brazil.

Introduction: Hypothalamus is a gray matter structure located below the thalamus and is part of the limbic system, presenting an important role in sleep, appetite and emotion. Reviewing the literature, we can find hypothalamic volume analysis variability between authors leading to inconsistent findings related to neurodegenerative diseases. For instance, while *Goldsteind et al* [1] found increased volume in the hypothalamus of patients, *Klomp et al* [2], reported preserved volumes. In the case of Huntington disease, *Gabery et al* [3] found no difference between the volume of the hypothalamus of patients and control subjects, whereas *Barlett et al* [4] found a reduction in the gray matter of hypothalamus in patients. Although it was believed that hypothalamic average

volume was approximately 4cm^3, more recent studies have shown that it does not have even half of this value. In this study we compare the reported hypothalamic volumes in the literature. **Methods:** In order to assess hypothalamic volume variation on the literature and try to understand its origin, we used the search string: (hypothalamus AND segmentation AND volume AND MRI AND (3T OR "3 tesla" OR 3-tesla)) on PubMed and ScienceDirect. It returned 3 results on the first and 18 on the second. After eliminating repetitions, we had 18 papers. From those, 1 is about another structure, 1 is about diffusion images and 3 have no comparable results. Eight of these studies are cluster and/or voxel-based and 1 is written in other language than english or portuguese. **Results:** After all exclusions, we compared the volumes reported on four different studies (Tab1). **Discussion/Conclusion**: Our literature review showed that hypothalamus volume is not consistent between authors (Tab.1). For instance, analysing only control groups, using [5] as reference, there is 24.25% of hypothalamic volume variation between [5] and [6] and 3.73% between [5] and [7]. We did not compare [8] since the authors reported patient and control volumes on the same test set, and volume variations could be disease-related. For being a small structure with low contrast, it is hard to define the morphological borders and authors follow different protocols for manual segmentation. Our next step is to define a robust method to obtain a reliable gold standard and create an automated method based on it.

Table 1. Hypothalamic volumes reported on the literature.

Author	Database	Volume (mean ± std)
Tognin et al (2012) [5]	26 healthy controls 26 with schizophrenia	910 ±10mm^3 for control group 960±11mm^3 for patients
Schindler et al (2013) [6]	10 healthy subjects	1130.64±103.48 mm^3
Bochetta et al (2015) [7]	18 patients with bvFTD 18 controls	944±73 mm^3 for control group 783 ±113 mm^3 for patients
Wolff et al (2018) [8]	23 healthy controls 20 with bipolar depression 41 with major depression	703± 53 to 732 ± 63 mm^3 for the right hypothalamus and from 719± 75 to 752± 54 mm^3 for the left hypothalamus

References: [1]Goldstein, JM et al.; doi: 10.1016/j.biopsych.2006.06.027 [2] Klomp, A. et al.; doi: 10.1017/S1461145711000794 [3] Gabery, S. et al.; doi: 10.1371 / journal.pone.0117593; [4] Barlett, D. et al.; doi: 10.1016/j.nbscr.2018.07.001 [5]Toning, S. et al.; doi: [6] Schindler, S. et al.; doi: 10.1016/j.pscychresns.2018.04.007; 10.1016/j.pscychresns.2012.10.006; [7] Bochetta, M. et al.; doi: 10.1007/s00415-015-7885-2; [8] Wolff, J. et al.; doi: 10.1016/j.pscychresns.2018.04.007

UNRAVELING THE EPIGENETIC MECHANISMS INVOLVED IN MESIAL TEMPORAL EPILEPSY WITH HIPPOCAMPAL SCLEROSIS

J. C. Geraldis[1], D. B. Dogini[1], W. Souza[1], A.M. Canto[1], S.H. Avansini[1], M. K.M. Alvin[2], F. Rogerio[3], C.L. Yasuda[2], B. S. Carvalho[4], F. Cendes[2], I. Lopes-Cendes[1]

[1]Department of Medical Genetics and Genomic Medicine, [2]Department of Neurology, [3]Department of Anatomical Pathology; School of Medical Sciences; [4]Department of Statistics Institute of Mathematics, Statistics and Scientific Computing; University of Campinas (UNICAMP); and the Brazilian Institute of Neuroscience and Neurotechnology, Campinas, SP, Brazil.

Introduction: Whole-genome bisulfite sequencing (WGBS) is the current gold-standard approach to study DNA methylation, one the most important epigenetic modifications. WGBS provides the complete DNA methylation profile, including different regions, as introns, exons and promoters. Mesial temporal lobe epilepsy (MTLE) associated with hippocampal sclerosis (HS) is one of the most frequent and most severe types of epilepsy. For these patients, a surgical procedure may be a therapeutic alternative and tissue obtained in these surgeries can be studied. Since epigenetic mechanisms play a relevant role in many neurological disorders, we aim to investigate whether a different methylation profile is present in tissue obtained from patients with MTLE+HS using WGBS. **Materials and Methods:** DNA was extracted from the hippocampal tissue with confirmed HS using the phenol-chloroform protocol and quantified with the *Qubit High Sensitivity* (*Thermo Fisher*) kit. We have analyzed 11 samples from patients and four controls from autopsy. In addition, samples from patients were divided into two groups: **i)** with less than 20 years of disease duration (n = 5); and **ii)** with more than 20 years of disease duration (n = 6). Next, we performed the bisulfite conversion and the preparation of sequencing library using the Accel-NGS Methyl-Seq DNA Library Kit (*Swift Biosciences*). Then, whole-genome sequencing was performed (*Illumina NovaSeq 6000*) and data were treated with the bioinformatic tools *TrimGalore* and *Bismark*, and the statistics package *BSSeq*. To analyze differentially methylated regions (DMR), *BSmooth* was used. **Results:** This is still an ongoing study and to date we found more than 1,000 differentially methylated regions when comparing to patients to controls. The identification of the differentially methylated regions is underway as well as the correlation of the methylation profiles with the transcriptomic profile of the same tissue. **Discussion/Conclusion**: We have identified many differentially methylated regions in tissue from patients with MTLE+HS, suggesting that epigenetic modifications may play an important role in the underlying mechanisms leading to HS. The identification of specific methylated regions and its correlation with gene-expression data may indicate new targets that could be used for therapeutic purposes in the future.

USE OF ASSISTIVE TECHNOLOGY IN THE REHABILITATION OF PATIENTS WITH STROKE

Dias, A. S.[1], Barros, G. S.[1], Min, L. L.[2,3], Brandão, A. F.[3,4], Tedrus, G. M. A. S.[5], Souza, R. C. T.[6]

[1]Medical School, PUCCAMP, [2]School of Medical Sciences, UNICAMP, [3]Brazilian Inst. of Neuroscience and Neurotech., BRAINN-UNICAMP, [4]Institute of Physics Gleb Wataghin, UNICAMP, [5]Neurology Dept., PUCCAMP, [6]Physiotherapy Dept., PUCCAMP.

Introduction and Hypothesis: Strokes are thromboembolic phenomena that have varying origins, classified according to the Trial of Org 10172 [1] in Acute Stroke Treatment (TOAST). Assistive technologies enable new solutions for the rehabilitation of problems caused by neural amputations or neurological injuries through medical interventions performed through neuroengineering. However, one of the problems related to the use of assistive technologies available in the market for the rehabilitation of stroke patients is the high cost, which hinders its implementation in the Brazilian Unified Health System (SUS) [2] and private clinics. The development of new interactive game software that uses only Kinect sensors and low-cost notebooks can be a way out of the problems presented since they are cost-effective compared to other technologies. The use of "Virtual Puzzle" software, developed by researchers at the BRAINN and Eldorado Institutes (which uses a Kinect sensor as interaction device), stimulates the motor and cognitive functions [3,4]. Also, technologies used through virtual reality in conjunction with traditional rehabilitation techniques may outperform traditional ones when employed alone, once occurred significant improvement in tone and movement ability of patients, increasing their quality of life. **Objective:** Demonstrate the influence of "Virtual Puzzle" software on the performance of hemiparesis patients during the rehabilitation process. **Materials and Methods:** The selection of stroke patients comes from the registration list of the Physiotherapy service of the Pontifical Catholic University of Campinas (PUC-Campinas). There will be two structured weekly sessions with an initial 15 minutes of application of virtual reality software and 45 minutes of conventional therapy. The sessions have a room provided for this purpose in the physiotherapy clinics (PUC-Campinas) and the data recorded at the beginning and the end of treatment to compare both samples. **Relevance:** Neurorehabilitation is a sensitive topic in the area of health and public spending, due to the increasing number of stroke patients, the severity of the disease and its psychosocial impacts on ageing in the Brazilian population. In this context, enabling means to reinsert the neurological patient into the labour market through cheap and effective rehabilitation methods becomes imperative to counter the growing economic expense in clinics and hospitals. Expenses for the care of a stroke patient in the United States can reach up to $ 140,048 [5], including rehabilitation, hospitalization, and treatment of underlying sequelae. The development of this project makes it possible to create evidence for the use of cheaper technology to improve performance during the rehabilitation process and prognosis.

References: [1] Chung, J. W. et al. Trial of ORG 10172 in Acute Stroke Treatment (TOAST). J Am Heart Assoc. Aug 11;3(4), 2014. [2] Brasil. Sistema Único de Saúde (SÚS): estrutura, princípios e como funciona. Ministério da Saúde. Available in http://www.saude.gov.br/sistema-unico-de-saude, 2019. [3] Brandão, A. F. et al. Gesture Collection for motor and cognitive stimuli: Virtual Reality and e-Health prospects. J Health Inform, v. 10:1, p. 9-16, 2018. [4] Brandão, A. F. et al. RehabGesture: an alternative tool for measuring human movement. Telemedicine and e-Health J, v. 22:7, p. 1-6, 2016. [5] Alves, M. B. et al. Custo-benefício de protocolos para o acidente vascular cerebral: experiência do Hospital Israelita Albert Einstein. Einstein: Educ Contin Saúde. p. 39-41, 2009.

VIRTUAL-REALITY BASED NEUROREHABILITATION OF A CHRONIC STROKE PATIENT WITH SENSORY-MOTOR DEFICIT

J. A. Feitosa[1,2], R. F. Casseb[2,3], A. Camargo[2,4], B. C. S. M. Guedes[4], M. M. Pereira-Novo[4], B. R. Ballester[5,6], P. Omedas[5,6], P. Verschure[5,6,7], T. D. Oberg[4], L. L. Min[2,4], G. Castellano[1,2]

[1]Neurophysics Group, IFGW, UNICAMP, Campinas, Brazil; [2]BRAINN, Campinas, Brazil; [3]Calgary University, Calgary, Canada; [4]Neurology Dept., FCM, UNICAMP, Campinas, Brazil, [5]SPECS, Universitat Pompeu Fabra, Barcelona, Spain; [6]Institute for Bioengineering of Catalonia (IBEC) and Barcelona Institute of Science and Technology (BIST), Barcelona, Spain; [7]Catalan Institute of Advanced Studies (ICREA), Barcelona, Spain.

Introduction: Hemiparesis is the most common impairment following stroke, affecting directly stroke survivors' independence and quality of life. As mortality related to stroke has been decreasing over the years, functional recovery has become a global health issue. In this context, virtual reality (VR) systems have been extensively used as an option to conventional rehabilitation. VR rehabilitation is associated to a lower dropout rate. This work aimed to detect brain changes associated with the Rehabilitation Gaming System [1] treatment of the upper limbs of a chronic stroke patient with sensory-motor deficit using resting-state functional magnetic resonance imaging (rs-fMRI). **Materials and Methods:** A 54-year old male with three years after ictus underwent rs-fMRI scanning and clinical assessment at three time-points: before the first rehabilitation session, after 12 and after 24 sessions. The sessions were composed of 20 min of VR, 20 min of conventional physiotherapy and another 20 min of VR therapy. To analyze the images, we modeled the brain as a 264-ROI graph using Power's functional atlas [2]. Pearson's correlation was determined for each pair of nodes and the correlation matrix was binarized maintaining only the 20% strongest correlations. Graph metrics (degree, clustering coefficient and betweenness centrality) were computed for the three adjacency matrices corresponding to the three data acquisitions. Then, the relative variation of the metrics was calculated between 1st to 2nd, 2nd to 3rd and 1st to 3rd time-points and plotted over an MNI brain cortical surface. Only graph metric changes larger than 10% were considered. **Results:** The betweenness centrality presented differences in areas related to visual and auditory functions on the left (contralesional) hemisphere (all time intervals) and on the left sensorimotor cortex (1st to 2nd time-points). Variations of the order of 10-80% were detected at the right supramarginal gyrus from 2nd to 3rd and from 1st to 3rd time-points. Clinical assessments showed changes on: shoulder abduction (3 to 4) and forearm flexion (4 to 5), on MRC scale; dynamometry from 10 to 20 kg; spasticity from 2 to 1; Fugl-Meyer scale for hand (6 to 13), sensibility (4 to 10), total motor function (35 to 45) and total upper extremity (55 to 102). **Discussion/Conclusion**: Some studies show that the right supramarginal gyrus plays an important role in proprioception [3,4]. The increase on betweenness centrality detected in this region may be related to clinical improvements (decreasing on muscle tone, gains on range of motion and grip and inclusion of the member on daily living activities), since somatic sense is crucial to proper motor execution. In short, the method was efficient to detect brain changes due to the treatment. Nevertheless, statistical methods must be explored to achieve better estimation of variations significance.

References: [1] Cameirao MS et al., doi: 10.1186/1743-0003-7-48; [2] Power et al., doi: 10.1016/j.neuron.2011.09.006; [3] Ben-Shabat et al., doi: 10.3389/fneur.2015.00248; [4] Kheradmand et al., doi: 10.1093/cercor/bht267

WHOLE EXOME SEQUENCING ANALYSIS IN PATIENTS WITH DEVELOPMENTAL EPILEPTIC ENCEPHALOPATHY (DEE)

HT Moraes[1,4], CM Cavalcante[2], MM Guerreiro[2], MA Montenegro[2], B Henning[1,4], BS Carvalho[3,4], AC Coan[2], I Lopes-Cendes[1,4]

[1]Department of Medical Genetics and Genomic Medicine, [2]Department of Neurology; School of Medical Sciences; [3]Department of Statistics, Institute of Mathematics, Statistics and Computer Science; University of Campinas, UNICAMP, Campinas, SP, Brazil and the [4]Brazilian Institute of Neuroscience and Neurotechnology (BRAINN), Campinas, SP, Brazil.

Introduction: The DEEs are a heterogeneous group of early-onset epilepsies characterized by different types of seizures, usually resistant to treatment, and a high-risk of global developmental delay, combined with cognitive dysfunction [1]. The diagnosis of the DEEs is still primarily based on clinical and EEG information, but the etiology remains unknown in most patients. However, recent developments in the molecular genetics techniques significantly improved the detection of mutations in patients with DEEs [2,3]. In this scenario, the main objective of this study is to search for the genetic causes of DEEs state-of-the art molecular technologies combined with different methods of analysis for complex genetic data. **Materials and Methods:** This is still an ongoing project and to date, we have performed whole exome sequence (WES) in 100 patients with different DEE syndromes and who had no previous genetic testing performed. Patients were assessed in different clinical centers in Brazil following a structured clinical protocol. The diagnosis of DEE was confirmed by consensus among a group of neurologists with expertise in childhood epilepsy. The DNA libraries were prepared using Sure Select all exons V6 protocol (Agilent Technologies) and were sequenced in Hiseq 4000 platform (Illumina). The raw data were processed, and the results were analyzed using the Varstation platform (www.varstation.com). For genetic variant selection, two initial filters were used: i) read depth (≥10), allele frequency in the control population (≤1%), and exonic consequence (everything different from 'synonymous SNV'; single nucleotide variants); ii) a panel of 129 known genes already related to the DEEs. The variants of interest were selected using three criteria: predicted as deleterious by the variant effect predictors, final variant consequence in the protein, and the presence on dbNSP and CLINVAR databases. **Results and discussion:** Our preliminary results show a mean read depth (RD) of 30X, and the mean percentage of targets with RD of at least 10X was 89%. The mean number of genetic variants identified per patient before the filters was 19,5341, and after the two bioinformatics filters had been applied was 22. Among these variants, we selected 63 variants of interest for further studies in 49 individuals and located in 41 genes. Considering the exonic consequences of the variants, 51 are missense, 5 are nonsense, 4 are frameshift indel, 2 are in-frame indel, and one is affecting a splicing site. In view of the ACMG (American College of Medical Genetics) classification for variant pathogenicity, 52 are of uncertain significance (VUS), 9 are likely pathogenic, one is likely benign, and one is pathogenic. **Conclusion**: Although still preliminary our results indicate that the bioinformatics algorithms used in the present study were efficient to identified genetics variants of potential clinical interest in 49% of patients with DEE.

References: [1] McTague *et al.*, doi: 10.1016/S1474-4422(15)00250-1; [2] Berkovic *et al.*, doi: 10.1016/S1474-4422(15)00199-4; [3] Mercimek-Mahmutoglu *et al.*, doi: 10.1111/epi.12954.

WHOLE-GENOME DNA METHYLATION PATTERN IN PATIENTS WITH JUVENILE MYOCLONIC EPILEPSY

B. S. Lopes[1], D.C.F. Bruno[1], W. Souza[1], B. S. Carvalho[3], M.K.M. Alvim[2], C.L. Yasuda[2], F. Cendes[2], I. Lopes-Cendes[1]

[1]Departament of Medical Genetics and Genomic Medicine, [2]Department of Neurology; School of Medical Sciences, [3] Department of Statistics, Institute of Mathematics, Statistics and Scientific Computing. University of Campinas (UNICAMP) and the Brazilian Institute of Neuroscience and Neurotechnology (BRAINN), Campinas, SP, Brazil.

Introduction: Juvenile myoclonic epilepsy (JME) is the most frequent type of genetic generalized epilepsy [1]. Although candidate genes have already been proposed for JME, most patients do not have mutations in specific genes [2,3]. More recently, differences in the methylation of the promoter region of the *BRD2* gene has been suggested as a possible mechanism leading to increased predisposition to JME [4]. Therefore, the present study aims to investigate the whole-genome methylation pattern in patients with JME. **Materials and Methods:** To date, we studied three patients with JME and three control individuals, Total genomic DNA was obtained from the peripheral blood and genomic converted with bisulfite using the EZ DNA Methylation-Gold Kit by Zymo Research. Whole-genome sequencing libraries were constructed with the Accel-NGS Methyl-Seq DNA Library Kit by Swift Biosciences. Subsequently, whole-genome bisulfite sequencing (WGBS) was performed in a HiSeq X Illumina. Raw sequencing data were trimmed using the TrimGallore software, and the filtered reads were aligned to the reference human genome (GRCh38). The Bismark software was used to calculate the proportion of methylation along the human genome, and the Bsseq program from the Bioconductor package was used to analyze differentially methylated regions (DMRs) in CpG contexts. **Results:** Overall, we obtained 470 million reads per sample sequenced with an average of 21% GC content. A unique alignment of reads was around 80%, with only 11% of duplications. Overall, we found more than 58 million methylated loci, with a 9x average coverage of GpGs regions. Finally, the comparison between the methylation pattern observed in patients with JME and controls identified 2,000 DMRs. **Discussion/Conclusion**: We have shown a remarkable difference in the methylation pattern of patients with JME in comparison with controls. Although our results are still preliminary and based in small sample size, we present here suggestive evidence that DNA methylation may be indeed involved in the mechanism underlying JME. Additional analysis is underway to precisely localize and analyze the possible functional impact of the differentially methylated regions found. **Supported by**: FAPESP .

References: [1] Mirian S.B. Guaranha et al., doi: https://doi.org/10.1016/j.seizure.2010.10.004., [2] Santos BPD et al., doi: 10.1371/journal.pone.0179629. eCollection 2017. [3] Chen T et al., doi:10.2147/NDT.S142032 [4] Pathak S, Miller J, Morris EC, Stewart WCL, Greenberg DA. Epilepsia. 2018 May;59(5):1011-1019. doi: 10.1111/epi.14058. Epub 2018 Apr 2.